

**A STUDY OF THE PREPARATION AND CHARACTERIZATION
OF BISMUTH TELLURIDE AND BISMUTH OXIDE
THIN FILMS**

**Thesis submitted by
PRADEEP, B.
in partial fulfilment of the
requirements for the Degree of
Doctor of Philosophy**

**SOLID STATE PHYSICS LABORATORY
DEPARTMENT OF PHYSICS
Cochin University of Science and Technology**

1986.

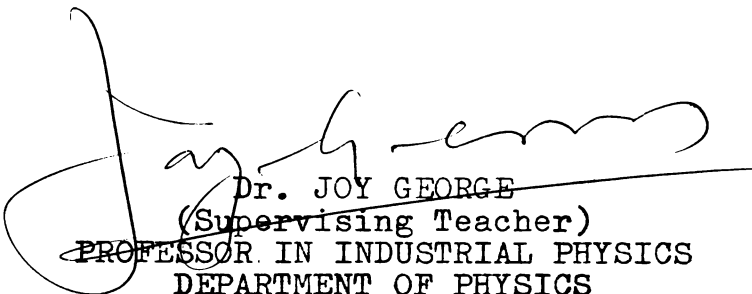
To the loving memory of my beloved father.

To my mother for her constant encouragement.

CERTIFICATE

Certified that this thesis is based on the work done by Mr. Pradeep, B. under my guidance in the Department of Physics, Cochin University of Science and Technology and no part of this has been presented by him for any other degree.

Cochin-22
10th Nov. 1986.


Dr. JOY GEORGE
(Supervising Teacher)
PROFESSOR IN INDUSTRIAL PHYSICS
DEPARTMENT OF PHYSICS
COCHIN UNIVERSITY OF SCIENCE AND
TECHNOLOGY.

DECLARATION

Certified that the work presented in this thesis is based on the original work done by me under the guidance of Professor Joy George in the Department of Physics, Cochin University of Science and Technology, and has not been included in any other thesis submitted previously for the award of any degree.

Cochin-22
10th Nov. 1986.


PRADEEP, B.

SYNOPSIS

A STUDY OF THE PREPARATION AND CHARACTERIZATION OF BISMUTH TELLURIDE AND BISMUTH OXIDE THIN FILMS

From the point of view of solid state technology, the V-VI family of compounds includes some very promising materials. The value of the forbidden band gap in this family varies from 0.15 eV (Bi_2Te_3) to 4.2 eV (Sb_2O_3). Some members of the family are good semiconductors (Bi_2Te_3 , Sb_2Te_3 , Sb_2S_3) and some others, insulators (Bi_2O_3 , Sb_2O_3). Bi_2Te_3 and Sb_2Te_3 and their alloy systems have been commercially used as thermoelectric generators and coolers. Sb_2S_3 and Bi_2S_3 are good photoconductors and have been used in television pick-up tubes, experimental solar cells etc. Bi_2O_3 is a good insulator and its uses include optical coatings, Schottky barrier solar cells etc. Also Bi_2O_3 and Sb_2O_3 exhibits polymorphism and hence are interesting from the point of view of structural crystallography.

In this thesis is reported the preparation and characterization of two compounds, viz. Bi_2Te_3 and Bi_2O_3 of this family in thin film form.

Thin films of V-VI compounds can be prepared using various methods, viz. vacuum evaporation of the compound, three temperature method and chemical methods. Direct evaporation of the compound in many cases is impracticable either due to the decomposition of the compound upon heating in vacuum or due to the chemical reactivity of the molten compound with ordinary boats or crucibles used for evaporation. Decomposition of the compound during evaporation leads either to non-stoichiometric films or to layered films. Three temperature method developed by Guenther /1/ overcomes the above defects of single source evaporation and has been satisfactorily used for the deposition of many V-VI compounds. In this method the component elements of the compound are evaporated separately at suitable rates and they are made to impinge on a substrate kept at a temperature which will not allow the condensation of the component elements, but only of the compounds.

Three temperature method has been successfully used here for the preparation of Bi_2Te_3 films. The bismuth flux and tellurium flux are approximately $2-3 \times 10^{14}$ atoms $\text{cm}^{-2}\text{S}^{-1}$ and $3-4 \times 10^{15}$ atoms $\text{cm}^{-2}\text{S}^{-1}$ respectively. The substrate temperature is in the range 530-545K. X-ray diffraction studies have shown

that these films have no particular orientation on the substrate surface. Electrical measurements show that the films have a carrier concentration of 1.2×10^{20} electrons cm^{-3} and a mobility of $100 \text{ cm}^2 \text{ Volt}^{-1} \text{ s}^{-1}$. Thermoelectric power measurements show that these films have a high thermoelectric power of $350 \mu \text{VK}^{-1}$.

Several authors have reported the preparation of bismuth oxide films by the oxidation of bismuth films in air. The results obtained in each case do not agree with one another. Often the films obtained are a mixture of the different phases of Bi_2O_3 . This is due to the polymorphism of bismuth oxide. Also there has been no systematic study on the dependence of the phases formed on the temperature of oxidation and on the medium of oxidation. In order to shed more light on this problem, a systematic study of the oxidation of bismuth films in different atmospheres like air, super-heated steam, nitrogen, and partial vacuum has been undertaken. The temperature of oxidation is varied from 500K to 650K. X-ray diffraction studies have been made of the different films prepared by these techniques and the different single phase films of $\beta - \text{Bi}_2\text{O}_3$ (tetragonal phase),

α - Bi_2O_3 (monoclinic phase) and γ - Bi_2O_3 (cubic phase) obtained have been confirmed.

Another method of preparation of Bi_2O_3 discussed in this thesis is the three temperature method. Here bismuth is evaporated into an atmosphere of oxygen. The impingement rate of bismuth atoms onto the substrate surface is varied from 3.5×10^{14} atoms $\text{cm}^{-2}\text{S}^{-1}$ to 5.6×10^{15} atoms $\text{cm}^{-2}\text{S}^{-1}$. The substrate temperature is also varied from room temperature to higher temperatures. Only β -phase films are obtained by this technique. It is also found that no film has been obtained, when the substrate is maintained above the melting point of bismuth.

Unfortunately films of Bi_2O_3 prepared using the above method is of poor quality due to the incorporation of unreacted bismuth in the growing film. This is a consequence of the high activation energy (>1 eV) needed for the reaction between bismuth and oxygen. Activation energy may be supplied to the reactants by activating the reactive gas suitably and this process is known as activated reactive evaporation (ARE) /2/. In the present case an electron beam with an energy ≈ 100 eV has been used to activate the

reactive gas. Good quality films of Bi_2O_3 have been obtained using this technique.

Bismuth flux was varied from 3.4×10^{15} atoms $\text{cm}^{-2}\text{S}^{-1}$ to 1.5×10^{16} atoms $\text{cm}^{-2}\text{S}^{-1}$. The substrate temperature has been varied from 300K to 650K. The films prepared at low substrate temperatures are amorphous in nature. Increase in substrate temperature leads to the formation of polycrystalline films. As evidenced by the x-ray diffraction studies it is seen that at constant oxygen pressure, for low bismuth evaporation rate, $\beta - \text{Bi}_2\text{O}_3$ and at high evaporation rate $\alpha - \text{Bi}_2\text{O}_3$ are obtained. Refractive index, absorption coefficient, and band gap of these films have been determined from the study of the optical properties of these materials.

Heat mirrors are multilayer structures which allow the transmission of the visible light but has a high reflectivity for heat radiations. These structures can be used in incandescent lamps, where it will increase the efficiency and in glass panes and windows of buildings where it will give better insulation. Heat mirrors using layers of Bi_2O_3 and gold have been fabricated. Visible transmission and IR reflection

have been optimised by varying the thickness of the Bi_2O_3 and gold layers and the results have been presented.

References:

1. K.G. Guenther in "The Use of Thin Films in Physical Investigations", edited by J.C. Anderson, Academic press, London (1966), p.213.
2. R.F. Bunshah and A.C. Raghuram, J. Vac. Sci. & Tech., 9 (1972) 1389.

CONTENTS

	Pages
INTRODUCTION	1
Chapter I - SEMICONDUCTOR PHYSICS	9
1.1 Band structure	9
1.2 Intrinsic and extrinsic semiconductors	16
1.3 Hall effect	20
1.4 Thermoelectric power	24
1.5 Amorphous semiconductors	25
1.6 Optical properties of semiconductors	29
References	42
Chapter II - THIN FILM PREPARATION METHODS	43
2.1 Introduction	43
2.2 Chemical methods	43
2.3 Physical methods	46
2.3.1 Sputtering	46
2.3.2 Evaporation	49
2.4 Reactive evaporation	52
2.5 Activated reactive evaporation	61
References	66
Chapter III - EXPERIMENTAL TECHNIQUES	68
3.1 Measurement of electrical conductivity	68
3.2 Measurement of Hall voltage	73
3.3 Measurement of thermoelectric power	79

3.4 X-ray diffraction	81
3.5 Thin film thickness measurements	84
3.6 Determination of optical constants of thin films	87
3.7 Oxidation of metal films	93
3.8 Preparation of compound films by reactive evaporation	96
3.9 Preparation of compound films by activated reactive evaporation	103
References	107
 Chapter IV - REACTIVELY EVAPORATED FILM OF BISMUTH TELLURIDE	 109
4.1 Introduction	109
4.2 Experimental	110
4.3 X-ray diffraction studies	112
4.4 Electrical properties	112
4.5 Conclusion	123
References	124
 Chapter V - BISMUTH OXIDE FILMS PREPARED BY THE OXIDATION OF BISMUTH FILMS	 126
5.1 Introduction	126
5.2 Experimental	128
5.3 Results	131

5.4 Discussion	136
5.5 Conclusion	147
References	148
Chapter VI - BISMUTH OXIDE FILMS PREPARED BY REACTIVE EVAPORATION	150
6.1 Introduction	150
6.2 Experimental	151
6.3 Results and discussion	152
6.4 Annealing of films	157
6.5 Conclusion	161
References	163
Chapter VII - BISMUTH OXIDE FILMS PREPARED BY ACTIVATED REACTIVE EVAPORATION	165
7.1 Introduction	165
7.2 Experimental	166
7.3 Results and discussion	169
7.4 Annealing of films	173
7.5 Conclusion	176
References	177
Chapter VIII - OPTICAL AND ELECTRICAL PROPERTIES OF β - Bi₂O₃ FILMS	178
8.1 Introduction	178
8.2 Experimental	179

8.3 Results and discussion	181
8.4 Conclusion	192
References	193
Chapter IX - PREPARATION OF HEAT MIRRORS USING BISMUTH OXIDE FILMS	195
9.1 Introduction	195
9.2 Theory	197
9.3 Experimental	200
9.4 Results and discussion	203
9.5 Conclusion	208
References	209

INTRODUCTION

An independent and important branch that has developed recently is the physics of thin films. This deals with systems which have only one common property, namely, that one of their dimensions is very small, though all other physical properties may be different. Thin layers of oil floating on the surface of water, with their fascinating colours, have attracted men's curiosity from time immemorial. The first evaporated thin films of metal were probably the deposits obtained by Faraday /1/ by exploding metal wire in an inert atmosphere. The possibility of depositing thin metal films in a vacuum by Joule heating of platinum wire was discovered by Nehrwoold /2/. Scientific interest in thin films, both fundamental and applied, began with their application first in optics and later in electronics. Optical applications are mainly for the preparation of reflecting coatings on mirrors, decorative coatings on plastics, antireflection coating in lenses, interference filters, optical filters, beam splitters, etc. Electronic applications are mainly in integrated circuits and in the preparation of passive and

active components for the microminiaturization of electronic devices. Applications of thin films in optoelectronics and integrated optics are also worth mentioning, for example, in phototubes, photoresistors, photovoltaic cells, TV-camera tubes, electro-luminescent panels, etc.

Thin films are also used as protective coatings to prevent corrosion, friction, etc. In India, a thin layer of tin has been used from ancient times to protect copper utensils from corrosion. Iridium thin films are used in certain applications on account of their good lubricating property. Relay contacts are coated with thin films of rare metals in order to prevent burning etc. due to arcing. Hard coatings are also available using the so called diamond like carbon (i-carbon) compound films.

Optimum material properties in device applications cannot be achieved by a single element. Hence scientists tried alloys and compounds and it was found that the properties can be optimised by a combination of two or more elements. Germanium, silicon and selenium were the earlier known and most used elemental semiconductors. Later the electrical

active components for the microminiaturization of electronic devices. Applications of thin films in optoelectronics and integrated optics are also worth mentioning, for example, in phototubes, photoresistors, photovoltaic cells, TV-camera tubes, electro-luminescent panels, etc.

Thin films are also used as protective coatings to prevent corrosion, friction, etc. In India, a thin layer of tin has been used from ancient times to protect copper utensils from corrosion. Iridium thin films are used in certain applications on account of their good lubricating property. Relay contacts are coated with thin films of rare metals in order to prevent burning etc. due to arcing. Hard coatings are also available using the so called diamond like carbon (i-carbon) compound films.

Optimum material properties in device applications cannot be achieved by a single element. Hence scientists tried alloys and compounds and it was found that the properties can be optimised by a combination of two or more elements. Germanium, silicon and selenium were the earlier known and most used elemental semiconductors. Later the electrical

properties of thin films of several III-V group compound semiconductors such as GaAs and InSb and II-VI compound semiconductors such as CdS and CdSe have been extensively explored for use in device applications.

There are various methods for depositing thin films of various materials. Out of which vacuum evaporation is the most widely used method. Direct evaporation of the compound in many cases is impracticable either due to the decomposition of the compound upon heating in vacuum or due to the chemical reactivity of the molten compound with ordinary boats or crucibles used for evaporation. When the compound dissociates in vacuum, the volatile component will be given off first, resulting in layered films, if all the evaporated material stick to the substrate, or a nonstoichiometric film of the compound, or a film of nonvolatile component, if the volatile component does not stick to the substrate, at the substrate temperature used. The compound film may be reproduced from the layered film by annealing it in an inert atmosphere at a suitable temperature. This method is applicable only to certain compounds, but

is rather time consuming. Single source evaporation is not applicable in the case of materials having high melting point, such as carbides, nitrides, etc.

Günther's three temperature method overcomes all these difficulties. This method is based on the fact that continuous condensation of a given vapour at given deposition rate is possible only if the substrate temperature drops below a critical temperature. By this method it is possible to deposit a compound film by suitably choosing, the substrate temperature at which elemental materials will not stick to the substrate, and partial pressures to the elemental vapours. This technique was the forerunner of modern day Molecular Beam Epitaxy (MBE).

In the three temperature method, the low chemical reactivity of the constituent elements leads to the need of high partial pressure of the volatile component, for a high rate of deposition. Because of this high partial pressure, the particles may be scattered and may affect the film quality even though the stoichiometry is maintained. This difficulty can be overcome by ionizing one of the

reactive elements. For this, a method was developed by Prof. Bunshah of UCLA and is known as Activated Reactive Evaporation (ARE). By this method TiC films were deposited at a high deposition rate by activating the acetylene gas using a low voltage electron gun. One further improved method of this was reported as Reactive Ion Plating (RIP). In this method the ionized components are accelerated to the negatively biased substrates. Films with very good adhesion, microhardness, etc. could be obtained by this method.

In this thesis is reported the preparation and properties of two compounds of V-VI family, viz. bismuth telluride and bismuth oxide, in thin film form. In the first chapter is given the resume of basic solid state physics relevant to the work reported here. In the second chapter the different methods of thin film preparation are described. Third chapter deals with the experimental techniques used for preparation and characterization of the films. Fourth chapter deals with the preparation and properties of bismuth telluride films. In next four chapters, the preparation and properties of bismuth oxide films are discussed in detail. In the last chapter the use

of Bi_2O_3 films in the fabrication of Heat mirrors is examined and discussed.

Part of the work reported in this thesis has been published in the form of following research papers:

1. "Preparation and properties of co-evaporated bismuth telluride (Bi_2Te_3) thin films".
Solid State Communications, 56 (1985) 117.
2. "Oxidation of bismuth films in air and superheated steam".
Thin Solid films, 144 (1986) 255.
3. "A method for the preparation of dielectric films by activated reactive evaporation using resistively heated sources".
Rev. Scientific Instruments (in press).
4. "X-ray diffraction studies of Bi_2O_3 films prepared by reactive and activated reactive evaporation".
Thin Solid films (in press).
5. "Thermal oxidation studies of bismuth films"
XVII National Seminar on Crystallography,
Dec. 20th-22nd, 1985, I.I.T., Madras, p.31.

6. "Bismuth oxide (Bi_2O_3) films prepared by activated reactive evaporation".
Proc. Solid State Physics Symposium,
Dec. 27th-30th (1985), Nagpur University,
Vol. 28C, p.335.
7. "A field stabilized electromagnet for Hall effect studies"
(Communicated).
8. "Optical properties of β - Bi_2O_3 thin films"
(Communicated).
9. "Preparation of Heat mirrors using bismuth oxide films"
(Communicated)

References:

1. M. Faraday, Phil. Trans., 147 (1857) 145.
2. R. Wairwold, Ann. Physik, 31 (1887) 417.

CHAPTER I

SEMICONDUCTOR PHYSICS1.1 BAND STRUCTURE

A great deal of work had been carried out on semiconductors before any satisfactory theory had been put forward to account for their properties. The first application of quantum mechanics to the motion of electrons in solids was the treatment of conduction of electricity in metals by A. Sommerfeld /1/. Here, the electrons are assumed to move in a field-free space, the fields of force due to atomic cores and other electrons being smoothed out except at the boundary of the solids. Here, these forces are supposed to attract the electron strongly if it moves outside the boundary. It is assumed that they set up an impenetrable potential barrier which holds the electrons in the solid. This theory enabled such phenomena as field emission and thermionic emission to be discussed in terms of potential barriers of finite height. But this theory gives no explanation of the vast difference in the properties of metals, semiconductors and insulators.

The next step was to take into account the interaction of the valence electrons with the atomic cores assuming these to be placed at the lattice points of the crystal. These electrons are still assumed to move independently but the smoothed out potential used by Sommerfeld is replaced by a periodic potential (figure 1). The particular feature of a potential of this form is that it is periodic having the same periodicity as the lattice. Motion of electrons in such a periodic potential was discussed by F. Bloch /2/ and a most fundamental result came to light which changed completely the whole approach to the problem of electronic motion in crystalline solids. It turns out that in a perfect periodic lattice the electron may move freely and is not scattered by the individual atoms of the lattice but only by deviation from perfection. The path over which an electron is to be regarded as free is determined only by the imperfections of the lattice and for a perfect crystal is infinite.

In Sommerfeld's theory, the allowed energy levels for the valence electrons of a crystal of

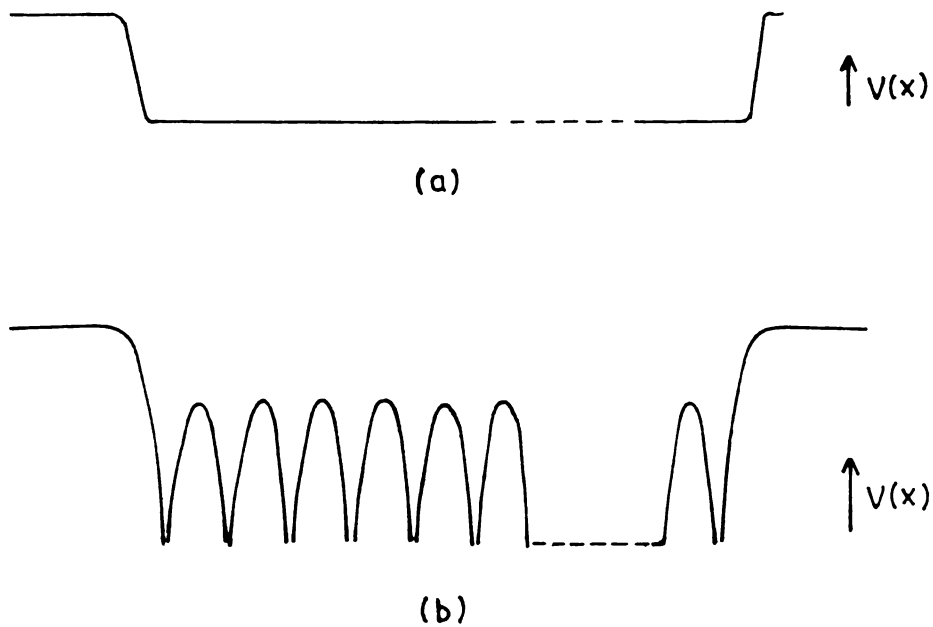


Figure 1. Potential energy of electrons in crystalline solid (a) Sommerfeld model, (b) Periodic potential due to atomic cores.

macroscopic dimensions lie very close together and their values extend from nearly the bottom of the potential trough in which the electrons move to indefinitely high values. When periodic potential is introduced, however, the energy levels are confined to certain allowed bands of energy, separated by regions in which no energy levels are allowed. For the inner electrons these allowed bands are extremely narrow and corresponds to the atomic levels; for the valence electrons the bands are quite broad. The arrangement of levels is shown in figure 2. Each band consist of many closely spaced levels and for many purposes may be regarded as a continuum. When we come to allocate electrons to these levels, however, we must remember that they are discrete and that there exists a definite number of them. Just as the inner levels in a heavy atom are all filled with electrons, so all the levels in the lower allowed bands are filled, and it is only the upper bands which may be wholly or partially unoccupied by electrons.

We can arrive at the energy band picture of solid in another way. Consider N atoms of a

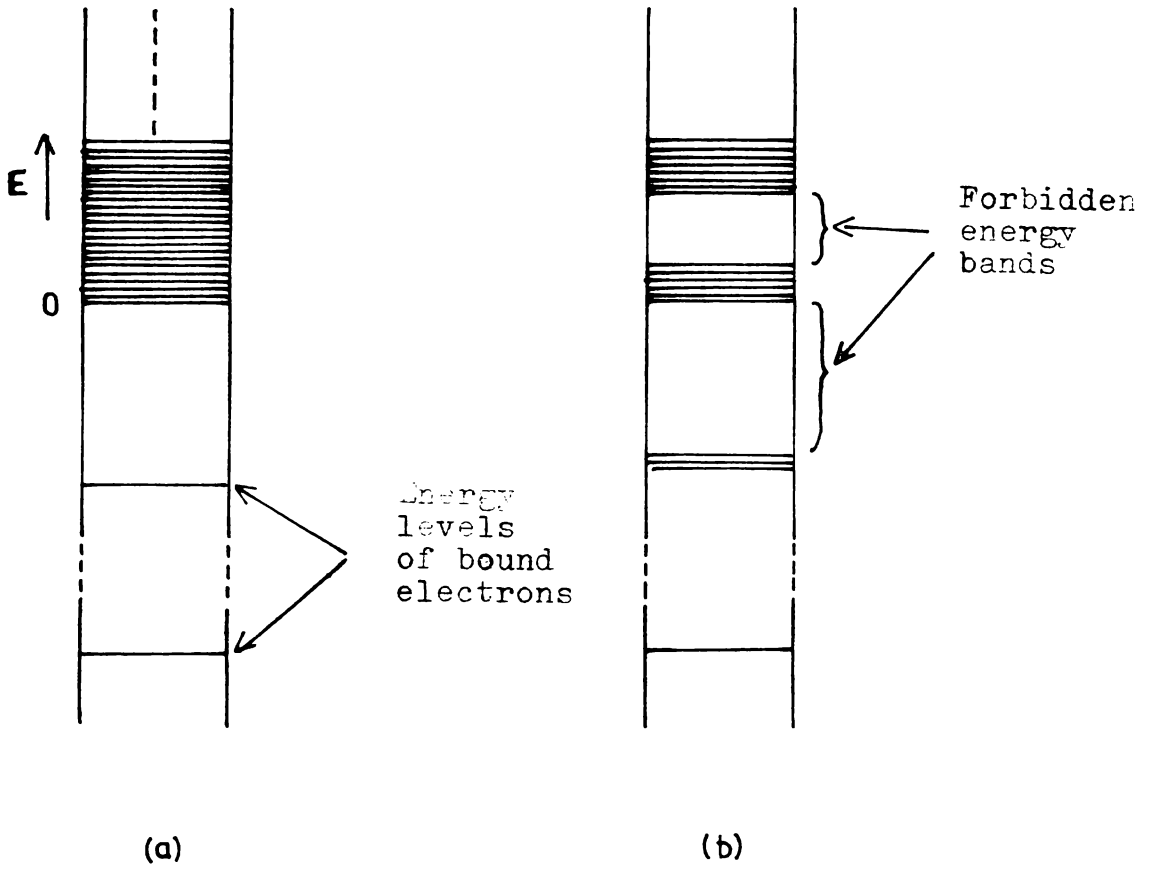


Figure 2. Energy levels of (a) Sommerfeld model,
(b) Periodic lattice.

substance and arrange them at a sufficiently large distance from each other but in such a way that this arrangement reproduces the crystalline structure of the material. We can ignore the interaction between the atoms and consider them free, since the separation between the atoms is large. In each of these atoms, there are degenerate levels with degeneracies equal to the number of differently oriented similar orbits in corresponding subshells. Now let the atoms approach, retaining the mutual arrangement. As the atoms come closer, they begin to experience the influence of their approaching neighbours. Due to this interaction, degeneracy of the energy levels splits into N nondegenerate levels. It could seem therefore that each atom should contribute the same set of nondegenerate sublevels into the energy spectrum that characterized the crystal as a whole. For the deep - lying levels the perturbation will be very small compared with the attractive force of the nucleus and the splitting will be very small. But in the case of valence electrons, the splitting may be quite large and in fact neighbouring band may overlap.

This shows that there is an entire band of allowed energy levels alternate with bands of forbidden energy levels. The electrons in the outermost levels are taking part in electronic conduction. The outer most filled level is called the conduction band and the next lower level is called the valence band. The physical properties of solids determined by the degree of filling of the energy bands and can be divided into conductors, insulators and semiconductors.

Substances having a partially filled energy spectrum above the completely filled energy band are called conductors. The electrons in this partially filled band are taking part in electrical conduction. In certain substances, there are absolutely empty bands above completely filled bands. If the forbidden gap between this empty and filled band is very high, ie. of the order of several electron volts, the excitation of electrons from the valence band to conduction band is not easy and hence conduction will not be possible even at higher temperatures. Such materials are known as insulators. If the forbidden gap is small, the electrons from the valence band can be thermally

excited to the conduction band. These thermally excited electrons can contribute to electrical conduction and hence the conductivity increases with rise of temperature. These type of substances are identified by Wilson /3/ as semiconductors. Figure 3 shows the band structure of metals, insulators and semiconductors.

1.2 INTRINSIC AND EXTRINSIC SEMICONDUCTORS

In an intrinsic semiconductor at temperatures different from absolute zero, a certain number of electrons may be excited thermally from the upper filled band to the conduction band, creating some unoccupied states; at the top of the filled band. This vacancy created will behave like a positive charge and are called holes. It moves in a direction opposite to electrons in an applied electric field. Both electrons in the conduction band and holes in the valence band contribute to electrical conductivity. The conductivity σ in presence of electrons and holes is given by

$$\sigma = (ne \mu_e + pe \mu_h) \quad (1.2.1)$$

where n and μ_e are the concentration and mobility of electrons respectively and p and μ_h are that of holes.

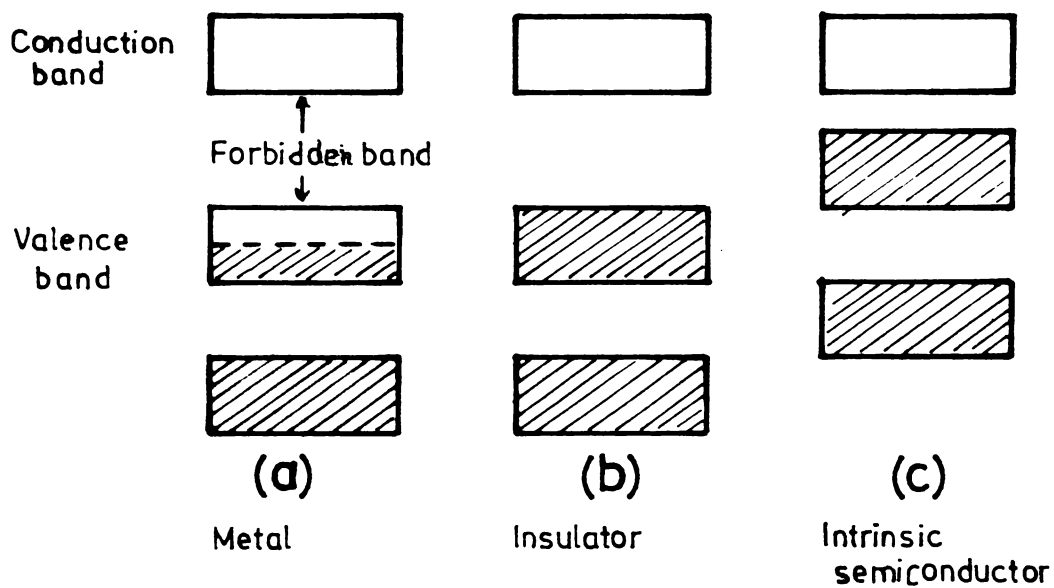


Figure 3. Energy bands for (a) metal, (b) insulator
(c) intrinsic semiconductor.

In an intrinsic semiconductor the number of electrons is equal to the number of holes. The carrier concentration is given by the expressions

$$n = N_c \exp (E_F/k_B T) \quad (1.2.2)$$

$$p = N_v \exp \left[- (E_F + E_g)/k_B T \right] \quad (1.2.3)$$

where N_c and N_v are the density of states in the conduction band and valence band respectively, E_F is the Fermi level, E_g is the forbidden energy gap, k_B is the Boltzmann's constant and T is the absolute temperature. N_c and N_v are given by

$$N_c = 2 (2 \pi m_e^* k_B T/h^2)^{3/2} \quad (1.2.4)$$

$$\text{and } N_v = 2 (2 \pi m_h^* k_B T/h^2)^{3/2} \quad (1.2.5)$$

where m_e^* and m_h^* are the effective mass of electrons and holes respectively.

Since $n = p$,

$$\begin{aligned} n = p &= 2(2 \pi k_B T/h^2)^{3/2} (m_e^* m_h^*)^{3/4} \exp (-E_g/2k_B T) \\ &= A \exp(-E_g/2k_B T) \end{aligned} \quad (1.2.6)$$

where A is a constant.

The carrier concentration in an intrinsic semiconductor increases very rapidly with temperature.

But the change in mobility with temperature is comparatively small. Hence the conductivity, which is proportional to the number of carriers, can be expressed as

$$\sigma = \sigma_0 \exp(-E_g/2k_B T) \quad (1.2.7)$$

where σ_0 is a constant.

In certain semiconductors the conductivity may be controlled by impurities. This type of semiconductors are called extrinsic semiconductors or impurity semiconductors. The addition of impurity to the semiconductor is called doping. Impurity atoms that can give up electrons are called donors and atoms which can accept electrons from the valence band, leaving holes in the band are called acceptors. If a material is doped with donor atoms, the conductivity of the material will be controlled by electrons and the material is said to be n-type semiconductors. If the acceptors are used for doping, holes will be set free in the valence band and the conductivity will be controlled by these positively charged holes. Such materials are called p-type semiconductors. The density of free electrons (n_c) in the conduction band due to a donor with activation energy E_d is given by the expression

$$n_c = (2n_d)^{1/2} (2\pi m_e^* k_B T/h^2)^{3/4} \exp(-E_d/k_B T) \quad (1.2.8)$$

where n_d is the donor density. It is to be noted that n_c is proportional to the square root of donor concentration. Hence, carrier concentration and hence conductivity of a semiconductor can be controlled by doping. A similar expression holds for the case of acceptors also.

1.3 HALL EFFECT

When a magnetic field is applied at right angles to the direction of current flow in a conductor, an electric field is developed in a direction perpendicular to both the direction of the current flow and of the magnetic field. This is known as Hall effect, and the developed voltage, Hall voltage.

Consider an n-type material with a current density ' j ' in the X-direction and a magnetic field of induction ' B ' in the Z-direction as shown in figure 4. The Hall voltage ' E ' developed will be in the Y-direction. Then the Hall coefficient ' R ' is defined by the equation

$$E = RjB \quad (1.3.1)$$

Considering the current, as a stream of electrons moving through the solid, an electron travelling with a velocity ' v ' will experience a Lorentz force Bvs .

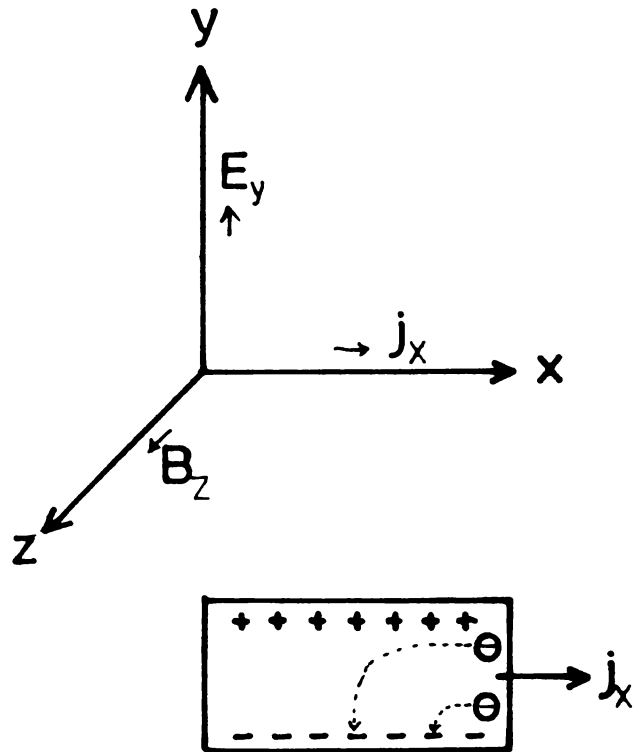


Figure 4. Origin of Hall field and Hall effect.

In free space electrons will be deflected in a direction perpendicular to the plane of B and v . But the current inside a solid is confined within the bounds of the solid. A few electrons will at first be deflected by B , but they will create an electric field which will counter balance the Lorentz force acting on the bulk of the current carriers, so enabling the current to continue flowing as before. The electric field is therefore given by

$$Bve = eE \quad (1.3.2)$$

Now the relationship between current density and the electron velocity is

$$j = nev \quad (1.3.3)$$

where n is the electron concentration.

From equation (1.3.2) and (1.3.3)

$$E = - \frac{1}{ne} B j \quad (1.3.4)$$

Electronic charge is considered as negative and hence this - sign here.

Comparing equation (1.3.4) with (1.3.1)

$$R = - \frac{1}{ne} \quad (1.3.5)$$

Knowing Hall coefficient, the carrier concentration can be determined using this relationship.

We know that the electrical conductivity (σ) is given by

$$\sigma = ne\mu \quad (1.3.6)$$

where μ is the mobility of the carrier.

Hence,

$$|R|\sigma = \mu \quad (1.3.7)$$

From this mobility of the charge carrier can be calculated, knowing R and σ

Consider a typical specimen of length 'l' width 'b' and thickness 't'. Let a potential difference 'V' is applied between the two ends such that a current 'I' flows through the sample. Then the conductivity of the sample is given by

$$\sigma = \frac{I}{V} \frac{l}{bt} \quad (1.3.8)$$

Let V_H be the Hall voltage developed in a magnetic field of induction B . Then from equation (1.3.1)

$$R = \frac{V_H t}{I B} \quad (1.3.9)$$

Hence the Hall coefficient and hence mobility and concentration of carriers can be calculated. The sign of the Hall coefficient will give the information about the type of the charge carrier.

1.4 THERMOELECTRIC POWER

If the two ends of a long material is maintained at two different temperatures, a potential difference will be developed between the two ends of the material. This potential difference developed, depends only on the temperature difference between both the ends. This is known as thermoelectric effect.

Suppose the temperature at one end is T and that at the other end is $T + dT$. The potential difference developed between the two ends be dV . Then the thermoelectric power Q is defined as

$$Q = \frac{dV}{dT} \quad (1.4.1)$$

When one end of the sample is heated, the carriers there will get a high velocity and drift towards the colder end. This produces a disturbance in equilibrium distribution of carriers and sets up an electric field which opposes the flow of carriers. This electric field will be positive with respect to the cold end if the carriers are electrons and negative if the carriers are holes.

An expression for thermoelectric power can be derived in terms of electron concentration n in the

form

$$Q = \pm \frac{k_B}{e} \left[\left(\frac{5}{2} - S \right) - \ln \frac{nh^3}{2(2\pi m^* k_B T)^{3/2}} \right] \quad (1.4.2)$$

where + refers to p-type, - to n-type semiconductors. S is a constant depending on the relaxation time of the process, m^* is the effective mass of the charge carrier and k_B is the Boltzmann's constant.

1.5 AMORPHOUS SEMICONDUCTORS

Amorphous solids have received much attention in recent years. The most familiar example of an amorphous solid is ordinary glass. Another familiar case of an amorphous structure is that of a liquid. Structurally it has got no crystalline structure. The atoms appear to have a random distribution. In such material there is only a short-range order; this is due to the regular arrangement of lattice atoms in the immediate vicinity of the particular atom considered. Long-range order, due to the strict periodicity and hence the translational invariance of the crystal lattice, will be absent in such materials (figure 5).

Many amorphous substances exhibit significant electrical conduction. This type of conduction is associated with electrons rather than ions in the solid, because the contribution of ions to the

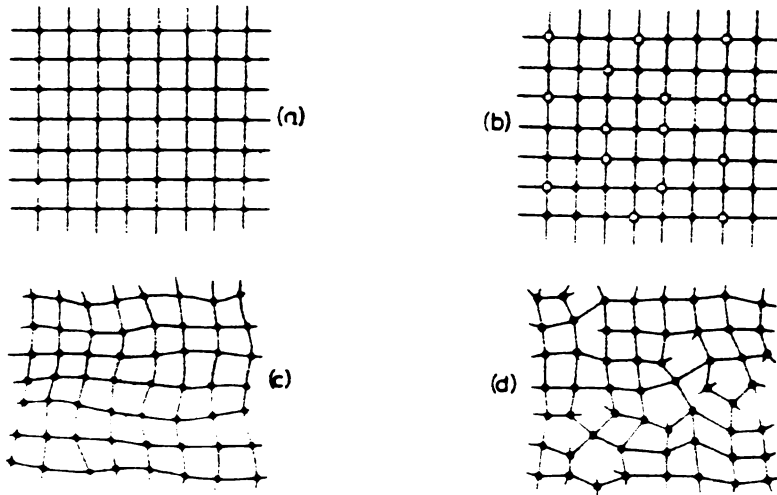
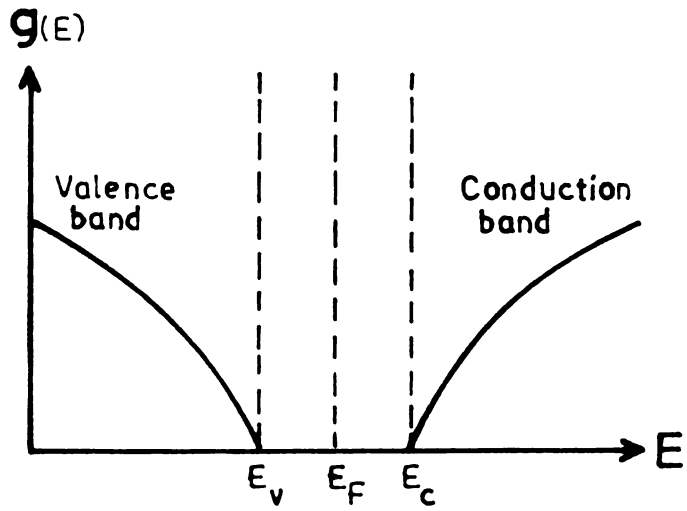


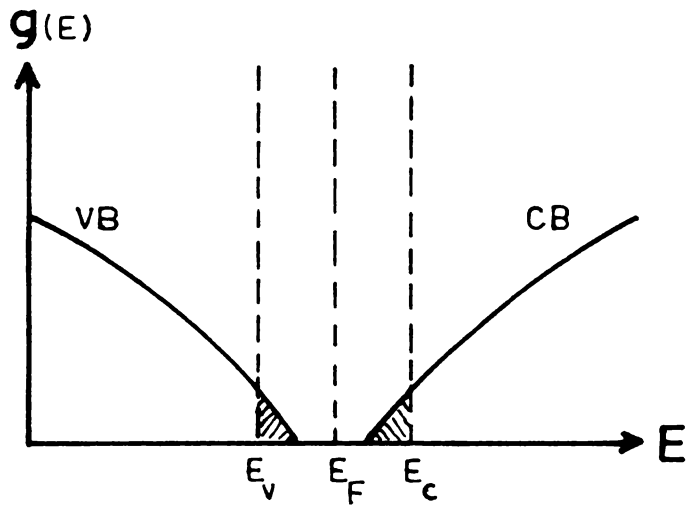
Figure 5. Possible types of lattice disorder: (a) ordered lattice, (b) compositional disorder: mixed crystal formation by statistical distribution of two sorts of atoms over the lattice sites, (c) positional disorder by distribution of the lattice, (d) topological disorder with simultaneous formation of dangling bonds.

conductivity is usually very small. Some amorphous substances show certain unusual switching properties, which could be important in applications such as switching and memory devices.

The knowledge of electronic states in an amorphous semiconductor is essential to understand the electrical and optical properties of material. Bloch theorem /2/ does not hold here, because of the presence of extensive disorder. Figure 6(a) shows the density of states $g(E)$ for a crystalline semiconductor. The bottom of the conduction band is at E_c , and the top of the valence band is at E_v . The range between these two energies, E_v to E_c , is the energy gap, where no electron can exist in a perfectly pure crystal. Figure 6(b) shows the density of states for the amorphous state of the same substance. In this case the density of states has extended into the gap from both the conduction band and the valence band side. Here the effect of disorder is to displace some levels right into the energy gap, creating the band tail. Although the shift here may not be large, it is significant, because the electron states in the tail have a different character from those in the remainder of the band.



(a)



(b)

Figure 6. Density of states $g(E)$ versus energy E for (a) a crystalline semiconductor, (b) an amorphous semiconductor.

1.6 OPTICAL PROPERTIES OF SEMICONDUCTORS

The most direct method for probing the band structure of semiconductors is the optical absorption studies. From the study of the frequency dependence of the absorption coefficient, we can determine the energy gap of the material. It is also possible to get information about the relative position of the valence band and conduction band extrema.

A plane electromagnetic wave travelling in an absorbing medium can be represented by the equations for electric and magnetic field

$$E = E_0 \exp - i(\mathbf{K} \cdot \mathbf{r} - \omega t) \quad (1.6.1)$$

$$H = H_0 \exp - i(\mathbf{K} \cdot \mathbf{r} - \omega t) \quad (1.6.2)$$

where \mathbf{K} is the complex propagation wave vector,

$$\mathbf{K} = \mathbf{K}_1 + i\mathbf{K}_2.$$

The above equations are solutions of Maxwell's equation for electromagnetic field in a medium with magnetic permeability unity.

The complex dielectric constant

$$\epsilon = \epsilon_1 + i\epsilon_2 = \epsilon_1 + \frac{i 4\pi\sigma}{\omega} \quad (1.6.3)$$

with the frequency dependent conductivity σ describes the response of the medium to the driving field $D = \epsilon E$.

The complex refractive index is defined as

$$N = n + ik = \epsilon^{1/2} \quad (1.6.4)$$

where n is the real refractive index and k , the extinction coefficient. The optical constants n and k are real positive numbers and can be determined by optical measurements.

From these we obtain

$$\epsilon_1 = n^2 - k^2 \quad (1.6.5)$$

$$\epsilon_2 = \frac{4\pi\sigma}{\omega} = 2nk \quad (1.6.6)$$

For homogeneous plane waves

$$K_1 = \frac{n\omega}{c}, \quad K_2 = \frac{k\omega}{c} \quad (1.6.7)$$

Substituting these in equation (1.6.1)

$$E_x = E_{0x} \exp\left[i\omega\left(\frac{nx}{c} - t\right)\right] \exp - \frac{\omega kx}{c} \quad (1.6.8)$$

This represents a wave travelling in x -direction with velocity (c/n) which is attenuated by $\exp(-\omega kx/c)$. The absorption coefficient α , defined by relative decrease of the intensity per unit distance in the propagation direction through $I = I_0 \exp(-\alpha x)$, is then

$$\alpha = 4\pi k/\lambda \quad (1.6.9)$$

The reflection R is referred as the ratio of the time averaged energy flow reflected from the surface to the

incident flow. For normal incidence, R is given by

$$R = \frac{(n - 1)^2 + k^2}{(n + 1)^2 + k^2} \quad (1.6.10)$$

when $k = 0$, ie. in the transparent range

$$R = (n - 1)^2 / (n + 1)^2$$

Different types of absorption

Fundamental absorption, free carrier absorption, excitonic absorption, impurity absorption etc. are the mechanisms which are responsible for absorption of electromagnetic radiation in semiconductors. In fundamental absorption, electrons can be excited from the valence band to the conduction band with the absorption of a photon of energy equal to the band gap of the material. The absorption coefficient in this case will be $\approx 10^5$ to 10^6 cm^{-1} . One of the characteristic features of semiconductor is that, on the low energy side of the absorption band, the absorption coefficient drops rapidly and the material becomes fairly transparent. This marked drop in absorption is called the absorption edge.

A free electron and hole capable of moving independently under the influence of an applied field will be produced by the excitation of an electron from the valence band to the conduction band. The system

of electron and hole mutually bound by their Coulomb attraction is known as exciton. The binding energy of exciton is about 0.01 eV and hence the excitation level falls slightly below the edge of the conduction band. The ground state ($n = 1$) excitonic level will be observed as absorption peak on the long wavelength side of the direct absorption edge. The exciton absorption is more pronounced in insulators than in semiconductors and can lead to strong narrow line absorption as in atomic spectra.

The absorption coefficient increases slowly with the increase of wave length beyond the absorption edge, due to the electronic transition within the conduction band or valence band. The process is referred to as free carrier absorption. The free carrier absorption takes place even when the energy of the incident photon is less than the forbidden gap of the material and frequently this absorption dominates the spectrum below the fundamental edge.

The transition between a neutral donor and the conduction band or between the valence band and the neutral acceptor can occur by the absorption of a low energy photon. For this absorption process the energy

of the photon must be at least equal to the ionization energy of the impurity. For donor levels lying deeper, the impurity absorption will be well separated from the fundamental absorption. For shallow impurities, the absorption spectrum will take the form of a series of lines in approximately the same position as would be expected for the exciton spectrum.

The fundamental absorption

Electron may be excited from the valence band to the conduction band by the absorption of a photon of energy approximately equal to the energy of the forbidden gap, E_g . There are two type of transition; those involving only photons and those involving photons and phonons. Transitions involving photons are called direct transition and those involving phonons, indirect transition.

Direct transition

If the valence band maximum and the conduction band minimum appear at the same point in the Brillouin zone at $K = 0$, the direct transition by the absorption of the energy approximately equal to the energy gap, E_g . Figure 7 shows a direct vertical optical transition near the fundamental absorption edge in a semiconductor.

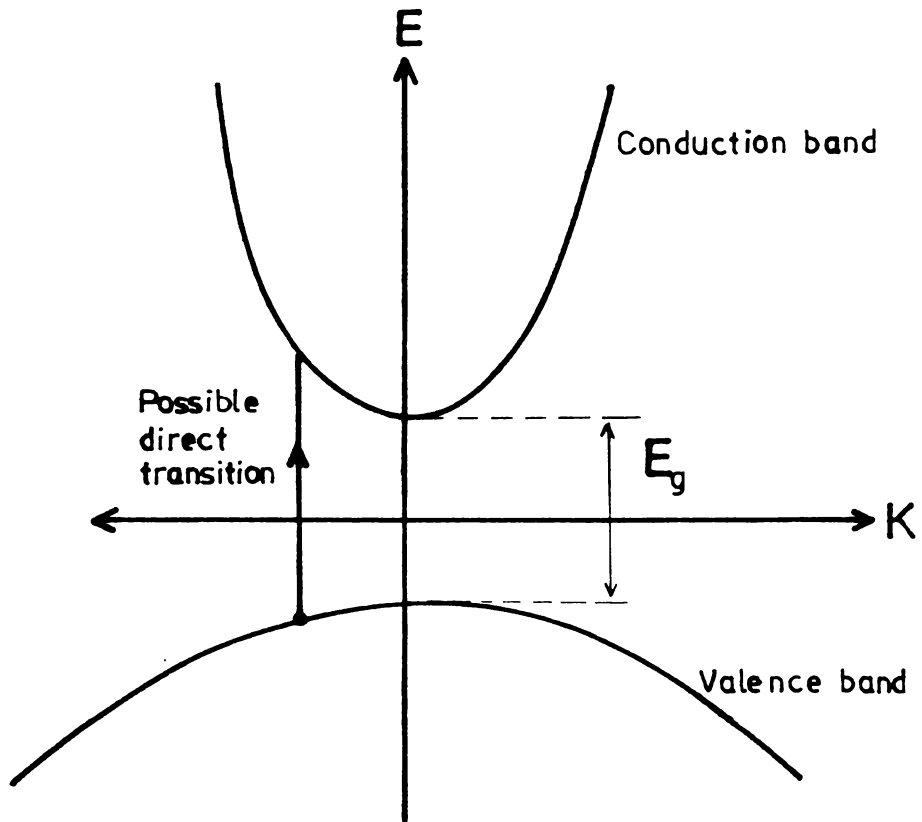


Figure 7. Direct transition from the valence band to the conduction band.

In an absorption process, crystal momentum must be conserved. The momentum of a photon h/λ is very small compared to the crystal momentum h/a , where λ is the wavelength of light and a is the lattice constant. The absorption coefficient $\alpha(h\nu)$ for a given photon energy $h\nu$ is proportional to the probability P_{if} for the transition from the initial state to the final state and to the density of electrons in the initial state n_i and to the density of available final state n_f . This process must be summed for all possible transitions between states separated by an energy difference equal to the photon energy $h\nu$.

$$\alpha(h\nu) = A \sum P_{if} n_i n_f \quad (1.6.11)$$

In the case of absorption transitions between two direct valleys where all the momentum-conserving transitions are allowed, the transition probability P_{if} is independent of photon energy. Every initial state at E_i is associated with a final state at E_f such that

$$E_f = h\nu - |E_i| \quad (1.6.12)$$

But in the case of parabolic bands

$$E_f - E_g = \frac{\hbar^2 K^2}{2m_e^*} \quad (1.6.13)$$

$$\text{and } E_i = \frac{\hbar^2 K^2}{2m_h^*} \quad (1.6.14)$$

Therefore,

$$h\nu - E_g = \frac{\hbar^2 K^2}{2} \left[\frac{1}{m_e^*} + \frac{1}{m_h^*} \right] \quad (1.6.15)$$

The density of state can be given by

$$\begin{aligned} N(h\nu) d(h\nu) &= \frac{8\pi K^2}{(2\pi)^3} dK \\ &= \frac{(2m_r)^{3/2}}{2\pi^2 \hbar^3} (h\nu - E_g)^{1/2} d(h\nu) \quad (1.6.16) \end{aligned}$$

where m_r is the reduced mass given by

$$\frac{1}{m_r} = \frac{1}{m_e^*} + \frac{1}{m_h^*}$$

The absorption coefficient is given by

$$\alpha(h\nu) = A (h\nu - E_g)^{1/2} \quad (1.6.17)$$

where A is a constant.

In some materials, quantum selection rules forbid direct transitions at $K = 0$, but allow them at $K \neq 0$, the transition probability increases proportionately to $h\nu - E_g$. Since the density of states linked in direct transitions is proportional to $(h\nu - E_g)^{1/2}$, the absorption coefficient for the forbidden transition has the spectral dependence

$$\alpha(h\nu) = B (h\nu - E_g)^{3/2} \quad (1.6.18)$$

where B is a constant.

Indirect transition

When a transition requires a change in both energy and momentum, a double transition process is required because the photon cannot provide a change in momentum. This situation can be overcome with the emission or absorption of phonons. Momentum is conserved by a phonon interaction. An indirect transition from the valence band to the conduction band is shown in figure 8. Phonons, the quantum of lattice vibration has a characteristic energy E_p . The minimum frequency for phonon assisted transition is given by

$$h\nu = E_f - E_i + E_p \quad (1.6.19)$$

for emission of a phonon, and

$$h\nu = E_f - E_i - E_p \quad (1.6.20)$$

for absorption of a phonon. In indirect transitions, all the occupied states of the valence band are connected to all the empty states of the conduction band. The density of initial states at an energy E_i is

$$N(E_i) = \frac{1}{2\pi^2 \hbar^3} (2 m_h^*)^{3/2} (E_i)^{1/2} \quad (1.6.21)$$

The density of states at E_f is

$$N(E_f) = \frac{1}{2\pi^2 \hbar^3} (2 m_e^*)^{3/2} (E_f - E_g)^{1/2}$$

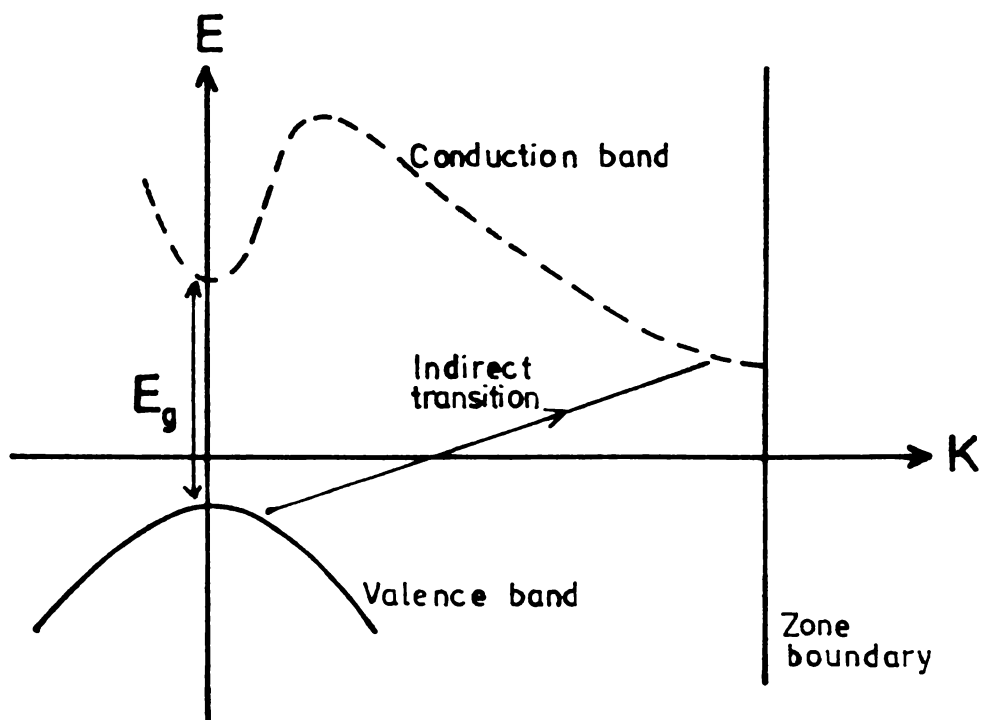


Figure 8. Indirect transitions from the valence band to the conduction band.

using equation (1.6.19)

$$N(E_f) = \frac{1}{2\pi^2 \hbar^3} (2m_e^*)^{3/2} (\hbar\nu - E_g \mp E_p + E_i)^{1/2} \quad (1.6.22)$$

The absorption coefficient is proportional to the product of the densities of initial states and final states integrated over all possible combinations of states separated by $\hbar\nu \mp E_p$; α is also proportional to the probability of interaction with phonons, which is a function $f(N_p)$ of the number N_p of phonons of energy E_p . The number of phonons is given by the Bose - Einstein statistics

$$N_p = \frac{1}{\exp(E_p/k_B T) - 1} \quad (1.6.23)$$

$$\alpha(\hbar\nu) = Af(N_p) \int_0^{(\hbar\nu - E_g \pm E_p)} (E_i)^{1/2} (\hbar\nu - E_g \mp E_p + E_i)^{1/2} dE_i \quad (1.6.24)$$

After simplification, absorption coefficient for a transition with phonon absorption is obtained as

$$\alpha_a = \frac{A(\hbar\nu - E_g + E_p)^2}{\exp(E_p/k_B T) - 1} \quad \text{for } \hbar\nu > E_g - E_p \quad (1.6.25)$$

The probability of phonon emission is proportional to $N_p + 1$. The contribution α_e to the absorption coefficient is given by

$$\alpha_e = \frac{A (h\nu - E_g - E_p)^2}{1 - \exp(-E_p/k_B T)} \quad \text{for } h\nu > E_g + E_p \quad (1.6.26)$$

where A is a slowly varying function of ν .

Since both phonon absorption and phonon emission are possible when $h\nu > E_g + E_p$, the absorption coefficient α_i is given by

$$\begin{aligned} \alpha_i &= \alpha_e + \alpha_a \\ &= \frac{A (h\nu - E_g \pm E_p)^2}{\exp(E_p/k_B T) - 1} \quad \text{for } E_g - E_p < h\nu \leq E_g + E_p \end{aligned} \quad (1.6.27)$$

In the case of indirect forbidden transition, an extra factor $(h\nu - E_g \pm E_p)$ is involved into the expression for α_e and α_a .

Therefore for forbidden transition, absorption coefficient is given by

$$\alpha_{if} = \frac{B (h\nu - E_g \pm E_p)^3}{\exp(E_p/k_B T) - 1} \quad (1.6.28)$$

The plot of $(\alpha h\nu)^2$ versus $h\nu$ for direct allowed transition, $(\alpha h\nu)^{2/3}$ for direct forbidden transition, $(\alpha h\nu)^{1/2}$ for indirect allowed and $(\alpha h\nu)^{1/3}$ for indirect forbidden transition, should always be

straight lines. By extrapolating these lines to $\alpha = 0$, we can obtain the band gap of the material.

Thus a careful and systematic study of optical properties can yield a lot of information regarding the material under study. This include the band gap of the material and the relative position of conduction band and valence band maxima in K-space. The dependence of absorption coefficient on photon energy near a transition can tell whether the transition is forbidden or allowed. The nature of transition can give information about the electronic states from which the transition took place. This will give a picture of the band structure of the semiconductor.

References:

1. A Sommerfeld, Z. Phys., 47 (1928) 1
2. F. Bloch, Z. Phys., 52 (1928) 555
3. A.H. Wilson, Proc. Roy. Soc. A, 133 (1931) 458.
A.H. Wilson, Proc. Roy. Soc. A, 134 (1931) 277.

CHAPTER II

THIN FILM PREPARATION METHODS2.1 INTRODUCTION

Thin films can be prepared by various methods depending upon the type of films required /1-6/. Generally, preparation methods can be broadly classified into two main groups. Chemical methods including electrochemical methods and physical methods. Out of which, physical methods received more attention because they result in the formation of very pure and well defined films. In practice they are applicable to almost all substances and a wide range of thicknesses. Chemical methods depend on a specific chemical reaction yielding the required film where as physical methods depends on the evaporation or ejection of the material by some means from a source.

2.2 CHEMICAL METHODS

Chemical methods are again sub-divided into the following methods:

Electrolytic deposition

In this method the substance to be deposited is present in a solution, in the form of ions. These

ions are attracted towards the cathode, by the applied potential and get deposited. The deposition is governed by the laws of electrolysis. The properties of the film deposited, eg. adhesion to the substrate, its crystal structure, etc., may be influenced by the composition of the electrolyte. By this method, it is possible to deposit only on metallic substrates and the film may be contaminated by the electrolyte.

Electroless deposition

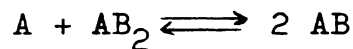
By this method metal films are deposited from a solution without the presence of an external field. The rate of deposition depends on the temperature of the bath and in some cases the deposition need to be stimulated by a catalyst.

Anodic oxidation

This method is used to deposit oxide films over certain metals (eg. Al, Ta, Nb, Ti & Zr). The metal anode dipped in the electrolyte attracts oxygen ions, by the influence of the applied electric field and get oxidized. The growth rate of the oxide layer depends on the current density and the temperature of the bath. For anodic oxidation it is possible to use either constant current or constant voltage method. By this method it is not possible to deposit a film of selected thickness.

Chemical vapour deposition

This method is widely used for the preparation of the monocrystalline films of high purity. If the material is deposited on substrate of the same material (eg. Si upon Si), the process is called homoepitaxy. When deposited on different substrate material, the process is called heteroepitaxy. Several type of chemical reactions are available, to carry out such deposition. One of them is the decomposition at high temperature, which is known as pyrolysis, another is decomposition caused by ultra violet or infrared light, which is called photolysis, of gaseous compounds. This may be represented as



where AB is a gaseous compound and A the substance which is desired to deposit.

Liquid phase epitaxy

This method of depositing semiconducting epitaxial films based on crystallization of semiconducting material dissolved in a suitable metal of low melting point (eg. Sn, In, Pb, Bi, Ga, etc.). A saturated solution at high temperature (1000°C) is prepared and then gradually cooled. The solution becomes super saturated and a crystalline phase begins to grow over the given substrate. The solution is then removed by chemical or mechanical means from the substrate.

Blodgett and Langmuir method

Fatty acids or higher alcohols are dissolved in a volatile solvent and one drop of the solution sprinkled on the surface of water. The molecules of the substance diffuse over the surface of water and the solvent evaporates. This film can be lifted up by the substrates. Films of different orientations can be prepared by changing the dipping angle of substrates.

2.3 PHYSICAL METHODS

Among the physical methods, the most important methods of preparation of thin films are the sputtering and vacuum evaporation. Both methods requires low pressure in the working space and hence a vacuum system is needed.

2.3.1 SPUTTERING

The surface atoms can be ejected from the surface of a material by the bombardment of energetic particles. The liberated components condense on surrounding area and consequently on the substrates placed. This process of preparation of thin films are called sputtering. There are various types of sputtering depending upon the method used to eject the atoms or molecules.

Glow discharge sputtering

In this method an electric field is applied between two electrodes in a gas at low pressure. The material to be deposited is used as the cathode and the substrates were placed on the anode. The factors influencing this technique are the pressure inside the system, current density, applied potential and the cathode area.

Bias sputtering

In this case the substrates are biased with a negative potential with respect to anode so that it is subjected to an ion-bombardment throughout the growth. This effectively cleans the substrate surface resulting films with good adhesion to the substrates.

Triode sputtering

In this case electrons are injected into the discharge by thermionically emitted from a filament. The total ionization and the ionization efficiency are increased by accelerating these electrons. A significant advantage of this system is the fine control of current density and hence the sputtering rate.

Assymmetric AC sputtering

An assymmetric AC supply is used for this purpose.

In the first half-cycle the substrate is charged positively and is bombarded by sputtering particles and molecules of the working gas. During the second half-cycle, the substrate is negatively charged and is bombarded by ions from the discharge cloud. These ions now have a lower energy because the amplitude of the voltage is smaller in the second half-cycle. Since the binding energy of impurities on the surface is usually lower than the binding energy of sputtered material, the bombardment removes these impurities and the sputtered particles are deposited during the subsequent half-cycle on a cleaned surface.

Ion-beam sputtering

By this method films can be prepared at pressures below 10^{-3} Torr. Ions are produced in a high pressure chamber and they are extracted to the differentially pumped vacuum chamber through suitable aperture.

R.F. sputtering

In this case ionization of the gas was produced by an R.F. field of several mega cycles. It can be used to sputter films directly from insulators and also possible to sputter at lower pressures.

Reactive sputtering

Films of oxides, nitrides, etc. of metals can be

prepared by introducing the reactive gas alongwith the inert sputtering gas into the sputtering system.

EVAPORATION

Vacuum evaporation is the widely used method of preparation of thin films. This method is comparatively simple and films of extreme purity can be prepared with proper experimental conditions.

The process of film formation consists of several physical stages.

- (1) Transformation of the material to be deposited into gaseous state.
- (2) Transfer of those atoms or molecules from source to the substrate.
- (3) Deposition of these particles on the substrate.
- (4) The rearrangement of these particles on the substrate surface.

It is a well known fact that atoms or molecules are liberated from a material by heating. Liquid to vapour transformation is called evaporation and solid to vapour transformation is called sublimation, during heating.

Resistive heating

Various methods are used to evaporate the materials in vacuum. Out of which the resistive heating is the most simple one. In this method a high current is passed through a refractory metal (eg. W, Mo, Ta, etc.) which is made in the form of a boat or filament, as required. The material, to be evaporated may be heated directly or indirectly. Direct heating means that the heating material will act as the supporting material for the evaporant. Indirect heating means that the material to be evaporated are supported by crucibles made of glass, quartz, alumina, etc. and they are heated with the heater windings.

Flash evaporation

Flash evaporation is a method used for rapid evaporation of a multicomponent alloy or compound. This is done by continuously dropping fine particles of the material on to a very hot surface. The powder may be fed to the hot surface by agitating the feed chute mechanically, ultrasonically or electronically.

Laser evaporation

A laser beam can be used to heat and vaporize the materials. The laser source can be placed outside

the vacuum system and the laser beam can be focussed onto the surface of the material, to be evaporated. The evaporation takes place from the surface only, because the laser penetration depth is small.

Electron beam evaporation

Vaporization of the material is caused by the electron bombardment. A stream of electrons are accelerated by a positive potential and focussed onto the material to be evaporated. The material absorb the energy of the electrons and will get vaporized. This method is capable of evaporating any material.

RF heating

RF or induction heating can be used to the material for evaporation, by suitably arranging the RF coils.

Arc evaporation

Very high temperature can be generated to evaporate refractory materials by striking an arc between two electrodes.

Molecular beam epitaxy

This is used for the epitaxial growth of films on single crystal substrates by slowly evaporating the

constituent elements of the film from Knudsen effusion cells onto substrates held at appropriate temperatures needed for chemical reaction, epitaxy and reevaporation of excess constituents. Epitaxial films of compound semiconductors are prepared by this method.

2.4 REACTIVE EVAPORATION

Reactive evaporation is a variant of Günthers Three Temperature Method /7/; which is based on the principle that for many binary system it has been found that a stoichiometric interval exists with a limited degree of freedom in selecting the individual components and substrate temperatures for the formation of a particular compound film.

The condensation flux N_k of a given vapour on a given substrate exceed zero only if the ratio P/P_e exceeds a critical value q_c , where P is the actual pressure and P_e the equilibrium vapour pressure.

$$\text{ie. } N_k > 0 \text{ if } (P/P_e) > q_c \quad (2.4.1)$$

At a given substrate temperature, the condition for progressive condensation can be represented in terms of incident flux as

$$N_k = 0 \text{ if } N_+ \leq N_{+c} (T) \quad (2.4.2)$$

$$N_k > 0 \text{ if } N_+ > N_{+c} (T) \quad (2.4.3)$$

where N_+ is the incident flux and N_{+c} is the critical value of the incident flux. If the incident flux exceeds the critical value, the condensation rises rapidly and approaches its maximum value given by

$$N_k \text{ max} = \alpha (N_+ - N_e) \quad (2.4.4)$$

where N_e is the reevaporation flux from the substrate surface and α the condensation coefficient..

Figure 1 shows the schematic representation of the state of affairs described above and may be represented in terms of critical temperature T_c , assuming a constant incident flux N_+

$$N_k = 0 \text{ if } T \geq T_c (N_+) \quad (2.4.5)$$

$$N_k > 0 \text{ if } T < T_c (N_+) \quad (2.4.6)$$

Thus by analogy with figure 1, the condensation can be represented as a function of substrate temperature as in figure 2, ie., below a critical temperature T_c the condensation starts spontaneously and quickly approaches a maximum.

Suppose the vapour phase consists of two components A and B, both being incident on the substrate under

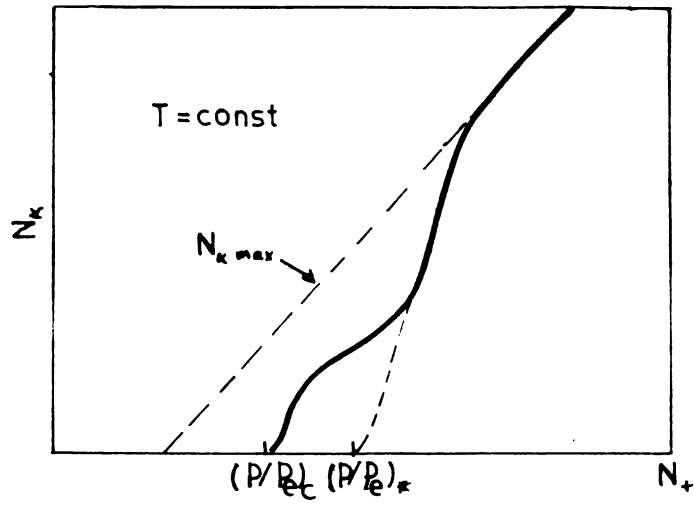


Figure 1. Variation of condensation flux N_k with the incident flux N_+ of the particles.

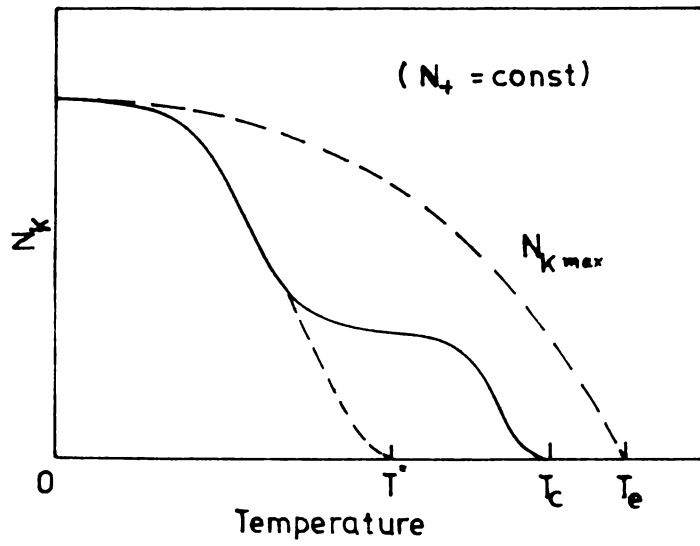


Figure 2. Variation of condensation flux N_k with substrate temperature T .

consideration. If the vapour density is low enough, we may neglect the collisions between particles of the components A and B in the vapour phase. However, interaction can take place between such particles within the adsorbed stage on the substrate surface. These interactions may lead to the formation of molecules.



where AB stands for all possible compounds $A_n B_m$. A rough estimate of the interaction probability on the surface gives a density

$$n_{AB} = \text{const. } n_A n_B \bar{D} \quad (2.4.8)$$

where n_A and n_B are the number of adsorbed atoms A and B and \bar{D} the mean diffusion coefficient. This is only a rough calculation because we are not considering the energies of the particles. We know that only if the particles collide with sufficient energy they will react to form the compound molecule. Since the number of adsorbed atoms is proportional to the actual vapour pressure P , or the incident flux N_+ of the particular vapour, the density n_{AB} should also be proportional to the product of incident flux ($N_{+A} N_{+B}$) or vapour pressure ($P_A P_B$).

In order to estimate the critical values which now apply, the equilibrium pressures P_{eA} , P_{eB} of the components and the value P_{eAB} of the compound must be considered. P_{eAB} usually corresponds to the dissociation pressure of the compound, and is equivalent to the pressure of the more volatile component (say, A) in equilibrium with the compound. Thus, the critical values of one component A in the presence of the other component B should vary as follows:

$$N_{+cA} (B) \ll N_{+cA} \quad (2.4.9)$$

$$T_{cA} (B) > T_{cA} \quad (2.4.10)$$

This means that at a given substrate temperature, it will be possible to condense A, in combination with B at a lower critical flux. Or in other words, it means that a higher substrate temperature may be used to deposit A in combination with B for a given flux of A.

At a given substrate temperature T and for incident flux $N_{+B} < N_{+cB}$, no condensation of any kind is possible while the incident rate N_{+A} is low. However, at a critical value $N_{+cA} (B)$, sufficient molecules AB are formed on the substrate, and nucleation and progressive condensation of the compound AB starts. This critical value itself depends on the incident flux of the

component B. With further increase of flux N_{+A} , no increase of condensation flux N_k is possible until, with $N_{+A} > N_{+cA}$, condensation of unreacted A takes place. Figure 3 shows the condensation diagram for two incident components A and B at a given substrate temperature.

The advantages of reactive evaporation can be summarised as follows:

- (1) There is no need to go through tedious and sometimes expensive metallurgical processes to prepare material in bulk before evaporation.
- (2) High temperatures ($> 2000^{\circ}\text{C}$) are frequently needed to evaporate high melting point carbides, nitrides and oxides. If resistive heaters are used, the film will get contaminated because of the evaporation of the heater material. High evaporation rates are also not possible which are essential in industrial processes. Reactive evaporation overcomes these difficulties because almost all metals evaporates with sufficient vapour pressure below 1500°C .
- (3) The stoichiometry can be adjusted by simply varying the individual evaporation rates and thus the charge carrier concentration and the type of conductivity of the compound can be controlled.

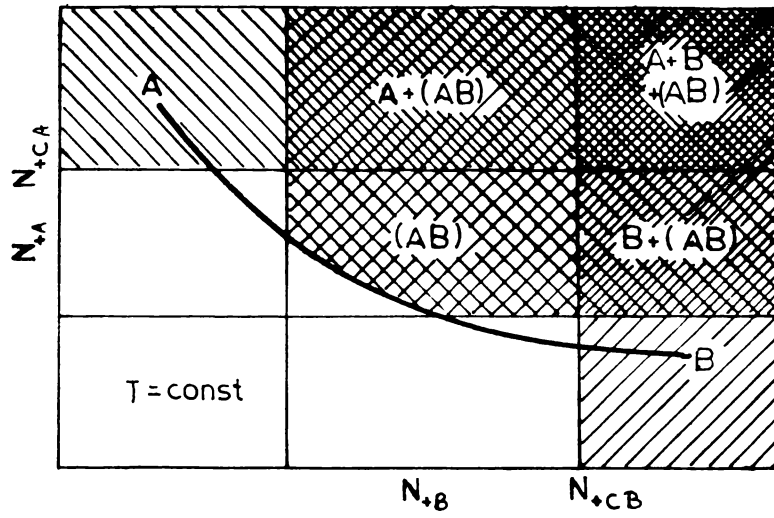


Figure 3. Condensation diagram for two incident components A and B.

- (4) Due to the wide disparity in vapour pressure between their constituent elements, thin films of many semiconducting compounds (eg. III-V compounds) cannot readily be prepared by the standard evaporation technique. This reactive evaporation overcomes this dissociation problem.
- (5) Amorphous films can be prepared by this method, since the lowest substrate temperature is dictated by the condensation temperature of the more volatile component and is usually low (eg. O_2 , S_2 , and Se).
- (6) Film growth can be started and stopped abruptly and hence abrupt interfaces are possible.
- (7) Deposits can be directly introduced in their elemental form and the doping level can be easily controlled.

This technique has been successfully employed for the preparation of many compound films such as Sb_2S_3 /8/, SnS_2 /9/, CuS /10/, $SnTe$ /11/, etc. Eventhough this technique has been so successfully used in the case of many technologically important compounds, it suffers from the following drawbacks which arise from the low chemical reactivity of the particles used for the film formation.

The use of large volatile flux and consequent wastage of the volatile element is a main drawback. When high deposition

rates are needed, large volatile flux leads to high volatile partial pressure (10^{-4} to 10^{-2} Torr) which reduces the mean free path and also scatters the non-volatile beam away from the substrate surface. Also the high pressure in the chamber reduces the evaporation rate of the non-volatile component.

2.5 ACTIVATED REACTIVE EVAPORATION

In the case of certain components, the reaction rate of elements to form their compound may be very low. The reaction rate may be increased in two ways. The first method is by increasing the translational energy of the particles so that they can overcome the potential barrier. The second method is by lowering the potential barrier itself, so that particles with very low energy can react together.

The translational energy of the particle can be increased by the temperature of the substrate where the reaction takes place. The substrate temperature cannot be increased beyond a certain range as this may increase the dissociation of the compound thus formed. Also the film formed may reevaporate from the substrate surface. Another way to increase the translational energy of particles is by increasing the source temperature. But, if the source

temperature is increased very much, the evaporation rate will also increase. The evaporation rate must be controlled in reactive evaporation. Hence the most versatile method of increasing kinetic energy of the particles is by ionizing the particles with suitable radiations or electron beams and accelerating them in electric fields.

The first method which used some of these techniques to increase the chemical reaction rate is the activated reactive evaporation (ARE) /12/ of Bunshah and Raghuram. Schematic diagram of the original experimental set-up is shown in figure 4. They used an electric field to activate the reactive gas, by using a low voltage probe. The probe was positively biased around 100V. The secondary electrons from the molten pool of the metal are attracted to this probe. These electrons ionize the reactive gas atoms generating a thick plasma. Due to the presence of this plasma, the chemical reaction rate is very much increased. Bunshah and Raghuram deposited TiC at a rate of $12 \mu\text{m}^{-1}$ at a source distance of 15 cm using this technique. It may be noted that Ti and the reactive gas, acetylene do not react together to form the compound TiC, in ordinary reactive evaporation.

In ARE the ions are not accelerated to the substrate and this is because, usually ions are positively

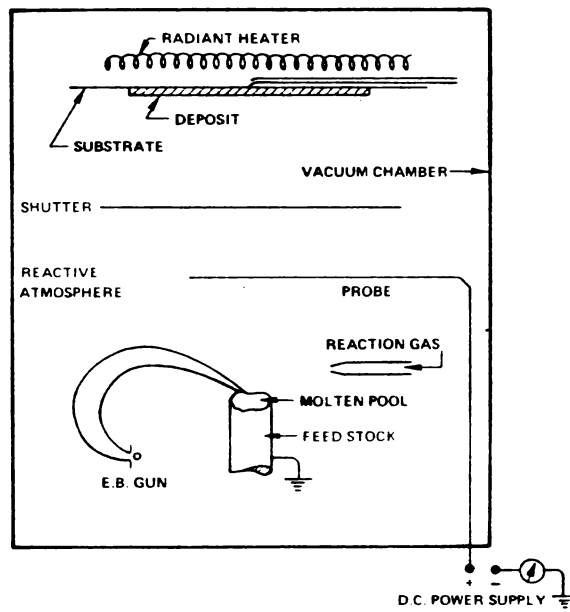


Figure 4. Schematic of the experimental arrangement for the activated reactive evaporation process.

charged and will be attracted only to the negatively charged pool of the metal which is in a direction opposite to that of the substrate. Also the applied electric field is confined to a small region above the source of the secondary electrons and ionization of the atoms predominantly takes place beyond this field. So the only increase in translational energy of the atom is from collisions with electrons. It can be shown that this energy is very low, and hence cannot be the cause for the large increase in chemical reaction rate in ARE.

In ordinary reactive evaporation the particles are not ionized and they have to collide with sufficient translational energy to overcome the potential barrier. But when one of the particles is ionized the activation energy for chemical reaction becomes very low or equal to zero. This is because of the inverse fifth power attractive force arising from point charge-induced dipole interaction between the ion and the molecule [13]. This increases the chemical reaction tremendously and hence the high deposition rate. Though chemical reaction rate is very much increased, there is still the problem of amorphous areas and unreacted elements getting entrapped in the growing film. This can be eliminated by choosing the substrate temperature during deposition. By

favourably choosing the substrate temperature, it is possible to reevaporate the amorphous areas and the unreacted species from the substrate surface, and hence good quality films are obtained. It is also found that if the ratio $T/T_b \approx 0.33$, films with optimum properties are obtained /14-16/, where T the substrate temperature and T_b the normal boiling point of the compound. This particular substrate temperature will also increase the diffusion into the reevaporated areas and microhole free films can be obtained. If, still higher substrate temperature is chosen, the crystalline areas of the film will also reevaporate, resulting in films with poor quality.

High substrate temperature is not practicable in all cases. Another method which gives all these beneficial effects is by giving additional kinetic energy to the ionized particles. This can be obtained by accelerating the ionized particles to the substrate by using an accelerating field. Such a method is known by various names like Biased Activated Reactive Evaporation (BARE) /17/ or Reactive Ion Plating (RIP) /18/. In this method substrate is kept at a high negative potential, around 3 KV, and the ions are accelerated towards the substrate.

REFERENCES:

1. K.L. Chopra, "Thin Film Phenomena", McGraw-Hill, New York, 1969, p.10.
2. L. Holland, "Vacuum Deposition of Thin Films", John Wiley, New York, 1961.
3. R.W. Berry, P.M. Hall and M.T. Harris, "Thin Film Technology", Van Nostrand Reinhold, New York, 1968.
4. R. Glang, in "Handbook of Thin Film Technology", L.I. Maissel and R. Gland (Eds.), McGraw-Hill, New York, 1970, p.1-3.
5. D.C. Campbell, "Use of Thin Films in Physical Investigations", J.C. Anderson (Ed.), Academic Press, London, 1966, p.11.
6. D.S. Campbell, "Physics of Nonmetallic Thin Films", C.H.S. Dupuy and A. Cachard (Eds.), Plenum Press, New York, 1976, p.9.
7. K.G. Günther, "The Use of Thin Films in Physical Investigations", J.C. Anderson (Ed.), Academic Press, London, 1966, p.213.
8. J. George and M.K. Radhakrishnan, Solid State Commun., 33 (1980) 987.
9. J. George and K.S. Joseph, J. Phys. D: Applied Physics, 15 (1982) 1109.

10. J. George and K.S. Joseph, *J. Phys. Chem. Solids*, 45 (1984) 341.
11. J. George and T.I. Palson, *Thin Solid Films*, 127(1985)233.
12. R.F. Bunshah and A.C. Raghuram, *J. Vac. Sci. Tech.* 9 (1972) 1389.
13. E.W. McDaniel, "Collision Phenomina in Ionized Gases", Sect. 3-6 and 6-3, Appendix II, Wiley, New York, 1964.
14. P.S. Vincett, W.A. Barlow, and G.G. Roberts, *J. Appl. Phys.*, 48 (1977) 3800.
15. P.S. Vincett, Z.D. Popovic, and L. McIntyre, *Thin Solid Films*, 82 (1981) 357.
16. P.S. Vincett, *Thin Solid Films*, 100 (1983) 371.
17. R.F. Bunshah, *Physical Vapour Deposition of Metals, Alloys and Compounds, New Trends in Materials Processing*, American Society for Metals, Metals Park, OH, 1976, p.200.
18. M. Kobayashi and Y. Doi, *Thin Solid Films*, 54 (1978) 67.

CHAPTER III

EXPERIMENTAL TECHNIQUES3.1 MEASUREMENT OF ELECTRICAL CONDUCTIVITY

The electrical conductivity of a semiconductor depends on the number of charge carriers available for conduction and the mobility of the charge carriers. All semiconductors may be considered as insulators at absolute zero. As the temperature is increased from absolute zero, the electrons in the closest defect level get excited to the conduction band and contribute to the conduction. If the temperature is further increased, the electrons from the next defect levels are excited and this process continues until all the defect levels are exhausted. If the defect levels are very close to the conduction band (very close to valence band in the case of holes), the conductivity may decrease with further increase of temperature due to the decrease in mobility of the charge carriers. After a short range the excitation of electrons from the valence band to conduction band may take place, and hence increase in conductivity and is known

as intrinsic region. In this region the activation energy required to excite the electron from valence band to conduction band must be equal to the band gap of the material.

Hence, the study of the conductivity with the variation of temperature can yield the informations regarding the defect levels as well as the band gap. The band gap can be determined from the slope of the $\ln \sigma$ Vs $1/T$ curve, where σ is the conductivity of the material and T the absolute temperature. Generally the intrinsic conduction sets in only at high temperatures. At such a high temperature the material may get melted.

It is not very easy to measure the conductivity of highly insulating films, since the measuring current is very low ($\sim 10^{-15}$ A). Good quality electrometer must be used in its maximum sensitivity range, to measure such a small current. The measurement must be performed in vacuum. Otherwise the humidity present in the atmosphere may short circuit the specimen and gives a higher value of conductivity. For this purpose an all metal cell was used, which is shown in figure 1. Cell can be evacuated to better than 10^{-2} Torr. A well smoothed DC supply was used for the heater, which maintained the sample at various temperatures. One end of the power supply was

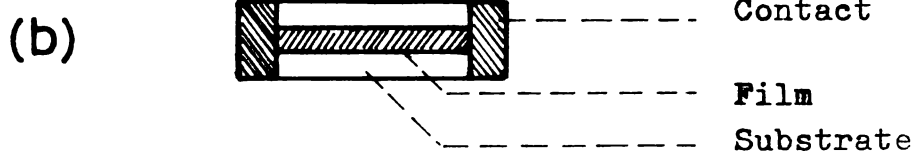
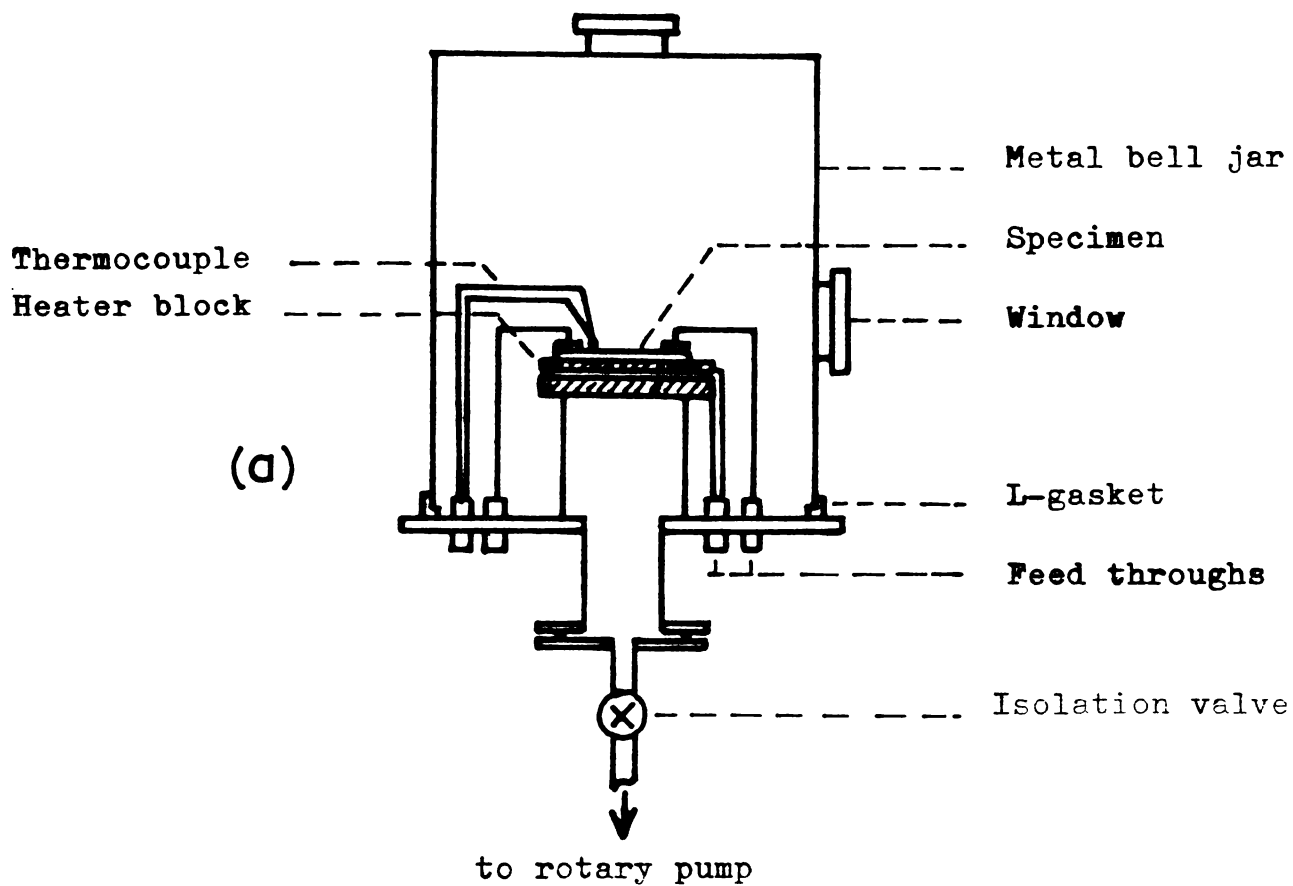


Figure 1(a). Measuring all for high resistance specimen.

(b). Typical specimen geometry.

earthed to eliminate the ripples, if present, which might induce large current through the specimen, masking the required signal. The measuring cell and heater block were also earthed to avoid electrical disturbances. A fine wire chromel-alumel thermocouple was used to measure the temperature of the specimen.

The metal contacts to the specimen to measure the conductivity must be ohmic in character. All the electrical insulations inside the chamber were done with teflon. The substrate was also so chosen that its resistance must be at least hundred times higher than the specimen, otherwise the substrate itself might short circuit the specimen leading to false results. The circuit used for measuring conductivity is shown in figure 2.

A well smoothed, regulated power supply, which can vary from 0 to 200 V was used for this measurement. Hewlett Packard 3465 A model digital multimeter was used to measure the voltage. The voltage shown in this meter was taken as the potential across the specimen, since the voltage drop across the electrometer was negligible. EA 815 model electrometer of ECIL was used to measure the current through the specimen.

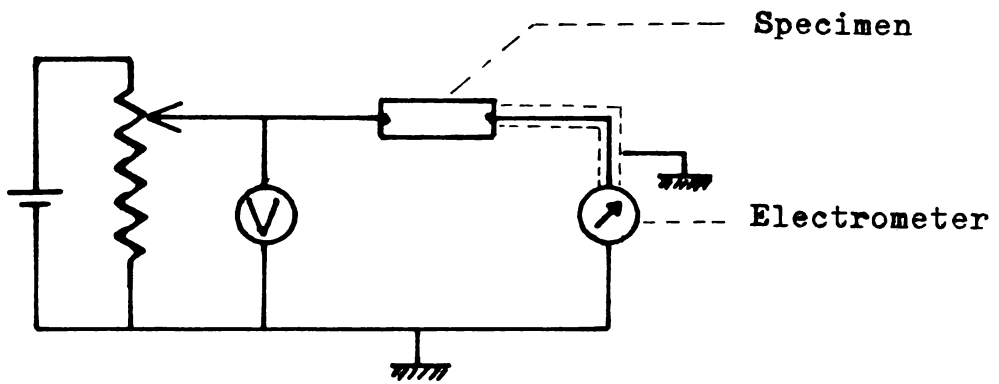


Figure 2. Circuit diagram for the measurement of conductivity.

3.2 MEASUREMENT OF HALL VOLTAGE

The carrier concentration and carrier mobility can be determined by the measurement of Hall voltage and conductivity. Conventional DC method is applicable only if the carrier mobility is greater than few $\text{cm}^2/\text{Volt Sec.}$, below which single or double AC method is to be used. This is because of the inverse proportionality of the Hall voltage and the carrier concentration. If the conductivity is very low, it is very difficult to send an appreciable amount of current through the specimen, so as to get a reasonable Hall voltage, without Joule heating. With the decrease of conductivity, noise may increase masking the required signal.

The circuit diagram used for the Hall effect measurements is shown in figure 3. The current through the specimen was maintained below 10 mA. The Hall voltage (V_H) developed across the film with the applied magnetic field was measured by a Hewlett Packard 3465 A digital multimeter which has a resolution of 1 μV . A Keithley 195 digital multimeter was used to measure the voltage applied to the specimen. The Hall voltage was measured by reversing the direction of current and magnetic field and the mean value was taken for further calculations.

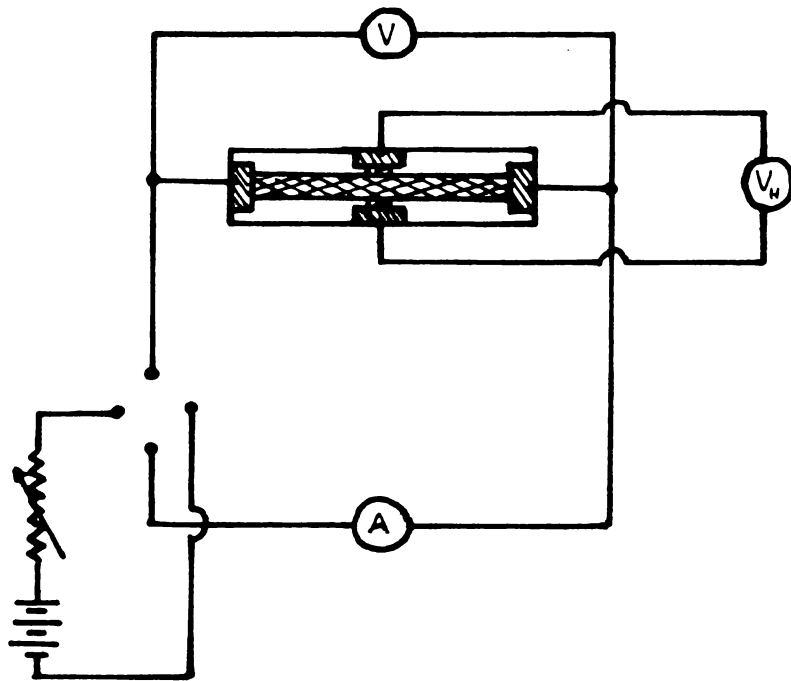


Figure 3. Circuit diagram for the measurement of Hall voltage.

The thermocouple output was read by a $3\frac{1}{2}$ digit, 200 mV digital panel meter (DPM). The cross section of the measuring cell is shown in figure 4, which is made of copper. Cell has got provision for cooling the sample down to liquid nitrogen temperature and heating to higher temperatures, and it is fully described in /1/. Measurements were carried out in a vacuum better than 10^{-2} Torr.

For this measurement a stabilized electromagnet has been designed and fabricated. The magnetic field can be varied from 0 to 0.5 Tesla. The magnetic field can be used both in AC and DC, since the core is laminated.

The magnet was constructed from transformer laminations stacked together, using the geometry show in figure 5. The stacked laminations were fixed using wooden frame. Here the pole separation is 2 cm and the central core area is 7.8 x 6.5 cms. No.14 gauge wire was used for the field coils. The maximum field obtainable is 0.3 Tesla for continuous operation and 0.5 Tesla for intermittent operation with forced air cooling.

The schematic diagram of the circuit used for the stabilization of the magnetic field /2/ is shown in figure 6. A standard resistance R_s is put in series with

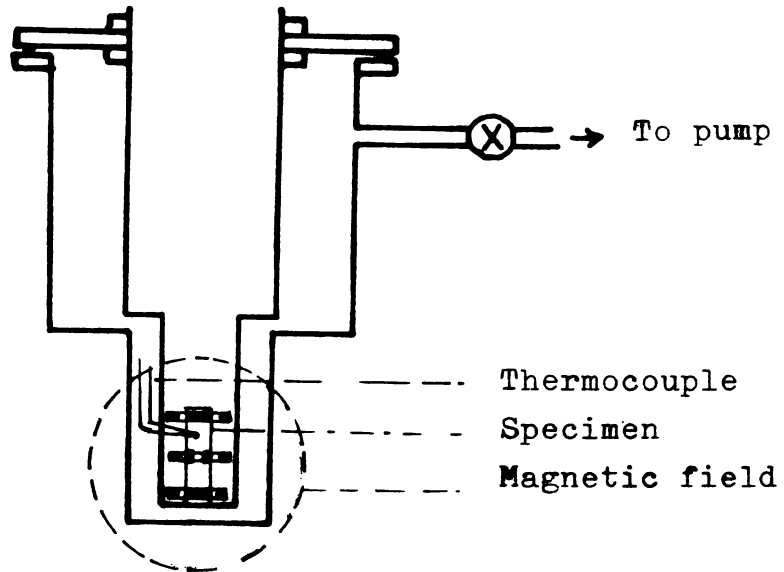


Figure 4. Cross section of the Hall effect measuring cell.

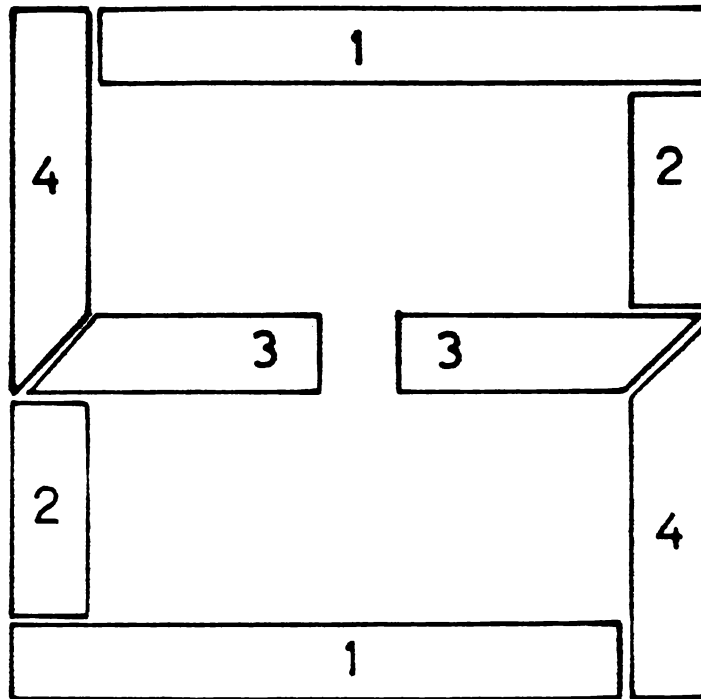


Figure 5. Geometry of the core lamination.

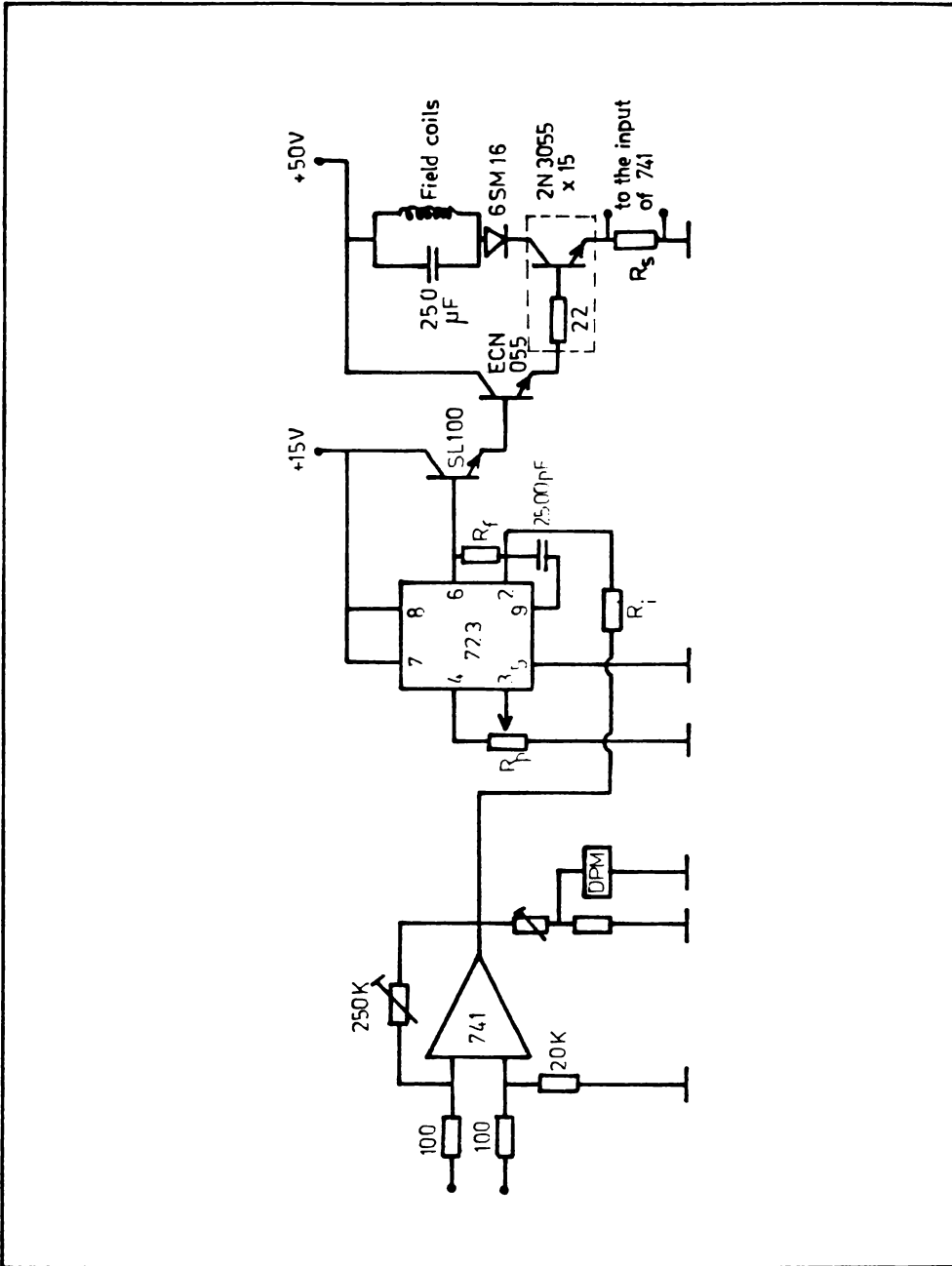


Figure 6. Schematic diagram of the stabilization circuit.

the field coils to sense the current flowing through it. The voltage developed across R_s is amplified by the differential amplifier (741 C) whose amplification is adjusted by the potentiometer in the feed back circuit such that at the maximum field the IC develops an output of 7V. Feed-back controlling is achieved by the use of the 723 voltage regulator IC. The field is set by the potentiometer R_p . The output of 723 is fed to a group of transistors connected with Darlington pair configuration. The amplification of 723 is limited to 100 by the resistors R_f and R_i to give stability to the system. Diode 6 SM 16 is put to prevent damage of the output transistors due to the back e.m.f. The magnetic field is displayed directly in Tesla by a $3\frac{1}{2}$ digit DPM suitably calibrated and connected at the output of the differential amplifier. The magnet has a field stability of 0.1% against 25% line voltage fluctuation.

3.3 MEASUREMENT OF THERMOELECTRIC POWER

Thermoelectric power measurements can be used to measure the effective mass of the charge carrier. It also enables us to determine the type of the charge carriers. Hall effect can also be used for determining the type of the charge carriers. But it is a rather difficult method,

because it requires a good deal of sample preparation and it is not applicable if the sample is highly insulating.

The technique used to determine the type of the charge carriers is known as the hot probe method. One probe of the microvoltmeter is heated with a soldering iron for a few minutes and both the probes are made to touch the sample and the deflection of the meter is observed. If the hot probe shows a positive deflection with respect to the cold probe, the sample is n-type and if the voltage is negative the sample is p-type.

For the measurement of thermoelectric power an all metal cell was used, which can be evacuated to better than 10^{-2} Torr. The cell is provided with a cold finger, which is used to cool one end of the sample down to liquid nitrogen temperature. The other end is provided with a micro heater to heat that end of the sample to the required temperature. A stainless steel plate is used to mount the specimen, since it has got relatively low thermal conductivity. The temperatures at both the ends and the middle of the sample were measured by using fine wire chromel-alumel thermocouples, and were read by 4½ digit, 200 mV DPM. The voltage developed across the sample was read by a digital multimeter, through suitable contacts made

to the ends of the sample. All electrical insulations inside the cell are done with teflon and the microheater was fed with a well smoothed DC supply. The cross section of the measuring cell is shown in figure 7.

3.4 X-RAY DIFFRACTION

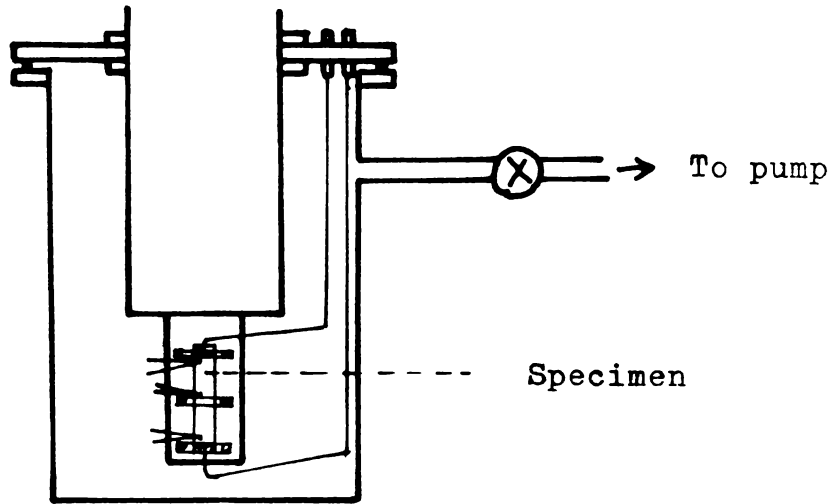
It is necessary to identify the compound films prepared by reactive evaporation. X-ray diffraction study which is a non-destructive technique was used to identify the compound and its structure. For this, the films must have a thickness $\geq 2000 \text{ \AA}$. Electron diffraction is also used for the identification of the material. It can be used for very thin films but the film has to be detached from the substrate.

The basic principle used in the x-ray diffraction is Bragg's law, which is

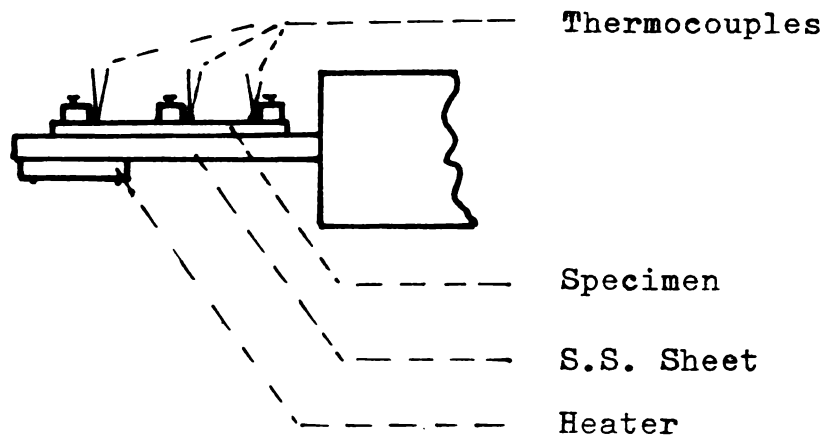
$$2 d \sin \theta = n \lambda \quad (3.4.1)$$

where d is the lattice spacing, θ the incident angle of the x-ray beam, n is an integer and λ the wavelength of the incident radiation.

Usually in x-ray diffractometers the x-ray source, specimen and the detector are so arranged to obey the Bragg's law. The specimen and the detector are rotated



(a)



(b)

Figure 7(a). Sectional view of the thermoelectric power measuring cell.

(b). Side view of the sample mount.

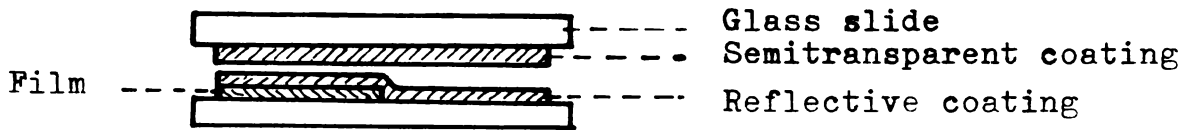
with an angular velocity ω and 2ω respectively to get various planes of diffraction. If thin films are used, the effective thickness of the films to the incident radiation varies as $t/\sin \theta$, where t is the thickness of the film and θ , the incident angle of the x-ray beam. And hence the diffracted intensity will also be a function of incident angle and this will not agree with the powder diffraction file (PDF), for comparison of intensities. X-ray diffraction can yield very good results if proper care is taken.

A Philips PW 1140/90 x-ray unit fitted with Philips PW 1050/70 goniometer was used for these studies. The detector was a proportional counter connected with a pulse height analyser. Filtered $\text{CuK}\alpha$ radiation was used. The accelerating potential applied to the x-ray tube was ≈ 30 KV and the tube current ≈ 16 mA depending on the specimens. The specimens were prepared on $4 \text{ cm} \times 2.5 \text{ cm}$ glass substrates with thickness greater than 2000 \AA and were scanned from $\theta = 10^\circ$ to 30° . The intensity of the diffracted radiation against 2θ was recorded by a recorder running in synchronization with the goniometer.

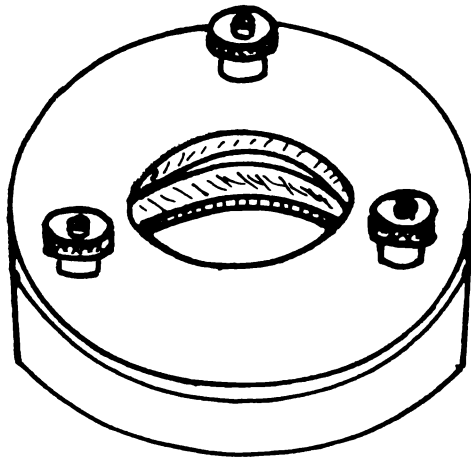
3.5 THIN FILM THICKNESS MEASUREMENTS

Multiple beam interferometry /3/ is a direct method of measuring the thickness of thin films. For measuring the thickness, half the portion of the film was etched down to the substrate along a straight line or masked during deposition. Then a highly reflecting film (eg. aluminium or silver) was deposited over the film and the bare substrate. Another semisilvered glass plate was then placed over this film, with the surface of both the films in contact (figure 8a). This assembly was clamped on a specially made jig, which has got three tilt adjustment screws as shown in figure 8b.

The interferometer setup is shown in figure 9. When the interferometer is illuminated with a parallel beam of monochromatic light, dark fringes in bright background with a step at the film boundary is observed. The three screws of the jig are adjusted to get equally spaced fringes perpendicular to the film step. The fringes show a displacement as they pass over the step. The spacing between the adjacent fringes corresponds to $\lambda/2$, where λ is the wave length of the monochromatic radiation used. Then the thickness of the film can be determined from the fringe displacement. The film thickness t is given by



(a)



(b)

Figure 8(a). Cross section of the film arrangement for the multiple beam interferometry.

(b). Jig for multiple beam interferometry.

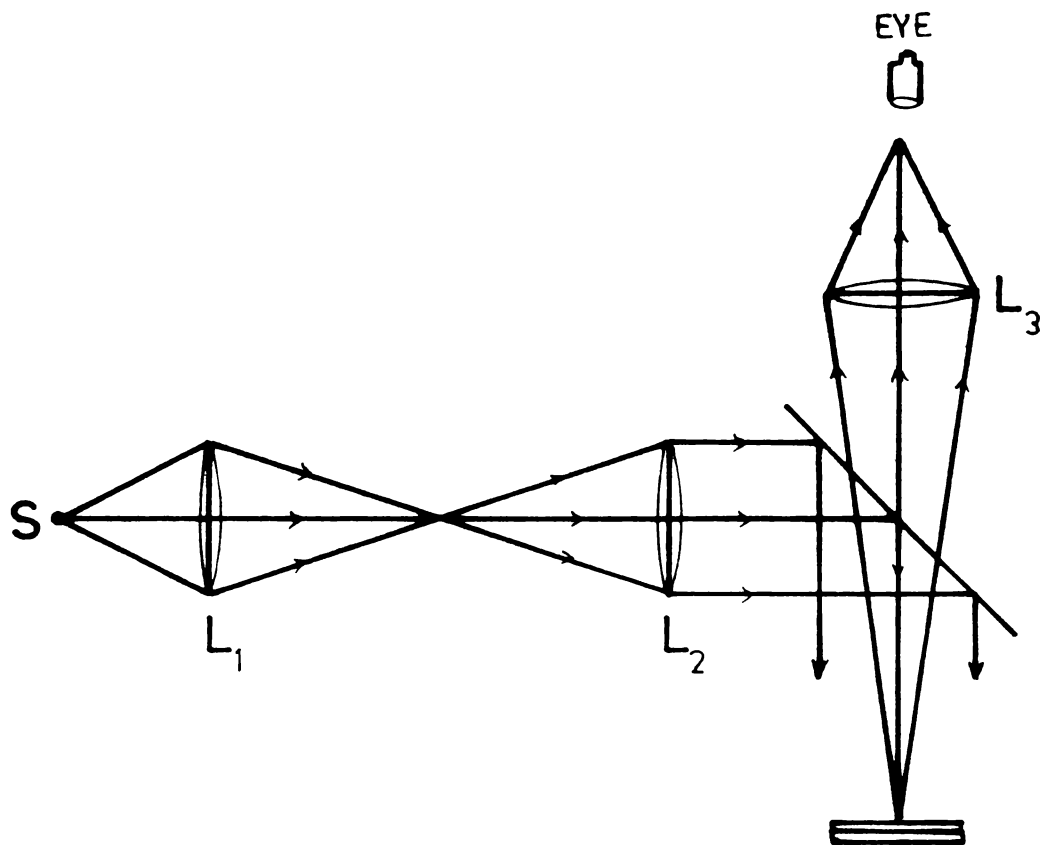


Figure 9. Set-up for multiple beam interferometry.

$$t = \frac{d}{D} \frac{\lambda}{2} \quad (3.5.1)$$

where d is the displacement and D the fringe spacing.

For getting sharp fringes it is necessary to coat the film and the bare substrate with highly reflecting material. The thickness of the reflective coating must be uniform, and the semisilvered plate must be as close as possible. The divergence of the incident parallel beam must be less than 3° . The incidence must be normal.

By carefully following the above conditions, narrow, well spaced fringes are produced and the thickness of the films are measured with an accuracy of $\pm 20 \text{ \AA}$.

3.6 DETERMINATION OF OPTICAL CONSTANTS OF THIN FILMS

From the point of view of applied research, the measurement of optical constants; refractive index n and extinction coefficient k of solids has got certain importance. Valuable informations regarding the structure and bonding of a solid can be obtained from the study of these quantities as a function of wave length. Also, n and k are the most important quantities in the optoelectronic applications of solids.

Spectroscopic ellipsometry, simultaneous measurement of transmission or reflection only are the usual

methods used to measure these quantities as a function of wavelength. Spectroscopic ellipsometry, which is the most precise technique, is applicable only in the regions of wavelength where polarizers and analyzers are available. It also requires lengthy mathematical calculations. One advantage of this method is the material need not be transparent to the radiation used. The simultaneous measurement of transmission and reflection is useful in any region of wavelength, if suitable light sources and detectors are available and also if the material is fairly transparent. In the highly absorbing regions of the spectra of a material, reflectivity measurements is the only available method.

A simple method to determine n , k and α , the absorption coefficient is given by Manifacier et. al. /4/. This method eliminates the tedious mathematical calculations and it can be easily performed with commercially available UV, Vis, NIR and IR spectrophotometers. Only the measurement of transmission through a parallel faced film in the region of transparency is sufficient to determine the real and imaginary part of the complex refractive index.

Figure 10 shows a film with complex refractive index $\gamma = n - ik$, bounded by two transparent media with

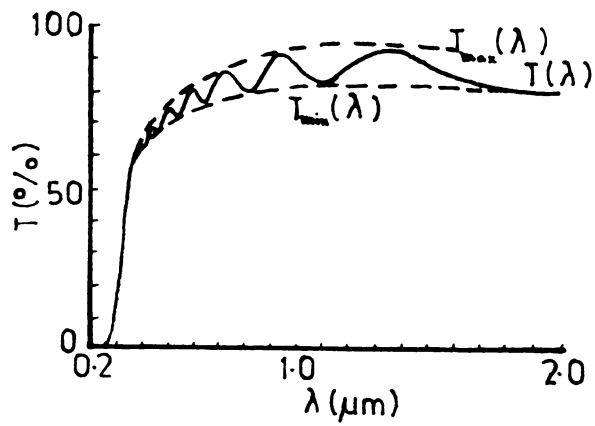
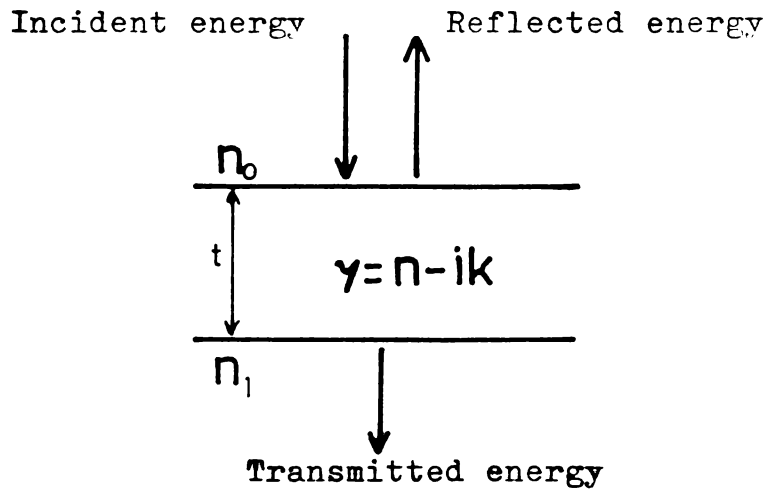


Figure 10. Reflection and transmission of light by single film alongwith a typical transmission spectra.

refractive indices n_0 and n_1 . Considering a unit amplitude for the incident light wave, in the case of normal incidence, the amplitude of the transmitted wave is given by

$$A = \frac{t_1 t_2 \exp(-2\pi i \gamma t / \lambda)}{1 + r_1 r_2 \exp(-4\pi i \gamma t / \lambda)} \quad (3.6.1)$$

in which t_1, t_2, r_1, r_2 are the transmission and reflection coefficients at the front and rear faces. The transmission of the layer is given by

$$T = \frac{n_1}{n_0} |A|^2 \quad (3.6.2)$$

In the case of weak absorption with $k^2 \ll (n-n_0)^2$ and $k^2 \ll (n-n_1)^2$,

$$T = \frac{16 n_0 n_1 n^2 \alpha'}{C_1^2 + C_2^2 \alpha'^2 + 2C_1 C_2 \alpha' \cos(4\pi n t / \lambda)} \quad (3.6.3)$$

where $C_1 = (n + n_0)(n_1 + n)$, $C_2 = (n - n_0)(n_1 - n)$ and

$$\alpha' = \exp(-4\pi k t / \lambda) = \exp(-\alpha t)$$

The maximum and minimum values of transmission are given by

$$T_{\max} = 16 n_0 n_1 n^2 \alpha' / (C_1 + C_2 \alpha')^2 \quad (3.6.4)$$

$$T_{\min} = 16 n_0 n_1 n^2 \alpha' / (C_1 - C_2 \alpha')^2 \quad (3.6.5)$$

Considering T_{\max} and T_{\min} as continuous functions of λ

through $n(\lambda)$ and $\alpha'(\lambda)$, which will be the envelop of the maxima, $T_{\max}(\lambda)$ and the minima, $T_{\min}(\lambda)$. Equating equations (3.6.4) and (3.6.5), we get

$$\alpha' = \frac{C_1 [1 - (T_{\max}/T_{\min})^{1/2}]}{C_2 [1 + (T_{\max}/T_{\min})^{1/2}]} \quad (3.6.6)$$

Then, from equation (3.6.4)

$$n = [N + (N^2 - n_0^2 n_1^2)^{1/2}]^{1/2} \quad (3.6.7)$$

where $N = \frac{n_0^2 + n_1^2}{2} + 2 n_0 n_1 \frac{(T_{\max} - T_{\min})}{T_{\max} T_{\min}}$

From these equations, refractive index n , extinction coefficient k and absorption coefficient α are determined.

The difference between film refractive index n and the substrate refractive index n_1 should be as great as possible to obtain good fringe pattern. The effective band width of the spectrophotometer should be kept smaller than the half width of the interference maximum. The sample must be parallel faced and homogeneous. Variation of n and k with wavelength should be small. These conditions are to be satisfied to get good results.

Another simple method may be used to measure α , in the region of fundamental absorption.

The transmission through a film on a transparent substrate in a medium of refractive index n_0 is given by

$$T = \frac{16 n_0 n_1 (n^2 + k^2) \exp(-\alpha t)}{[(n_0 + n)^2 + k^2][(n_1 + n)^2 + K^2]} \quad (3.6.8)$$

In weakly absorbing regions of the spectra, $n^2 \gg k^2$ this equation can be approximated to

$$T = \frac{16 n_0 n_1 n^2}{(n_0 + n)^2 (n_1 + n)^2} \exp(-\alpha t) \quad (3.6.9)$$

If we have two samples with thickness t_1 and t_2 and if the samples are put in the sample beam and reference beam of the spectrophotometer,

$$T_1 = \frac{16 n_0 n_1 n^2}{(n_0 + n)^2 (n_1 + n)^2} \exp(-\alpha t_1) \quad (3.6.10)$$

for the specimen in the sample beam and

$$T_2 = \frac{16 n_0 n_1 n^2}{(n_0 + n)^2 (n_1 + n)^2} \exp(-\alpha t_2) \quad (3.6.11)$$

for the specimen in the reference beam. The log of the ratio of the two transmissions are displayed by the spectrophotometer. Hence for any particular wavelength

$$\ln (T_2/T_1) = \alpha t \quad (3.6.12)$$

where $t = t_1 - t_2$. From this α may be determined.

The advantages of this method is, that it requires only simple calculations and one need not have to

know the refractive index of the film. The only disadvantage of this method is that a precise knowledge of the film thickness is necessary, since α depends on the differences in sample thickness, which is a small quantity.

For these measurements in the UV-Vis-NIR region a Hitachi, Model No.330, spectrophotometer was used, which can cover 2500 nm to 200 nm. For the measurements in UV-Vis region, a Hitachi 200-20 UV-Vis spectrophotometer was used. This can cover 900 nm to 200 nm with a light source change at 370 nm. A spectral band width of 2 nm was used in these measurements.

Measurements were made in the transmission mode of the spectrophotometer for the calculation of refractive index, absorption coefficient and extinction coefficient. Films were deposited on 3 cm x 1 cm x 0.1 cm, optically flat glass substrates for the NIR-Vis region and on quartz when measurements were to be made in the UV-Vis-NIR region.

3.7 OXIDATION OF METAL FILMS

The oxidation of bismuth films was performed in a setup shown in figure 11. The setup consists of a 4 cm diameter corning glass tube over which No.28

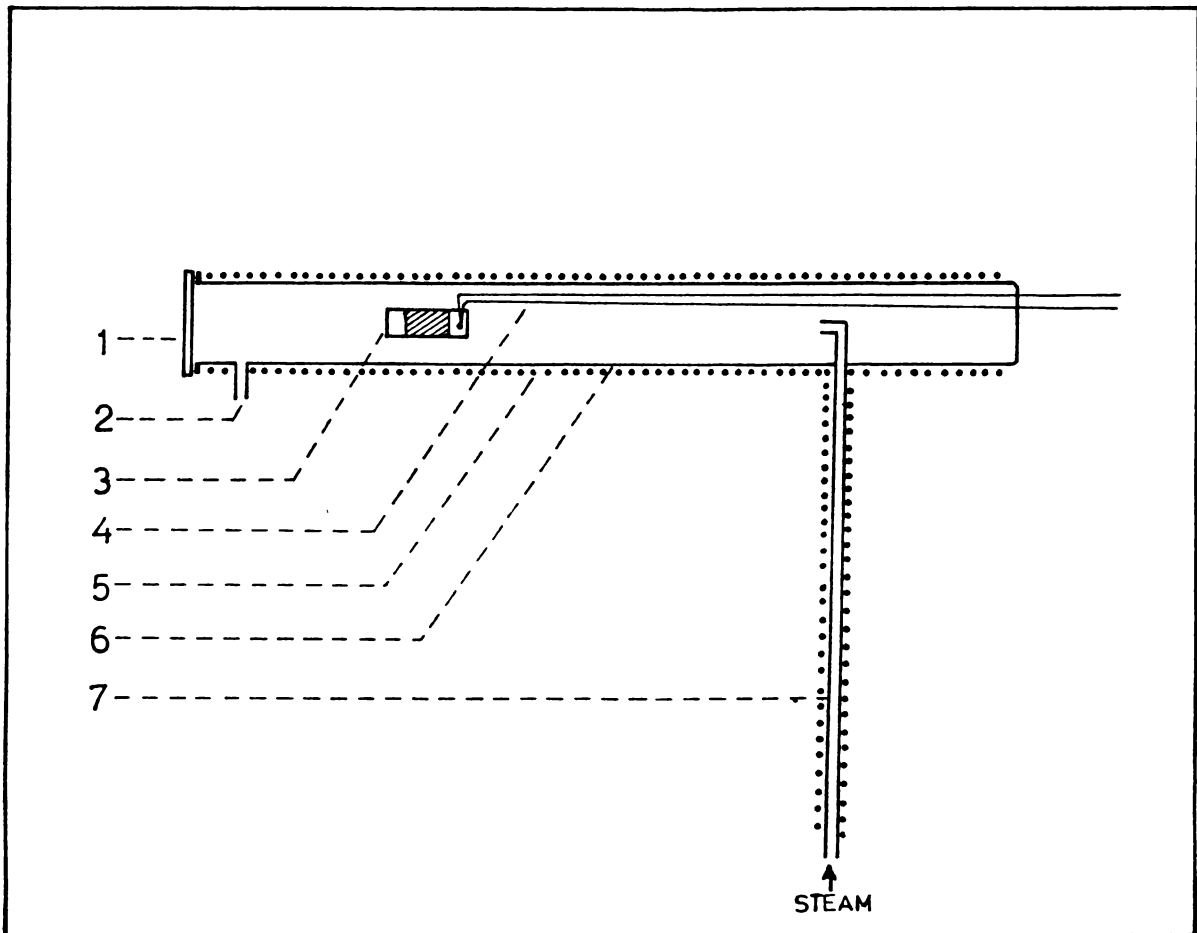


Figure 11. Experimental set-up for oxidation of bismuth films in different atmospheres.

- 1) Ground glass lid,
- 2) Out let,
- 3) Specimen,
- 4) Thermocouple,
- 5) Heater winding,
- 6) 4 cm diameter glass tube,
- 7) Narrow glass tube.

gauge Kanthal wire was wound. The steam or the required gas was admitted through the long and narrow glass tube, which was also wound with heater wire. The steam or the gas was heated to a high temperature before admitting into the furnace, using this winding. Otherwise the surface of the film may get cooled because of the flow of the steam or gas. The temperature inside the furnace was measured by a chromel-alumel thermocouple and controlled by a proportional temperature controller /5/ which was developed in this laboratory. An accuracy of ± 2 K was obtained even in such an open system. The thermocouple was placed near the specimen with the thermocouple head not touching the walls of the furnace. The heating rate of the furnace was around 2 K/Sec. The power to the narrow tube winding was supplied through a dimmerstat from a servo voltage stabilizer.

The flow of the super-heated steam was controlled by adjusting the power fed to the steam bath. The steam flow was measured by condensing the steam coming out of the exit port of the furnace and measuring the amount of vapour condensed.

The pressure inside the furnace was reduced by connecting a double stage rotary pump to the exit port

of the furnace and closing the inlet port using a rubber tube fitted with a glass stopper. The pressure inside was measured by a thermocouple gauge.

The bismuth films, deposited on 2.4 cm x 3.5 cm glass slides were used for the oxidation studies. The oxidation of bismuth films were performed at various conditions as follows:

- 1) At different temperatures in air
- 2) At different flow rates of super-heated steam and temperatures
- 3) At different low pressures and temperatures
- 4) At different atmospheres, viz. O_2 , N_2 and temperatures.

3.8 PREPARATION OF COMPOUND FILMS BY REACTIVE EVAPORATION

One of the methods used here for the preparation of compound films is reactive evaporation of the metal (Bismuth) in an atmosphere of the other element (Tellurium/Oxygen). This method of preparation is also known as Günther's technique /6/. Tellurium was evaporated from a quartz crucible placed in a conical basket of molybdenum wire. In the case of oxygen, the pressure inside the chamber was controlled with the help of a needle valve, through which oxygen was admitted.

The rate of evaporation G from a clean surface in vacuum, at a temperature T was calculated from the loss of weight per unit area per unit time and is given by the Langmuir expression /7/

$$G = P (M/2\pi RT)^{1/2} \quad (3.8.1.)$$

where P is the vapour pressure, M molecular weight of the material and R the gas constant. The relationship between the vapour pressure and temperature have been calculated for a wide variety of materials by various authors /8/.

For the purpose of reactive evaporation, the rate at which metal atoms arrive at the substrate is best expressed in terms of the deposition rate as obtained from the same source at the same temperature and distance, but in the absence of the reactive element flux /9/.

$$\frac{d N_m}{A_r dt} = \frac{N_a \rho_m d'}{M_m} \text{ atoms/cm}^2 \text{ Sec.} \quad (3.8.2)$$

where N_a is the Avogadro number, ρ_m the density of the metal film in g/cm^3 , d' the pure metal condensation rate in cm/Sec. , M_m the molar mass of the metal in gm/mol , and A_r the receiving surface area in cm^2 .

The impingement rate of oxygen molecules is given by

$$\frac{d N_{O_2}}{A_r dt} = 3.513 \times 10^{22} (M_{O_2} T)^{-1/2} P_{O_2} \text{ molecules} \quad (3.8.3)$$

where M_{O_2} is the molar mass of oxygen, T the gas temperature (300 K) and P_{O_2} the oxygen partial pressure in Torr.

Equations (3.8.2) and (3.8.3) are used to calculate the impingement rate of bismuth, tellurium and oxygen at the substrate surface for a given deposition rate.

The rate of deposition of the vapour on the substrate also depends on the source geometry, position of source relative to the substrate and the condensation coefficient. According to Knudsen cosine law, the rate of deposition varies as $\text{Cos } \theta / r^2$, for the ideal case of deposition from a uniformly emitting point source to a plane surface, where r is the radial distance of the substrate from the source and θ the angle between the radial vector and the normal to the substrate.

Vacuum system

The preparation of the compound films were

carried out in a conventional vacuum system fitted with a 12 inch glass bell-jar. The working chamber was evacuated by a 4 inch oil diffusion pump backed with a double stage rotary pump with a pumping speed 200 lits/minute. Better than 10^{-5} Torr can be attained even without the use of liquid nitrogen. Pirani gauge ($0 - 10^{-3}$ Torr) and Penning gauge (10^{-2} Torr to 10^{-6} Torr) are used to measure the pressure inside the working chamber.

The working chamber is provided with two high current (100 A, 10 V) sources for the evaporation of the element materials. The current for the substrate heater can be taken from the main supply through an 8 A dimmer-stat. An ion-bombardment cleaning system is fitted inside the chamber with a high tension supply (100 mA, 5 KV). The system is also provided with a narrow tube to admit the required gas, which is controlled by a needle valve. The substrate temperature was measured by a chromel-alumel thermocouple placed in contact with the substrate. The pressure used normally in the preparation of the films was 2×10^{-5} Torr and the normal pumping down time to get ultimate vacuum was around one hour.

Substrate cleaning

1 cm x 3.5 cm x 0.1 cm glass or quartz, optically flat substrates were first cleaned with industrial detergent

(Teepol), then washed in running water followed by distilled water. These were again cleaned with analytical grade acetone. The final cleaning was done by agitating the slides for 20 minutes in distilled water using an ultrasonic cleaner and then dried by a hot air blower. Immediately the substrates were loaded in the vacuum system and the substrates were further cleaned by ion-bombardment for 15 minutes before depositing the film.

Deposition of the film

After loading the system with required elemental materials of high purity and with the substrates properly masked, it was pumped to the ultimate vacuum. Then the substrates were heated to the required temperature and was measured by a chromel-alumel thermocouple placed in contact with the substrates. The output of the thermocouple was read by a $3\frac{1}{2}$ digit, 200 mV digital panel meter. High purity (5 N) Tellurium was evaporated from a quartz crucible, heated with a conical basket of molybdenum wire of 0.5 mm diameter. High purity (5 N) Bismuth was evaporated from a molybdenum boat. A thermocouple head was placed in contact with the lower surface of the boat, to read the temperature of the boat. The temperature of both the sources were controlled by adjusting the current

flowing through them. The metal source was covered with stainless steel heat shield, so as to prevent the radiant heat reaching the substrate. And hence the substrate temperature could be controlled within ± 5 K, during deposition. A schematic diagram of the setup is given in figure 12.

The temperature of the substrates was controlled by the current flowing through the substrate heater. When the temperature reached the required value, it was maintained at that temperature for 15 minutes. Then the current through the tellurium source was switched on and the current through it was slowly increased till the tellurium got melted, keeping the shutter over both the sources. Then the source current was reduced to the pre-calibrated value, for a certain tellurium flux and the current through the bismuth source was switched on and slowly increased, so that the boat attained the required temperature, read by the thermocouple. The shutter was withdrawn after giving a little time for the flux to stabilize. The individual elements from both the sources would meet at the substrate surface and combined to form the bismuth telluride, and was deposited on the substrate surface. After completion of deposition, the shutter was put back in position over the sources and the supply

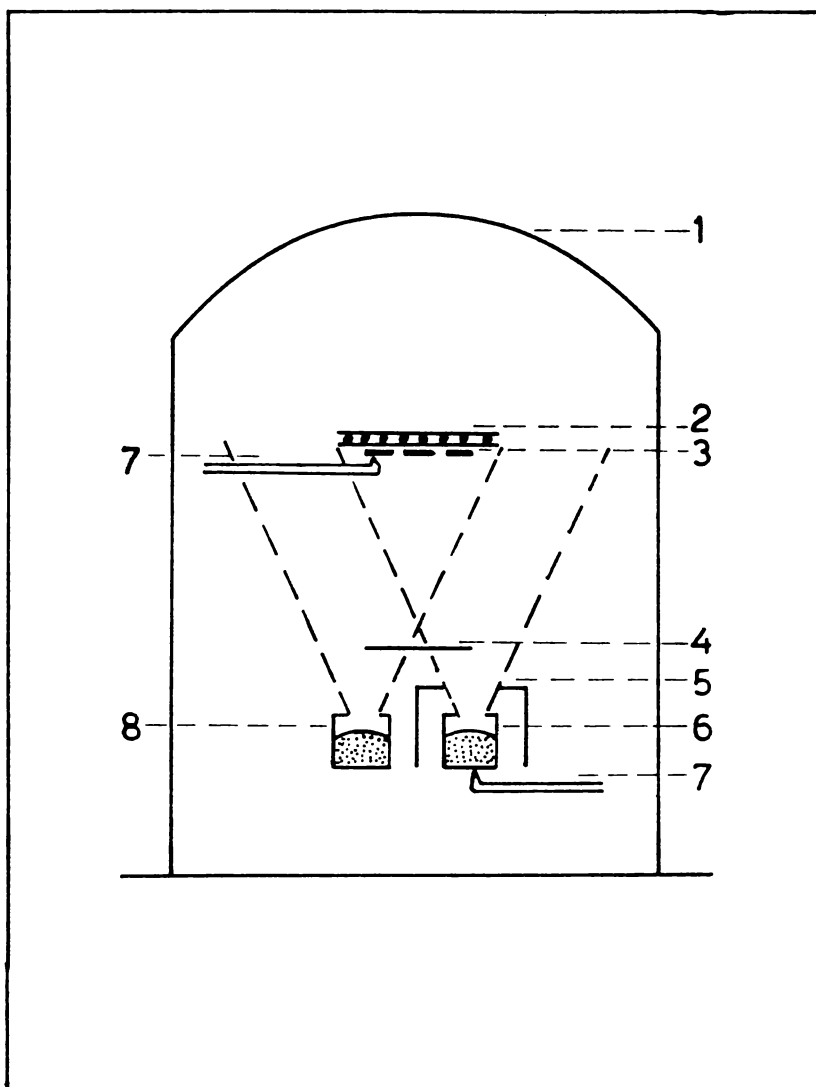


Figure 12. Schematic diagram of the experimental set-up

- 1) bell jar,
- 2) substrate heater,
- 3) substrates,
- 4) shutter,
- 5) heat shield,
- 6) bismuth source,
- 7) thermocouple,
- 8) tellurium source.

to both the sources switched off. The substrate temperature was also reduced slowly.

For the preparation of oxide films, tellurium source was replaced by oxygen source. Industrial grade oxygen was admitted to the chamber through a thin tube of 4 mm diameter. The flow of oxygen through this tube was controlled by a needle valve. The oxygen molecules coming out of the tube were directed towards the substrates. After the substrates attained the required temperature, oxygen was admitted and controlled by the needle valve so as to get a pressure $\sim 10^{-3}$ Torr in the chamber. After about 10 minutes the film deposition was done as described earlier.

3.9 PREPARATION OF COMPOUND FILMS BY ACTIVATED REACTIVE EVAPORATION

Certain metals will not readily form their oxide/nitride phases when reactively evaporated in an oxygen/nitrogen atmosphere. This is because of the high activation energy needed for chemical reaction (1 - 3 eV) to form the oxide/nitride phase. Another problem with the ordinary reactive evaporation is the low deposition rate. In order to overcome these difficulties, activated reactive evaporation (ARE) was developed by Prof. Bunshah of UCLA /10/. Here the required metal is evaporated from

an electron gun in the presence of the reactive gas. A small electrode, biased positively (100 - 200 V) and placed in between the electron gun and the substrate, accelerates the electrons from the electron gun. These electrons, colliding with the reactive gas, ionizes them making a plasma. Because of this, the chemical reaction rate is increased very much and high rate of deposition of several oxides, nitrides, etc. have been made possible /11/. One difficulty with the approach is the need for a commercial electron gun which may not be readily available in a laboratory.

Another modification of this method had been reported from Prof. Bunshah's laboratory /12/. Here the metal was evaporated from a suitable boat and uses a magnetic field together with an electron emitting filament made of thoriated tungsten to generate the plasma. The reactive gas pressure inside the chamber was 5×10^{-4} Torr. This method requires a magnetic field and the field coils are placed outside the vacuum chamber. Evidently this necessitates the use of glass bell-jars.

A modified version of the above method was used here for the preparation of bismuth oxide films and the setup is shown in figure 13. Here the use of the magnetic

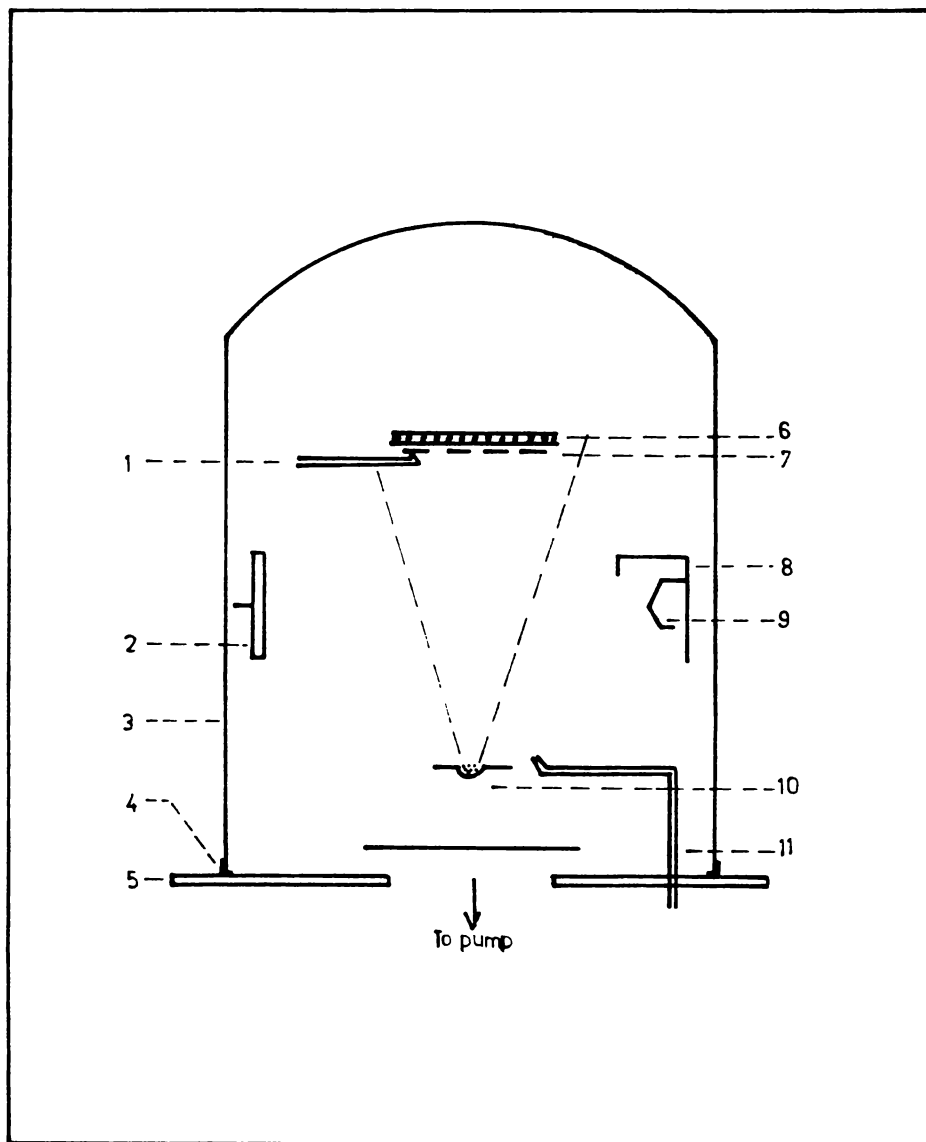


Figure 13. Schematic diagram of the experimental set-up for activated reactive evaporation.

- 1) thermocouple, 2) anode, 3) glass bell jar, 4) L-gasket, 5) base plate, 6) substrate heater, 7) substrate, 8) electron reflector and shield, 9) W-filament, 10) metal source, 11) Cu-tube for O₂ inlet.

field is dispensed with and metallic bell jars can obviously be used. Two electron emitters are used to obtain a high emission current, and a negatively charged reflector behind the emitters is used to direct the electrons towards the anode.

With ordinary reactive evaporation, bismuth will not form the oxide phase easily and the reported rate of deposition is only 0.05 - 0.2 Å/Sec. /13/. With the present setup it has been possible to get a very high rate of deposition. Here two tungsten wires of 0.5 mm diameter were used as the electron emitters. Anode was made of thick aluminium block of 8.5 cm x 8.5 cm x 1 cm dimensions and was biased at 100 V positive with respect to the cathode by a DC supply capable of supplying 2 A. The electron emitter was so shielded that small quantities of tungsten evaporating from the filament at such high temperatures would not reach the substrate. With this setup it is possible to maintain the glow discharge down to 5×10^{-4} Torr oxygen partial pressure.

Optical quality films of bismuth oxide were prepared using this setup and the details of the deposition procedure is given in chapter VII, 7.2.

Anode has to be cleaned after each deposition run because of the insulating nature of the bismuth oxide.

REFERENCES

1. V.J. Sebastian, M.Sc. Project, Department of Physics, University of Cochin (1982).
2. V. Narayanankutty, M.Sc. Project, Department of Physics, University of Cochin (1983).
3. S. Tolansky, "Multiple Beam Interferometry of Surface and films", Oxford Univ. Press, London (1948).
4. J.C. Manificier, J. Gasiot and J.P. Fillard, J. Phys. E, 9 (1976) 1002.
5. J. George, K.S. Joseph and C.K. Valsalakumari, Int. J. Electronics, 52 (1982) 299.
6. K.G. Günther in "The Use of Thin Films in Physical Investigations", J.C. Anderson (Ed.), Academic Press, New York, 1966, p.213.
7. S. Dushmen, "Scientific Foundations of Vacuum Technique", John Wiley, New York, 1962, p.17.
8. Ibid, p. 696.
9. R. Glang in "Hand Book of Thin Film Technology", L.I. Maissel and R. Glang (Eds.), McGraw Hill, New York, 1970, p.1-81.
10. R.F. Bunshah and A.C. Raghuram, J. Vac. Sci. & Tech., 9 (1972) 1389.

11. R.F. Bunshah, "Science and Technology of Surface Coatings", B.N. Chapman and J.C. Anderson (Eds.) Academic Press, London, 1974, p.361.
12. H.S. Randhawa, M.D. Mathews and R.F. Bunshah, Thin Solid Films, 83 (1981) 267.
13. A. Milch, Thin Solid Films, 17 (1973) 231.

CHAPTER IV

REACTIVELY EVAPORATED FILMS OF BISMUTH TELLURIDE4.1 INTRODUCTION

Bismuth telluride has received considerable attention because of its high thermoelectric properties. Extensive studies have been carried out on samples of bismuth telluride in the bulk form /1-6/. But not much work has been reported on thin films of bismuth telluride. Hanlein and Günther /7/ have reported the room temperature carrier concentration, carrier mobility and thermoelectric power of the Bi_2Te_3 films prepared by three temperature method. Goswami and Koli /8/ studied the films, prepared by evaporation from the bulk, which normally results in incongruent evaporation of the compound material and consequent lack of stoichiometry. Shing et.al. /9/ have also reported the room temperature carrier concentration and hole mobility of the films prepared by diode sputtering. Their films were also nonstoichiometric, which was caused by the dissociation of bismuth telluride during the sputtering process.

Here it is reported the preparation and the semiconducting properties such as conductivity, Hall coefficient and thermoelectric power in the temperature range from liquid nitrogen temperature to 350 K of stoichiometric films of bismuth telluride prepared by reactive evaporation.

4.2 EXPERIMENTAL

Bismuth telluride films were prepared by reactive evaporation, a variant of three temperature method, in which the individual elements were evaporated from separate sources and the compound films deposited on the substrate, which was kept at an elevated temperature. For many binary system it has been found that a stoichiometric interval exists with a limited degree of freedom in selecting the individual components and substrate temperature for obtaining a particular compound of the system /10, 11/.

Bismuth telluride films were prepared by reactive evaporation as described in chapter III, 3.8. The impingement rate of bismuth and tellurium atoms, on the substrate surface were calculated by using equation (3.8.2) of chapter III.

It has been found that good stoichiometric films

of bismuth telluride are obtained if the following deposition parameters are satisfied:

$$\text{Bismuth flux} = 2 - 3 \times 10^{14} \text{ atoms cm}^{-2}\text{Sec}^{-1}$$

$$\text{Tellurium flux} = 3 - 4 \times 10^{15} \text{ atoms cm}^{-2}\text{Sec}^{-1}$$

$$\text{Substrate temperature} = 530 - 545 \text{ K}$$

The films obtained had a metallic lustre and highly reproducible films were obtained under these conditions. The deposition rate of bismuth telluride film was 0.3 - 0.4 nm per second. All the films used in this study were prepared at a substrate temperature of $537 \pm 2\text{K}$.

At the high substrate temperatures (530 - 545 K) and low supersaturations used in the experiments, tellurium or bismuth will not stick individually to the substrate. Only a compound of bismuth and tellurium, which has got a low vapour pressure compared to Bi and Te will stick to the substrate. If the substrate temperature was lower than 530 K, the films had a smoky appearance with poor adhesion to the substrate. But if the substrate temperature was higher than 545 K, the films were discontinuous. This was probably due to the reevaporation of the compound film formed from certain preferential areas /12/.

4.3 X-RAY DIFFRACTION STUDIES

For x-ray diffraction studies the films were deposited on glass substrates of 3.5 cm x 2.4 cm x 0.1 cm dimensions and films of $\approx 3500 \text{ \AA}$ thick were used. An x-ray unit with Copper K α radiation was used for the diffraction studies as described in chapter III, 3.4. The x-ray diffractogram of typical Bi_2Te_3 film is given in figure 1. Table I gives the standard values of the x-ray powder diffraction data given by Francombe /13/ alongwith the data obtained in the present case. From this table it is clear that the present film contains only Bi_2Te_3 .

4.4 ELECTRICAL PROPERTIES

(a) Hall effect studies.

For Hall effect measurements the glass substrates were masked with proper masks made of mica sheet during the preparation of samples to get the specimen geometry shown in chapter III (figure 3). The Hall effect measurements were done in the all metal cell, (chapter III, figure 4) where the temperature could be varied from liquid nitrogen temperature to 500 K. Conventional four probe method /14/ was used for the Hall effect studies. The magnetic field used was 0.4 Tesla with a pole separation of 2 cm using the electromagnet described in detail in chapter III, 3.2

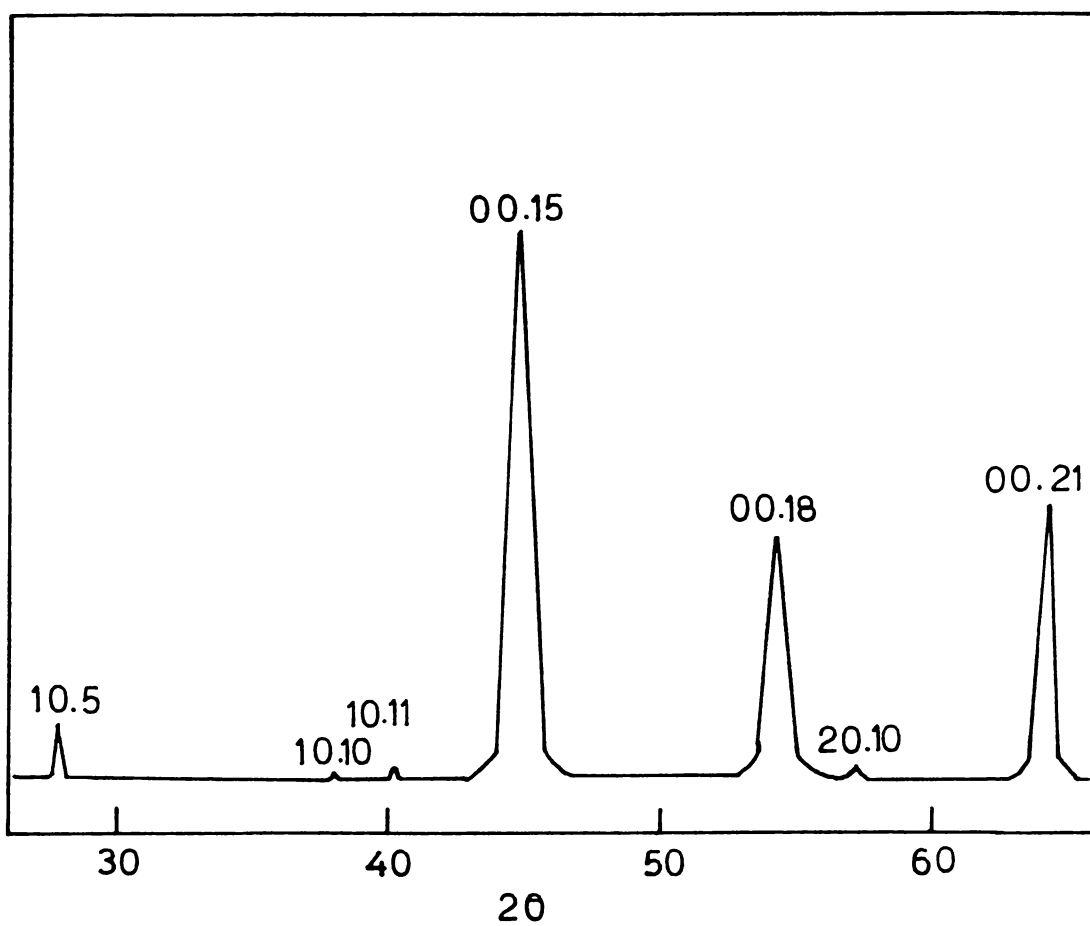


Figure 1. X-ray diffraction pattern of the film.

TABLE I

X-ray diffraction data for co-evaporated bismuth
Telluride films

hkl*	Standard pattern		Prepared film	
	d A.u.	I/I ₀	d A.u.	I/I ₀
1,0,5	3.22	100	3.21	10
1,0,10	2.378	55	2.366	1
1,0,11	2.237	11	2.238	2
0,0,15	2.032	40	2.025	100
0,0,18	1.694	5	1.688	44
2,0,10	1.610	16	1.609	2
0,0,21	1.452	6	1.448	50

*The hkl indices are referred to the hexagonal
structure cell.

Samples of dimensions $\approx 2000 \text{ \AA} \times 2.5 \text{ cm} \times 0.3 \text{ cm}$ were prepared on glass substrates. One glass slide was also placed side by side with the specimen substrates and which was used for the determination of film thickness after deposition. The thickness was determined by Tolansky's /15/ multiple beam interferometric method. After deposition, samples were cooled to room temperature. The samples were taken out of vacuum and the electrical contacts were made with silver paint which was found to give ohmic contact. Then the sample was fixed in the cell for Hall effect studies (described in chapter III, 3.2) and the measurements were performed in a vacuum better than 10^{-2} Torr. Measurements were carried out from 100 K to 375 K. Throughout the measurements the current through the sample was maintained at 2 mA and was read by a $3\frac{1}{2}$ digit, digital multimeter.

The variation of Hall coefficient (R) with temperature is given in figure 2. It is seen that the Hall coefficient is fairly constant in the lower temperature region, indicating that the extrinsic material is in the saturation range, where no further ionisation of impurities take place. The carrier concentration has been calculated from the familiar relation

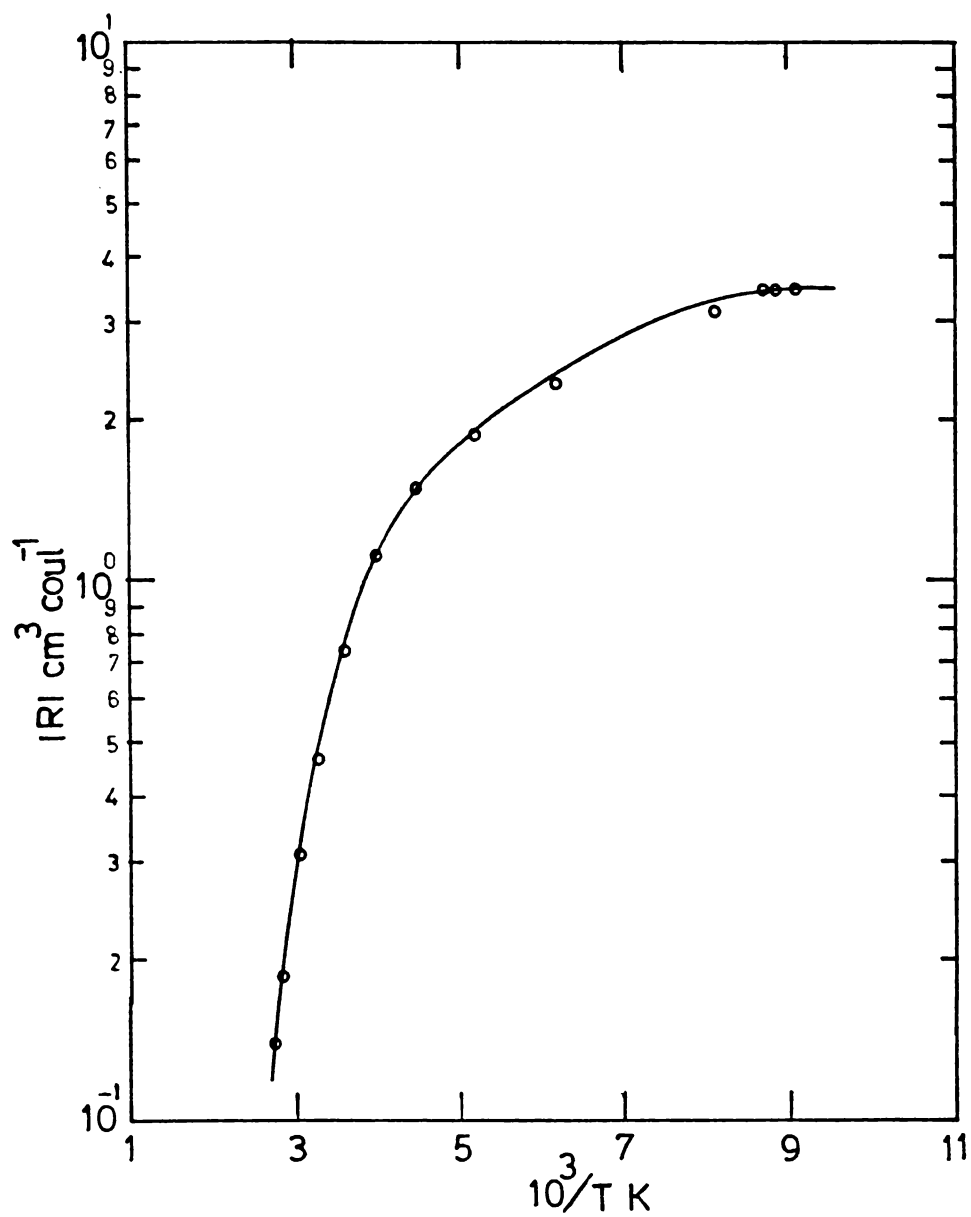


Figure 2. Variation of Hall coefficient with reciprocal of absolute temperature.

$$R = \frac{3\pi}{8} \frac{1}{ne} \quad (4.4.1)$$

where n and e are the electron concentration and electronic charge respectively; and is found to be $2 \times 10^{19} \text{cm}^{-3}$ at this saturation temperature region. For this concentration the degeneracy temperature has been estimated using the relation /16/.

$$T_{\text{deg}} = \left(\frac{3}{\pi}\right)^{3/2} \frac{h^2}{8 km} n^{2/3} \quad (4.4.2)$$

where k is the Boltzmann's constant, m the free electron mass, and h Plank's constant. From this we get a degeneracy temperature of 300 K. As the temperature is increased beyond the saturation region, the Hall coefficient is found to decrease slowly and near room temperature a very steep decrease in Hall coefficient is observed. This obviously is due to the film becoming intrinsic in nature. This type of behaviour has been reported in bismuth telluride in bulk form /2, 3, 6/. These authors have also been observed a sign reversal of Hall coefficient, and the temperature at which this takes place varies from sample to sample in each case /3/. But in the present case, it has not been able to observe any sign reversal upto 370 K.

(b) Conductivity studies

Conductivity measurements were also carried out alongwith the Hall effect measurements. Since bismuth

telluride being a material with high thermoelectric power and low thermal conductivity, the measuring current will produce a temperature gradient, which will cause a thermoelectric voltage across the conductivity probes. This was eliminated by taking one reading after the current had established a steady state temperature distribution and the current was immediately reversed, and a second reading was taken. Thus the temperature distribution for both the readings was maintained the same. From the average of these two readings, the conductivity was calculated.

Figure 3 shows the variation of conductivity (σ) with temperature. The conductivity decreases with temperature, becomes a minimum and then increases. The decrease from 100 K to 225 K is caused by increased lattice scattering. Above 225 K, the intrinsic region begins and the conductivity increases with temperature. Slope of $\log \sigma$ Vs $\frac{1}{T}$, in the intrinsic range gives the value of energy gap E_g to be 0.15 eV, which is in agreement with the values obtained in bulk samples /6, 17/. Figure 4 shows the variation of Hall mobility (μ) with temperature. Temperature dependence of mobility is found to be $T^{-1.8}$, which shows that lattice scattering is predominant and impurity scattering is not important.

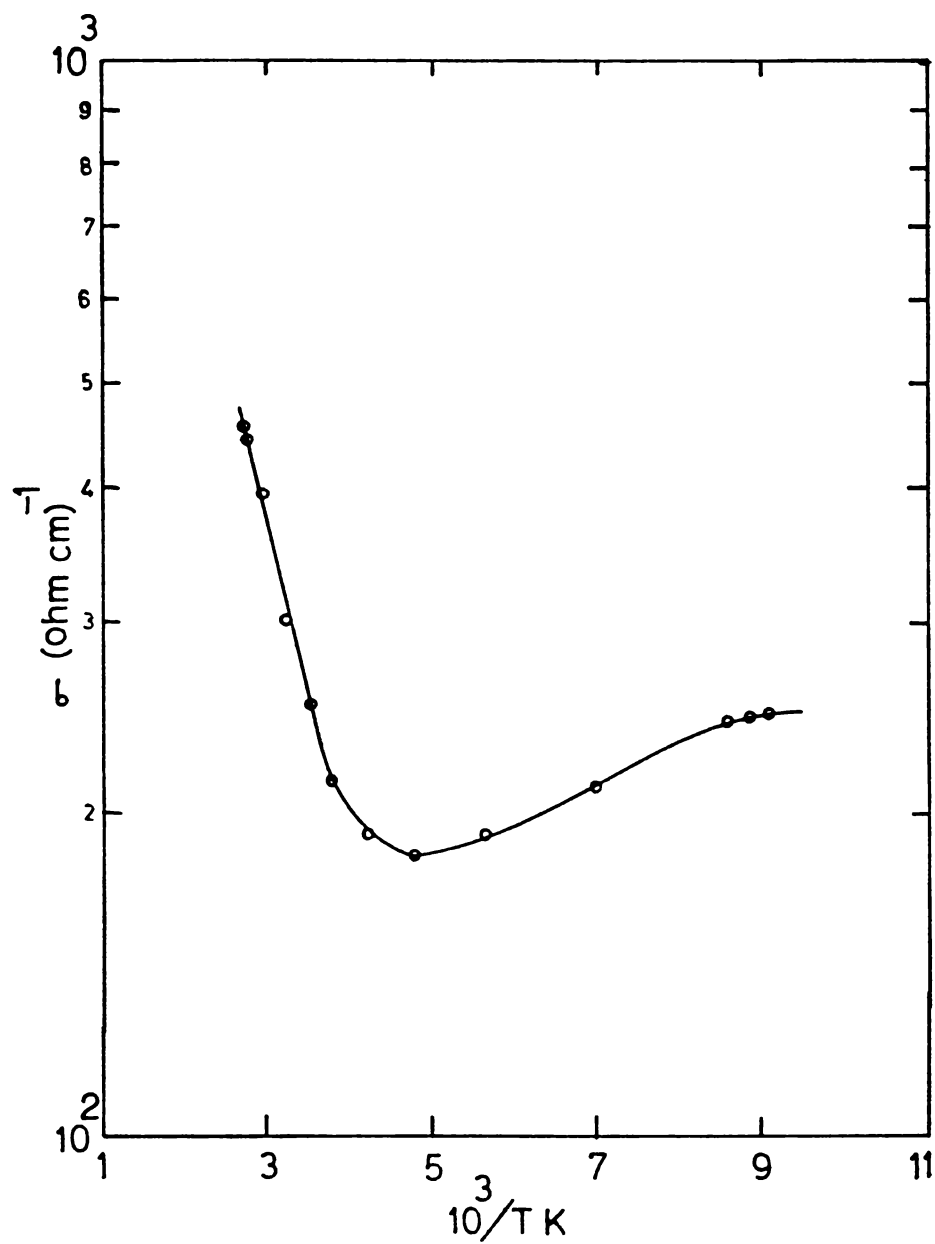


Figure 3. Variation of d.c. conductivity with reciprocal of absolute temperature.

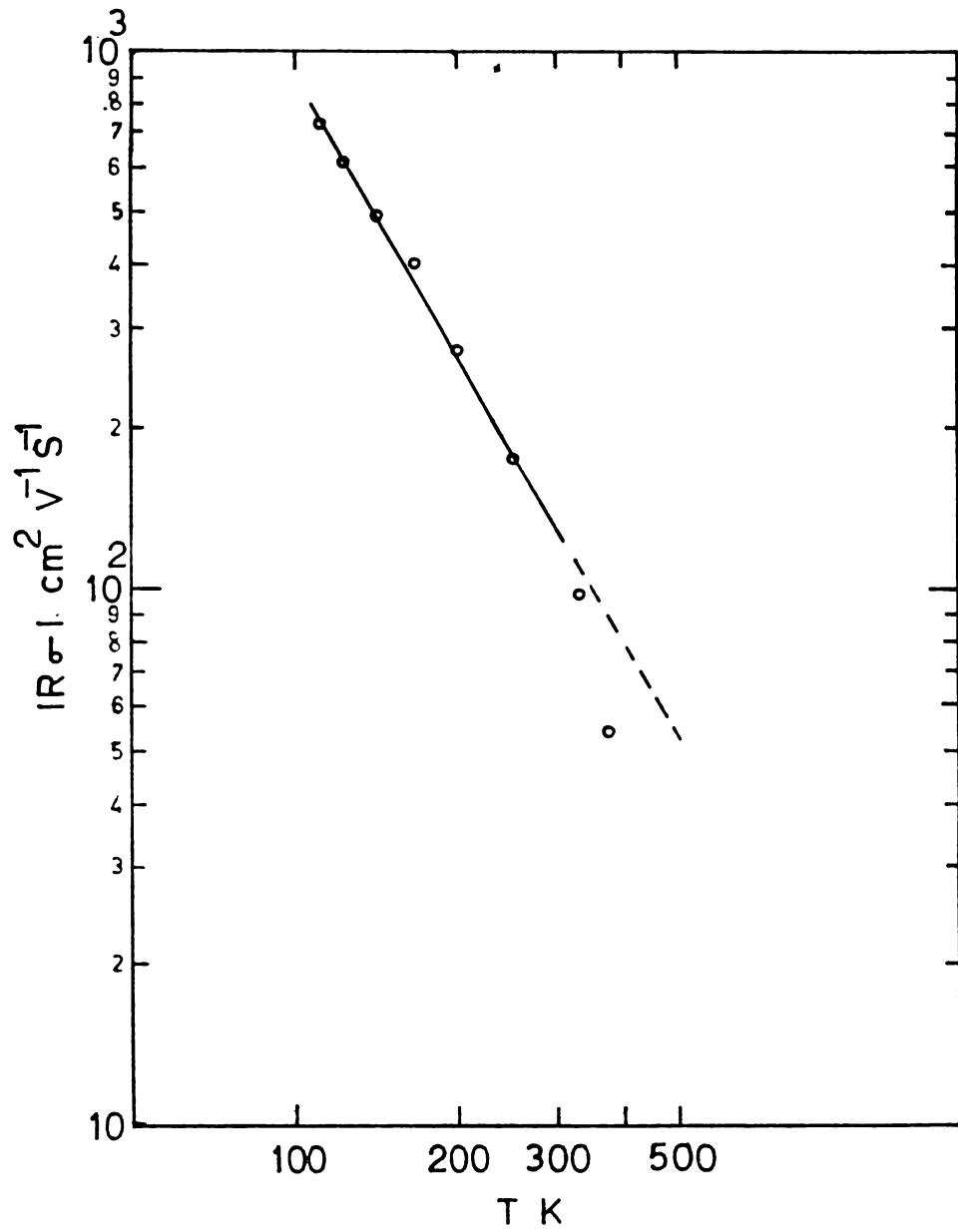


Figure 4. Variation of Hall mobility with absolute temperature.

(c) Thermoelectric power studies

For thermoelectric power measurements, samples were prepared on glass substrates, of dimension 2.5 cm x 0.3 cm. The thickness of the films used were $\approx 2000 \text{ \AA}$. After the preparation, the sample was transferred to the measuring cell described in chapter III, 3.3. Contacts to the specimens were made with silver paint. Thermocouples were placed in contact with the ends of the specimen, and a third thermocouple was placed at the middle of the sample. These thermocouples were fixed to the samples using teflon strips, to get firm contact with the sample, and the temperatures were read by 4 $\frac{1}{2}$ digit, 200 mV, digital panel meters. One end of the sample was cooled using liquid nitrogen and the voltage developed across the sample was noted by a digital multimeter. The other end of the sample was heated with the microheater. The maximum temperature difference used for the measurements between the two ends was 25 K. The readings were taken from 150 K to 400 K at a vacuum better than 10^{-2} Torr.

The variation of thermoelectric power (α) with temperature is shown in figure 5. Thermoelectric power is negative throughout the temperature range, suggesting that the sample is of n-type. n-type conductivity is

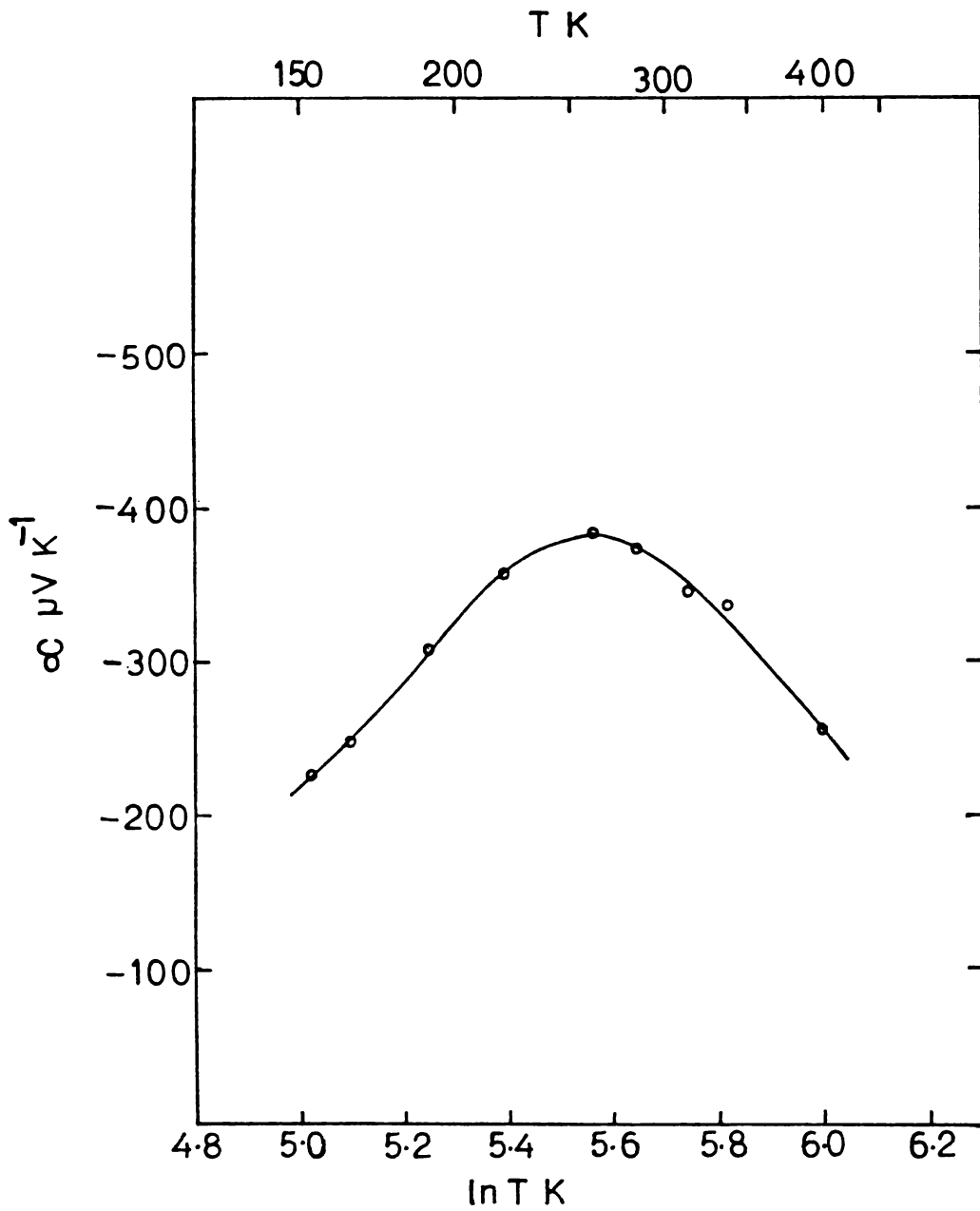


Figure 5. Variation of thermoelectric power with absolute temperature.

due to the incorporation of excess tellurium in the films /5/. It is seen that the thermoelectric power increases with increasing temperature upto 260 K, due to the degenerate nature of the material and attains a maximum value of $380 \mu\text{V/K}$. Then it is found to decrease with increase of temperature. The same phenomena has been observed in bulk bismuth telluride /4, 6/.

4.5 CONCLUSION

The films of bismuth telluride prepared by this method were stoichiometric and good quality films were obtained in the temperature range 530 K to 545 K. The films were of n-type with a carrier concentration $1.25 \times 10^{20} \text{ cm}^{-3}$ at room temperature. The energy band gap was found to be 0.15 eV. Thermoelectric power increased with increasing temperature upto 260 K and attained the maximum value of $380 \mu\text{V/K}$ and decreased with increase of temperature. The films obtained had a metallic lustre and good adhesion to the substrate.

REFERENCES

1. W. Haken, *Ann. Phys.*, 32 (1910) 291.
2. S. Shigetomi and S. Mori, *J. Phys. Soc. Japan*, 11 (1956) 915.
3. C.B. Satterthwaite and R.W. Ure, *Phys. Rev.*, 108 (1957) 1164.
4. H.J. Goldsmid, *Proc. Phys. Soc. (London)*, 71 (1958) 633.
5. C.H. Champness and A.L. Kipling, *Canad. J. Phys.*, 44 (1966) 769.
6. J. Black, E.M. Conwell, L. Seigle and C.W. Spencer, *J. Phys. Chem. Solids*, 2 (1957) 240.
7. W. Hanlein and K.G. Günther, *Naturwissenschaften*, 46 (1959) 319.
8. A. Goswami and S.S. Koli, *Indian J. Pure Appl. Phys.* 7 (1969) 166.
9. Y.H. Shing, Y. Chang, A. Mirshafii, L. Hayashi, S.S. Roberts, J.Y. Josefowicz and N. Tran, *J. Vac. Sci. Technol. A.*, 1 (1983) 503.
10. J. George and M.K. Radhakrishnan, *Solid-State Commun.*, 33 (1980) 987.

11. J. George and K.S. Joseph, J. Phys. D., 15 (1982) 1109.
12. P.S. Vincett, Thin Solid Films, 100 (1983) 371.
13. M.H. Framcombe, Phil. Mag. (GB), 10 (1964) 989.
14. E.H. Putley, "The Hall effect and related phenomena", Whitefriar's Press, London, 1960, p.24.
15. S. Tolansky, "Multiple beam interferometry of surface and films", Oxford Univ. Press, London, 1948.
16. W. Shockley, "Electron and holes in semi-conductors", Affiliated East-West Press, India, 1968, p.242.
17. T.C. Harman, B. Paris, S.E. Miller and H.L. Goering, J. Phys. Chem. Solids, 2 (1957) 181.

CHAPTER V

BISMUTH OXIDE FILMS PREPARED BY THE
OXIDATION OF BISMUTH FILMS

5.1 INTRODUCTION

A number of investigators /1-10/ have reported on the oxidation of thin bismuth films in air and the properties of resultant oxide films /11-14/. There is considerable disagreement among the different authors on the phases formed during oxidation. Aggarwal and Goswami /1/ reported two cubic phases with $a_0 = 5.65 \text{ \AA}$ and $a_0 = 7.02 \text{ \AA}$ and the well known tetragonal phase, when bismuth films were oxidized in air at temperatures of 525 K to 575 K. Zav'yalova et. al. /2/ obtained, on prolonged heating of bismuth films in air at 725 - 750 K, the tetragonal phase ($\text{Bi}_2\text{O}_{2.7-2.8}$, $a = 3.85 \text{ \AA}$, $c = 12.25 \text{ \AA}$). Hapase et.al. /3,4/ oxidized bismuth films and determined the activation energy for oxidation of bismuth films. Zav'yalova and Imamov /5/ claimed that they had obtained an orthorhombic bismuth oxide of unknown composition ($a = 6.22 \text{ \AA}$, $b = 4.33 \text{ \AA}$, $c = 35.1 \text{ \AA}$) and also a new tetragonal phase of $\text{Bi}_2\text{O}_{2.3-2.4}$ ($a = 3.85 \text{ \AA}$, $c = 35.1 \text{ \AA}$),

when they heated thin films of bismuth to 775 K in air or oxygen. Moreover Zav'yalova and Imamov /6/ reported that they obtained β - $\text{Bi}_2\text{O}_{2.5}$ thin films with tetragonal structure ($a = 10.93 \text{ \AA}$, $c = 5.63 \text{ \AA}$) when they oxidized bismuth films deposited onto amorphous colloid films at 475 - 525 K in air. Sharma and Pandey /8/ obtained at 451 K, tetragonal $\text{Bi}_2\text{O}_{2.33}$ or a mixture of $\text{Bi}_2\text{O}_{2.33}$ and α - Bi_2O_3 depending upon the film thickness. All these variations occur due to the polymorphism of bismuth oxide /15-18/.

In all these experiments the authors had to use very thin films ($\lesssim 500 \text{ \AA}$) since electron diffraction technique had been used in the identification of the phases. Also these films will be highly strained and may not show the behaviour of the bulk. Again some fixed temperatures were only used for oxidation, and no systematic study had been made on the influence of the oxidation temperature and the medium of oxidation on the phases formed. Also there has not been any report on the oxidation of bismuth films to prepare single phase films of α - Bi_2O_3 and γ - Bi_2O_3 .

Here it is reported the oxidation of comparatively thick films ($\approx 2500 \text{ \AA}$) of bismuth in air, superheated steam and partial vacuum. The temperature at

which the films were oxidized was varied in the interval 500 K to 640 K. X-ray diffraction had been used for identifying the phases present.

5.2 EXPERIMENTAL

(a) Preparation of Bismuth films

Bismuth films were prepared in a vacuum system equipped with a diffusion pump as described in chapter III, 3.8. The ambient pressure in the system at the time of deposition was $\sim 10^{-5}$ Torr. 99.999 percent pure bismuth was used for evaporation and was evaporated from a molybdenum boat at a rate of deposition $\approx 15 \text{ \AA/Sec.}$ Optically flat, cleaned glass substrates of dimensions 3.5 cm x 2.5 cm x 0.1 cm were used for the preparation of bismuth films. The substrates were kept at room temperature (300 K) during deposition. Films $\approx 2500 \text{ \AA}$ thickness were prepared for the oxidation studies. For the determination of activation energy, $\approx 500 \text{ \AA}$ thick films were also prepared. The thickness of the films were determined by Tolansky's multiple beam interferometry.

(b) Oxidation in Air

These bismuth films were taken out of the chamber and were oxidized as described in chapter III, 3.7.

The temperatures used, vary in the range 500 K to 640 K. Different heating, cooling and annealing conditions were used in the case of different films. Here slow heating means that the film and the furnace are heated from room temperature simultaneously to the required temperature of oxidation. Fast heating means that the film was put into the furnace which was already heated to the required oxidation temperature. Slow cooling means that the furnace and the film were allowed to cool gradually and in fast cooling the film was suddenly taken into the ambient after oxidation or annealing.

(c) Oxidation in Super-Heated Steam

Oxidation in super-heated steam was also performed in the same furnace. Steam was admitted to the furnace through the narrow tube, which is connected to a steam bath with a neoprene tube. The steam was heated to a high temperature, with the windings provided in the narrow tube, before entering furnace. Different heating, cooling and annealing conditions were used in the case of different films as discussed above. The glass lid was placed in position and the exit port was loosely closed with cotton waste, so as to maintain a little pressure of steam inside the furnace. The flow of super-heated steam was controlled by adjusting the

power fed to the steam bath. Steam flow was measured by condensing the steam coming out of the exit port and measuring the amount of vapour condensed. Three steam pressures, maximum (condensation rate 0.07 ml/Sec.), medium (0.015 ml/Sec.) and low (0.003 ml/Sec.) were used here.

(d) Oxidation in Partial Vacuum

This was also done in the same furnace as above, but with the glass lid placed in position with vacuum grease. The inlet port was closed with a stop-cock using a neoprene tube. The exit port was connected to a double stage rotary pump, through a neoprene tube. Pressure was measured by a thermocouple gauge connected with this tube. The pressure inside the furnace was controlled, using the stop-cock connected at the inlet port. The sample was put into the furnace and the system was evacuated to the required pressure. Then the furnace was heated to the oxidation temperature. Oxidation was carried out at different pressures below atmospheric to 10^{-1} Torr.

For the determination of the activation energy for oxidation, films of thickness $\approx 500 \text{ \AA}$ were used. Usually in these type of experiments, the time taken

for the onset of oxidation (t), after the furnace has attained the particular temperature used for oxidation, is taken and its variation with the oxidation temperature (actually $10^3/T$) is plotted to yield the activation energy /20/. But in the present set of experiments the onset of oxidation could not be determined unambiguously by naked eye and hence the time taken for the complete oxidation of the film was taken as ' t '. To avoid error in ' t ' which might result from this procedure, very thin films were used in these studies as these films will not take much time to complete the oxidation when once it is started.

5.3 RESULTS

Table I summarises the conditions of oxidation and the results obtained when bismuth films are oxidized in air. The corresponding diffractograms (selected) are given in figure 1a-c. β - Bi_2O_3 phase is that described in Powder Diffraction File (PDF) No.27-50 and α - Bi_2O_3 that described in PDF No.27-53.

Table II summarises the conditions of oxidation and the phases obtained when bismuth films are oxidized in super-heated steam. X-ray diffractograms are given in figure 2a-c.

TABLE I

Phases obtained when Bismuth films are oxidized in air

<u>Preparation conditions</u>			
Temper- ature of oxidation (K)	Annealing time in hour	Conditions of heating/ Cooling	Phases obtained
525	Nil	fast heating fast cooling	pure β - Bi_2O_3
550	Nil	fast heating fast cooling	predominantly β - Bi_2O_3 presence of α - Bi_2O_3
565	one	fast heating slow cooling	predominantly β - Bi_2O_3 presence of α - Bi_2O_3
565	one	slow heating fast cooling	predominantly β - Bi_2O_3 presence of α - Bi_2O_3
600	Nil	fast heating fast cooling	predominantly β - Bi_2O_3 presence of α - Bi_2O_3
600	one	fast heating slow cooling	predominantly β - Bi_2O_3 presence of α - Bi_2O_3
640	one	fast heating fast cooling	pure β - Bi_2O_3

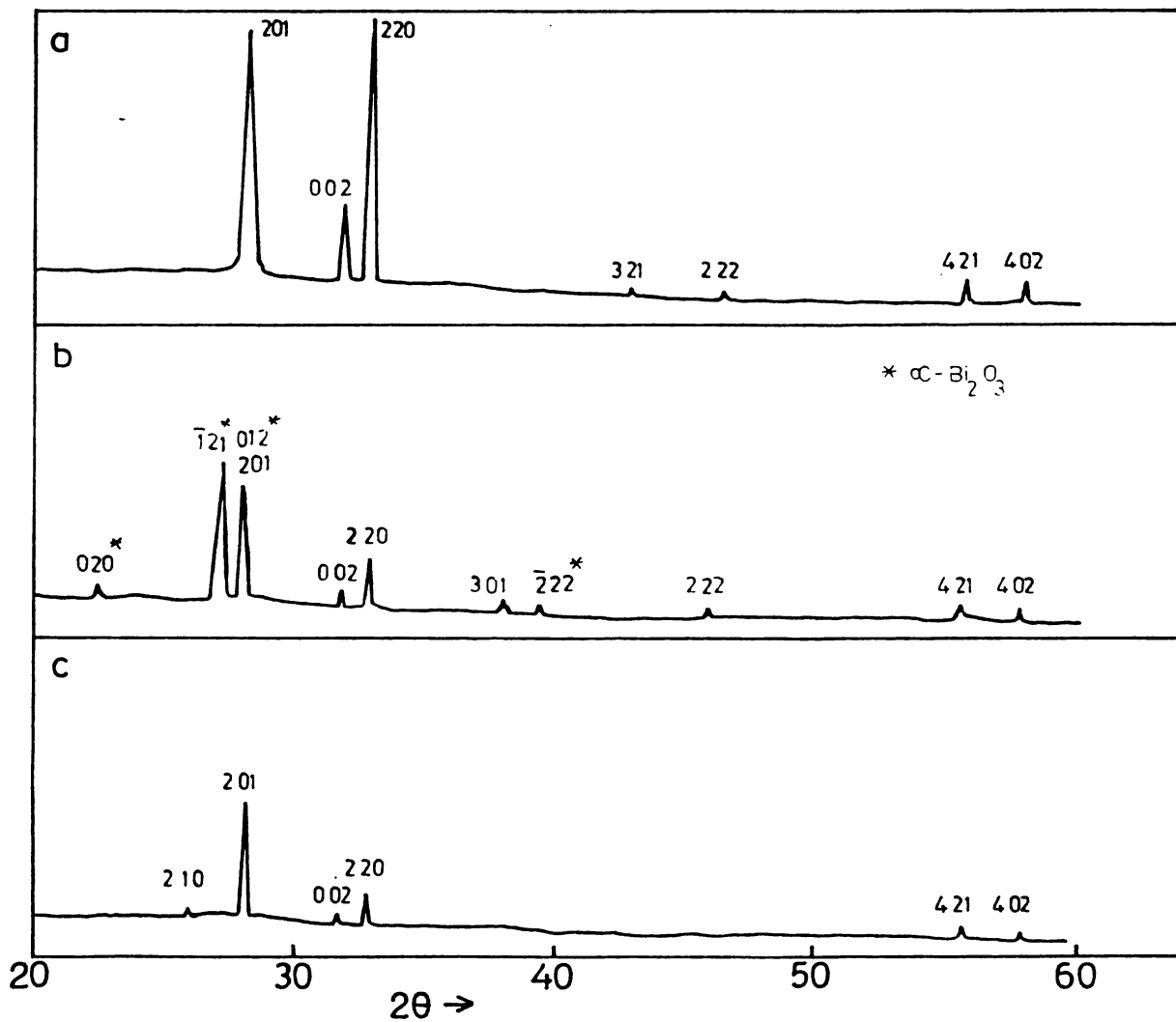


Figure 1. X-ray diffractograms of selected Bismuth oxide films, oxidized in air.

a. oxidation temperature 525 K; b. 550K; c. 640 K
 β - phase lines are shown without astricks.

TABLE II

Phases obtained when Bismuth films are oxidized in superheated steam

Preparation conditions				Phases obtained
Temperature of oxidation (K)	Annealing time in superheated steam in hour	Conditions of heating/cooling	Steam pressure	
525	Nil	fast heating fast cooling	medium	predominantly β - Bi_2O_3 presence of α - Bi_2O_3
550	Nil	fast heating fast cooling	low	equal proportions of α - Bi_2O_3 and β - Bi_2O_3
565	one	fast heating slow cooling without steam	medium	equal proportions of α - Bi_2O_3 and β - Bi_2O_3
565	one	slow heating fast cooling	medium	predominantly α - Bi_2O_3 presence of β - Bi_2O_3
575	Nil	fast heating fast cooling	medium	predominantly α - Bi_2O_3 presence of β - Bi_2O_3
640	one	fast heating fast cooling	medium	α - Bi_2O_3 traces of β - Bi_2O_3
640	half	fast heating slow cooling	maximum	pure α - Bi_2O_3

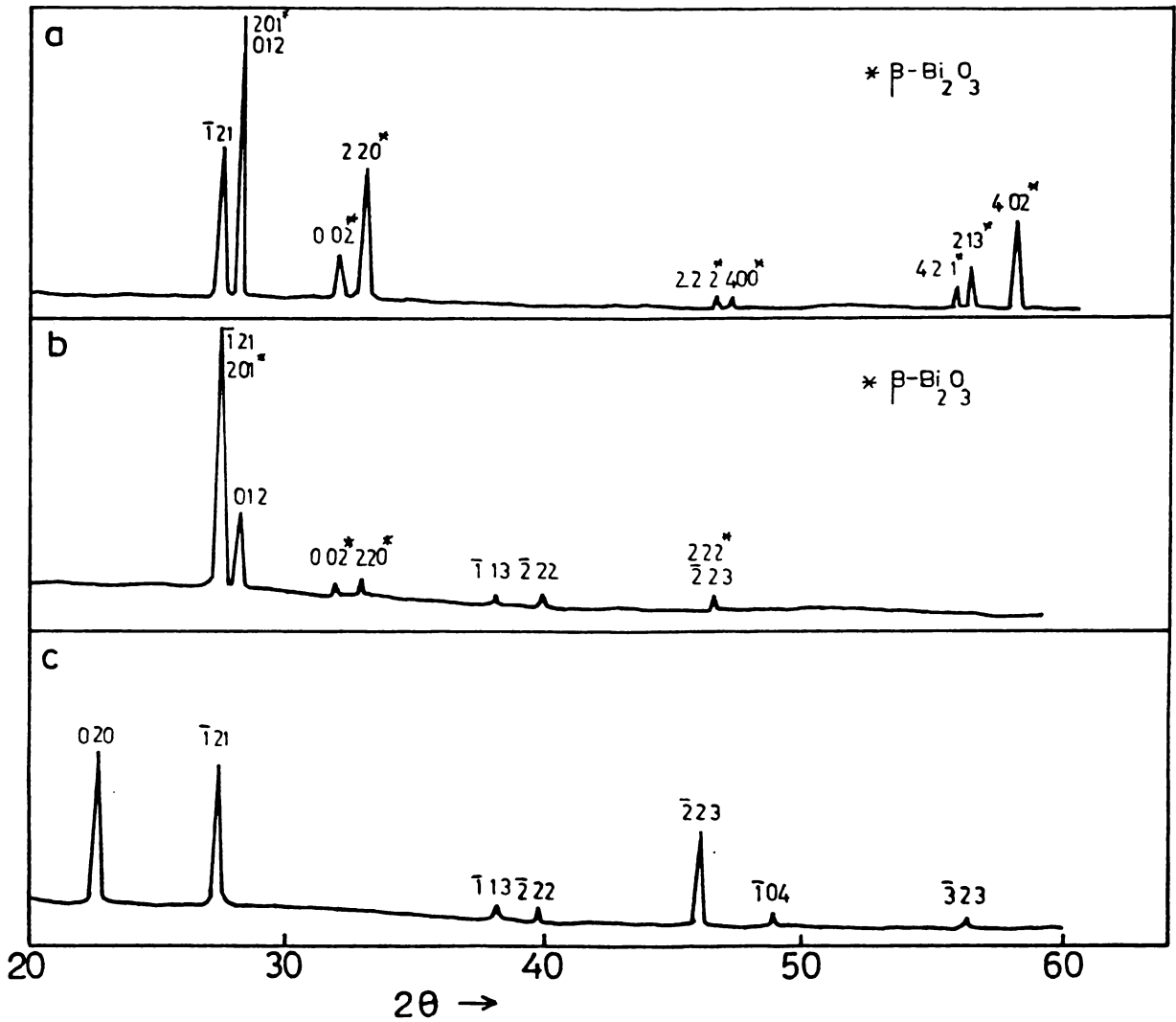


Figure 2. X-ray diffractograms of selected Bismuth oxide films, oxidized in the presence of steam.

a. 525 K; b. 550 K; c. 640 K

α - phase lines are shown without astricks.

Table III summarises the results of conversion between different phases of the oxide films and the diffractograms are given in figure 3a-c. The γ -phase described here is that given by Medernach and Snyder /18/ (BCC, $a_0 = 10.1 \text{ \AA}$).

Pure β - phase films have a transparent yellow appearance and pure α - phase and γ - phase films are completely transparent to visible light.

Figure 4 gives the time taken for the complete oxidation of bismuth films versus the reciprocal of absolute temperature used for oxidation. An activation energy of 1.5 eV for oxidation is obtained when fitted to a relation of the type $t = t_0 \exp (E_a/kT)$. Since at higher temperatures of oxidation in air, α - phase is also formed alongwith β - phase, the value of activation energy obtained may not be the true value of activation energy for the formation of the β - phase. The oxidation experiment was done on about 35 films to obtain a satisfactory value of E_a .

5.4 DISCUSSION

It can be seen from Table I that when bismuth films are oxidized in air at 525 K, pure β - Bi_2O_3 is

TABLE III

Conversion between different phases of Bismuth
oxide films

Preparation conditions	Conversion conditions				Phases obtained
	Temperature of conversion	Presence of air/super-heated steam	Annealing time in hour	Conditions of heating/cooling	
640 K prepared and annealed in air for one hour (β - phase)	640 K	steam	one	fast heating slow cooling in the presence of steam	α - Bi_2O_3
640 K prepared and annealed in super-heated steam for one hour (α - phase)	640 K	air	one	fast heating slow cooling	β - Bi_2O_3 and α - Bi_2O_3
525 K prepared in air (β - phase)	640 K	steam	one	fast heating slow cooling in presence of steam	γ - Bi_2O_3 (BCC)

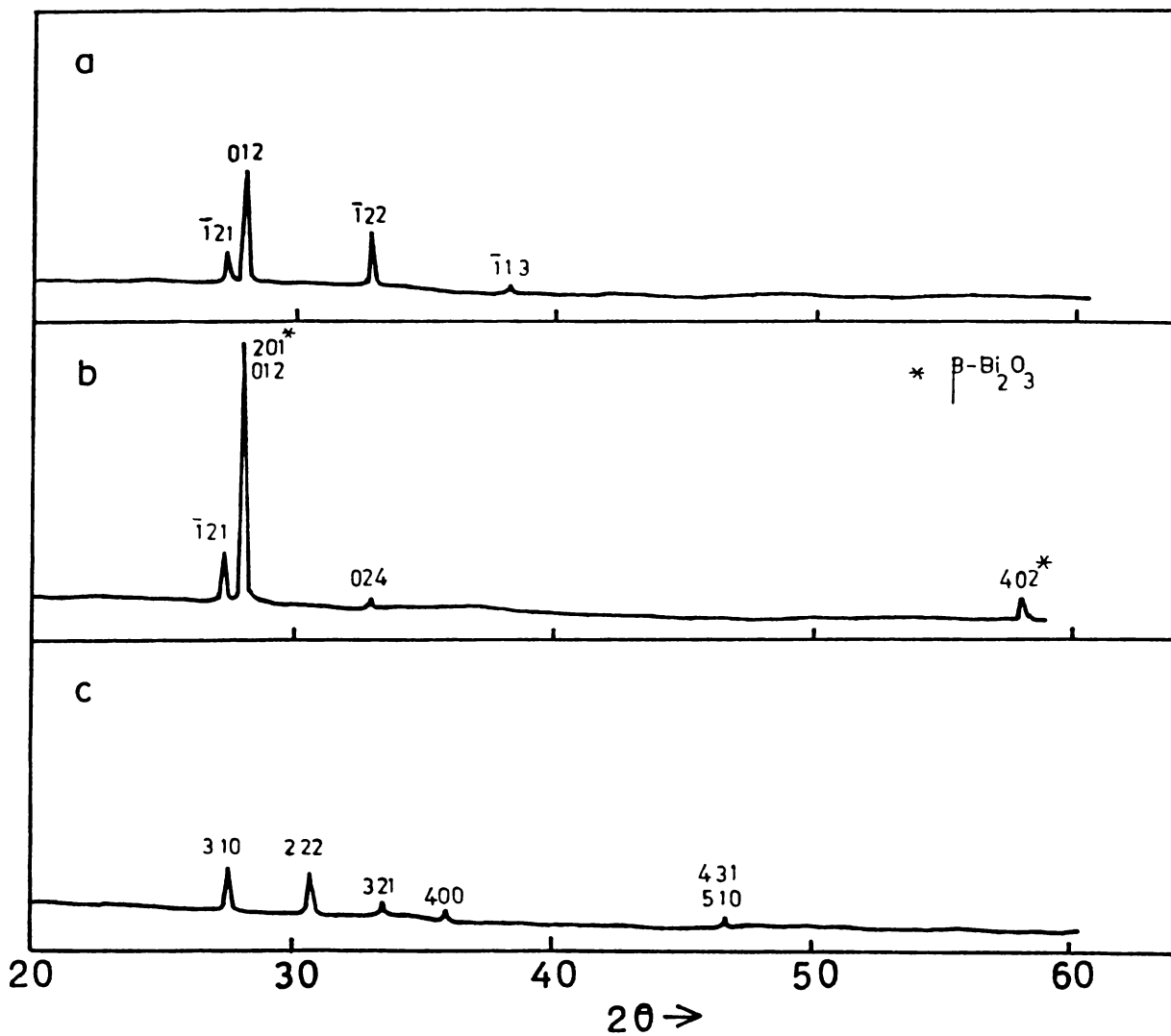


Figure 3. X-ray diffractograms of phase changed films of Bi_2O_3

a. $\beta \rightarrow \alpha$; b. $\alpha \rightarrow \beta$; c. $\beta \rightarrow \gamma$ (see text)

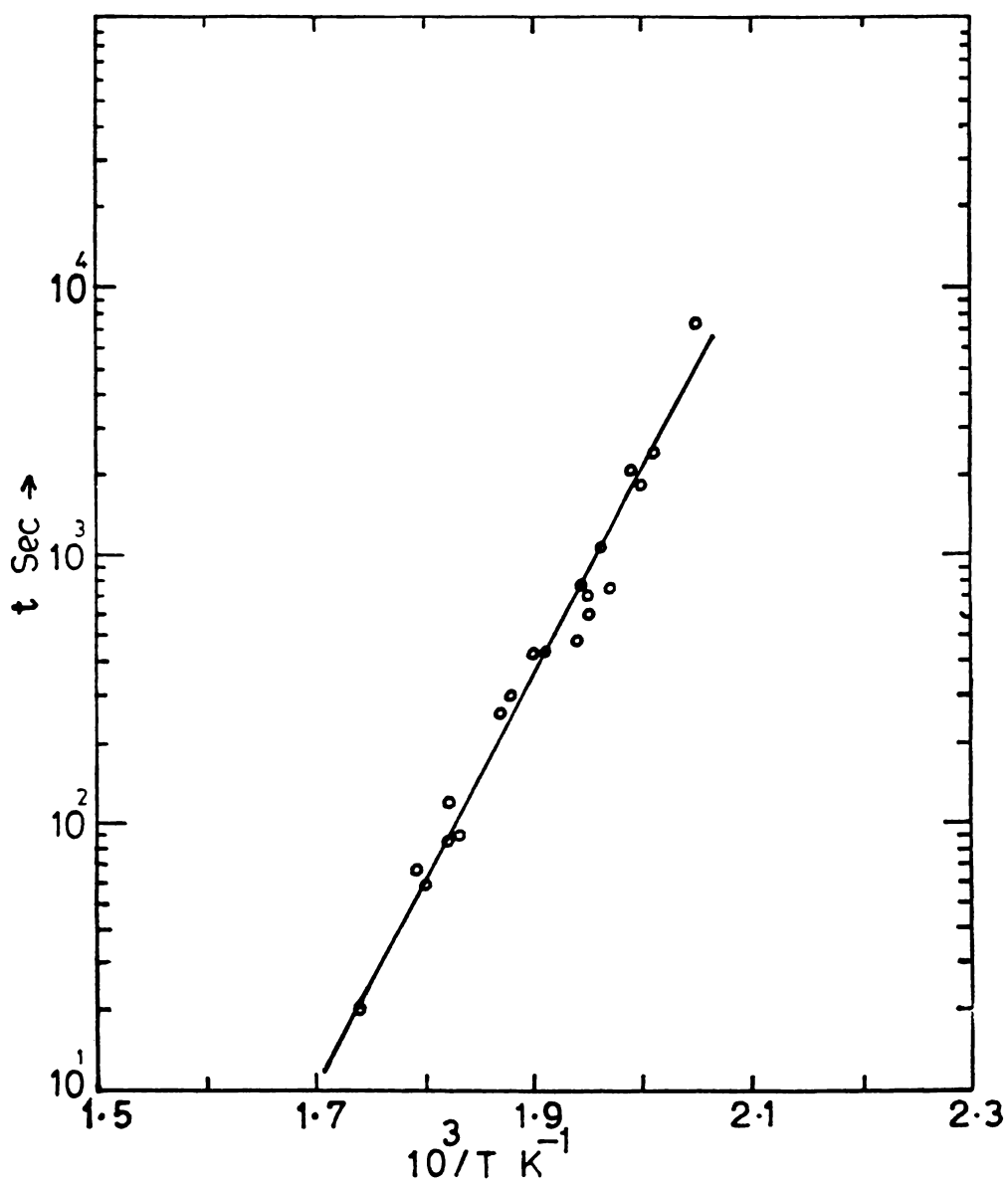


Figure 4. Plot of reciprocal of oxidation temperature versus time.

formed (figure 1a) and as the oxidation temperature is increased, a mixture of β - Bi_2O_3 and α - Bi_2O_3 is formed (figure 1b). In terms of the activation energy for chemical reaction, this may be explained by assuming that a lower activation energy is required for the formation of β - phase than that for the formation of α - phase. So at low temperatures, predominantly β - phase is formed and as the temperature is increased, a mixture of α - and β - phases is formed. Accordingly at higher oxidation temperatures one should get films containing pure α - phase. Experimental evidence do not confirm this (table I). When bismuth films are oxidized in air at 640 K and annealed for one hour at that temperature, pure β - Bi_2O_3 is obtained (figure 1c) instead of α - phase. As such it is clear that there is some other factor besides the activation energy for chemical reaction, which determines the final phase obtained. It will be shown below that it is the availability of oxygen which determines the Bi_2O_3 phase formed.

The activation energy needed for the formation of β - phase is approximately 1.5 eV, Hapase et.al. /3/ gives a value of 1.2 eV for oxidation of bismuth films and it compares favourably with our results. Using Arrhenious relation, the rate of reaction in a chemical

reaction which needs an activation energy of 1.5 eV, is plotted in figure 5. Here the rate of reaction at 500 K is taken as unity. From the curve it may be seen that at 550 K the reaction rate will be 20 times more than that at 500 K. And if the reaction is to continue at the same oxygen concentration as that is available for the reaction at 500 K, the air pressure must be increased 20 times. Since the air pressure is one atmosphere throughout the experiments, there will be deficiency of oxygen as the oxidation temperature of the films are increased and this short supply of oxygen seems to induce the formation of α - phase at higher oxidation temperatures. This is supported by the experimental observations to be described below.

When bismuth films are oxidized at 525 K in super-heated steam (medium pressure) it is seen that predominantly β - phase is formed with some presence of α - phase (figure 2a and table II). As the oxidation temperature is increased, the proportion of α - phase increases. When the films are oxidized in super-heated steam at 640 K and annealed at that temperature for half an hour and cooled in the presence of steam, pure α - phase is obtained. It can safely be assumed that water molecules will not decompose into its components (oxygen and

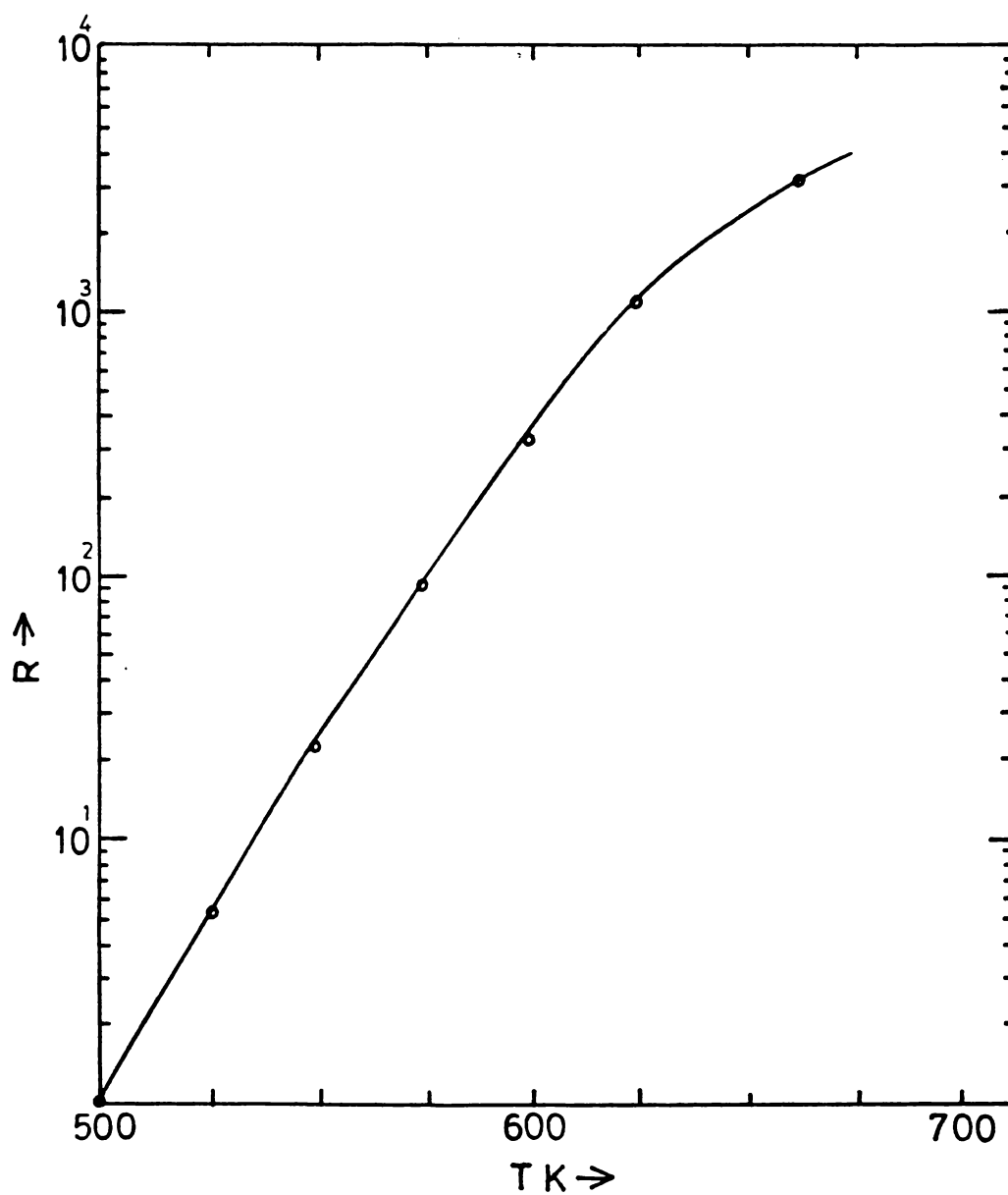


Figure 5. Rate of reaction R (in arbitrary units) versus temperature for a chemical reaction which needs an activation energy of 1.5 eV. Reaction rate at 500 K is taken as unity.

hydrogen) when heated to 640 K. The only effect of high temperature steam would be to displace the air present in the chamber considerably thereby reducing the effective oxygen concentration. It may also be noted that as the oxidation temperature is increased from 520 K, the rate of reaction (whatever be the activation energy) increases thereby necessitating a higher supply of oxygen. And so the percentage of α - phase increases as the oxidation temperature is increased. From this it can certainly be said that the deficiency of oxygen promotes the formation of the α - phase. When the steam pressure is reduced to medium pressure, (so that the concentration of air is increased) keeping the oxidation temperature at 640 K and even after an annealing for one hour in the presence of steam, trace quantities of β - phase still remains (table II). So it is clear that oxidation at any particular temperature in the presence of large quantities of air, always promotes the formation of β - phase, whereas oxidation in a medium which is deficient in oxygen always promotes the formation of α - phase. Again regarding the formation of β - phase at low oxidation temperatures in the presence of steam it can be seen that at low oxidation temperatures the rate of

chemical reaction is low (figure 5) and the supply of oxygen is sufficient to form β - Bi_2O_3 . But as the oxidation temperature is increased, the rate of chemical reaction increases and the oxygen supply will not be sufficient to make the whole film converted to β - phase. At 640 K with maximum steam pressure, we have only the α - phase.

To test the above model, bismuth films were oxidized in oxygen lean atmospheres created by evacuating the oxidation chamber to pressure down to 10^{-1} Torr. α - phase films were obtained when the pressure was ~ 10 Torr and this was confirmed by x-ray diffraction. For pressure above ~ 10 Torr, a mixture of α - phase and β - phase bismuth oxide was formed. Selected x-ray diffractograms are shown in figure 6a-c. This conclusively shows that oxygen lean atmospheres leads to the formation of α - phase and steam has no effect on the reaction other than displacing the air in the reaction chamber.

Formation of β - phase in an oxygen rich atmosphere and α - phase in an oxygen deficient atmosphere has been observed in the preparation of Bi_2O_3 films by activated reactive evaporation, which is discussed in detail in chapter VII.

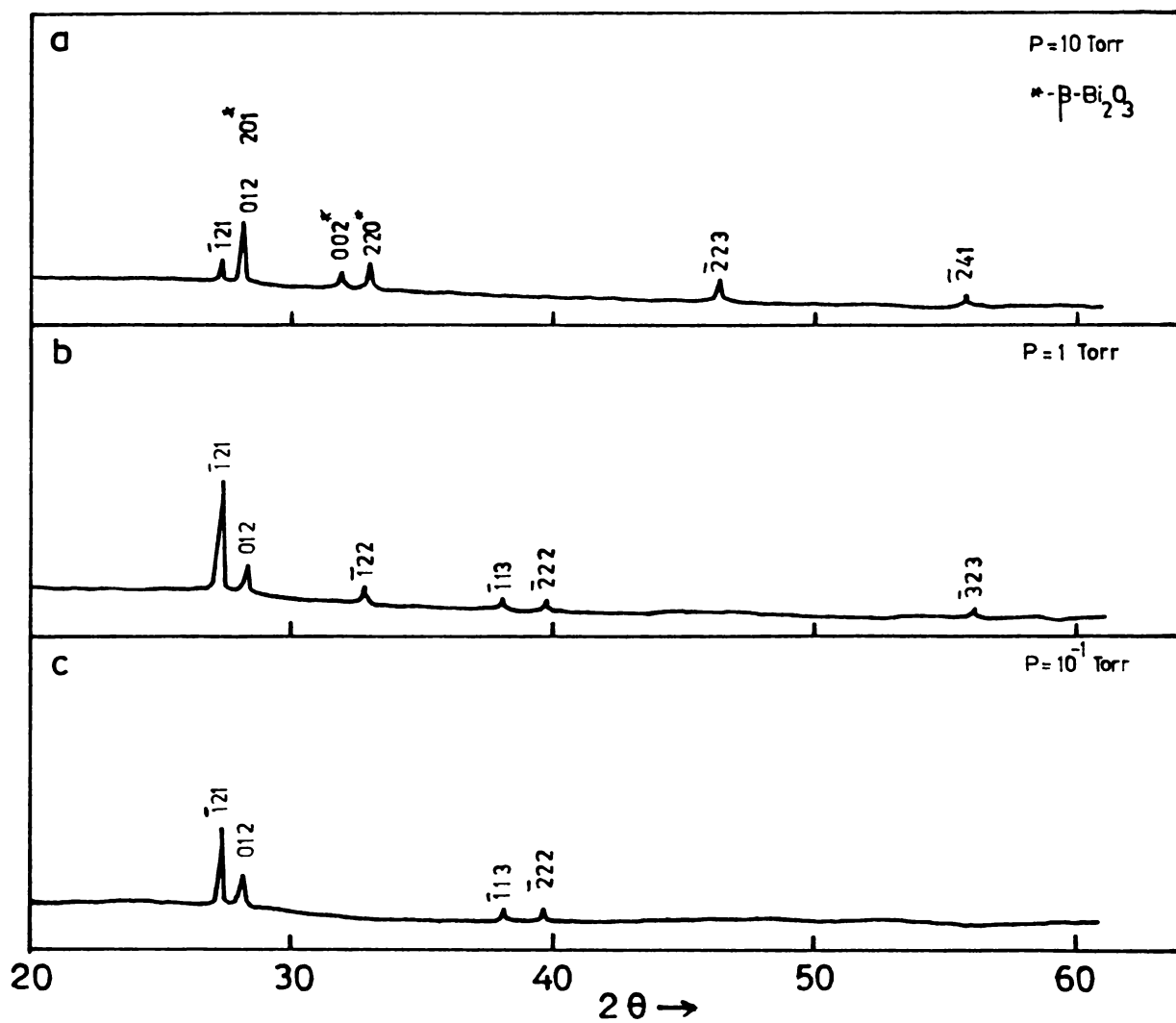


Figure 6. X-ray diffractograms of selected Bismuth oxide films, oxidized in partial vacua at 560 K
 a. 10 Torr; b. 10^0 Torr; c. 10^{-1} Torr
 · β - phase lines are shown with astricks.

Figure 3a shows that when a film prepared and annealed in air at 640 K (β - phase), is further annealed for one hour in steam, it is converted completely to α - phase (table III). This shows that a β - phase film can be converted to α - phase simply by heating it in an oxygen deficient atmosphere. Table III shows that even after one hour annealing in air, the α - phase film is not fully converted to β - phase (figure 3b). This may be due to the reported low temperature stability of the α - phase compared to the β - phase /15/.

The formation of pure β - Bi_2O_3 when bismuth film is annealed in air at 640 K (table I) is due to the conversion of α - phase in the mixture to β - phase on continued intake of oxygen at the high temperature. It has been reported by many authors that β - phase is the most oxygen rich of the various Bi_2O_3 phases.

Bismuth films oxidized in air at 525 K (β - phase) when heated to 640 K for one hour in steam and then cooled in the presence of steam, is completely converted to γ - phase (table III). Figure 3c shows the X-ray diffraction actogram of such a film. This means that there is some difference in the β - phases formed at 525 K and at 640 K which cannot be distinguished by X-ray diffraction.

Chemical analysis of the present β - phase films were not carried out to determine whether the β - phase obtained have the same chemical composition Bi_2O_3 or a variation like $\text{Bi}_2\text{O}_{2.5}$ as reported by Zav'yalova and Imamov /6/. But Medernach /21/ has shown that X-ray diffraction methods alone cannot differentiate between β - Bi_2O_3 and β - $\text{Bi}_2\text{O}_{2.5}$. By incorporating optical absorption measurements, electron microprobe and chemical analysis, he has shown that the β - form may be expressed as β - $\text{Bi}_2\text{O}_{3-x}$, since β - $\text{Bi}_2\text{O}_{2.5}$ is not an independent phase as suggested by Zav'yalova and Imamov /6/, but only on a non-stoichiometric β - Bi_2O_3 . How this factor contributes to the formation of γ - phase is not clear at present.

5.5 CONCLUSION

Single phase films of α - Bi_2O_3 , β - Bi_2O_3 , and γ - Bi_2O_3 have been prepared by oxidizing bismuth films. Bismuth films when oxidized and annealed in an oxygen rich atmosphere results in the formation of β - Bi_2O_3 whereas in an oxygen deficient atmosphere, α - Bi_2O_3 is produced. β - Bi_2O_3 films can easily be converted to α - phase by heating them in an oxygen deficient atmosphere and α - phase can be converted to β - phase by heating α - phase in an oxygen rich atmosphere.

REFERENCES

1. P.S. Aggarwal and A. Goswami, *Z. Naturforsch.*, Teil A. 13 (1958) 885.
2. A.A. Zav'yalova, R.M. Imamov, and Z.G. Pinsker, *Sov. Phys. Crystallogr.*, 9 (1965) 724.
3. M.G. Hapase, V.B. Tare, and A.B. Biswas, *Acta Metallurgica*, 15 (1967) 131.
4. M.G. Hapase, V.B. Tare, and A.B. Biswas, *Indian J. Pure. Appl. Phys.*, 5 (1967) 401.
5. A.A. Zav'yalova and R.M. Imamov, *Sov. Phys. Crystallogr.*, 13 (1968) 37.
6. A.A. Zav'yalova and R.M. Imamov, *Sov. Phys. Crystallogr.*, 16 (1971) 437.
7. A.A. Zav'yalova and R.M. Imamov, *Sov. Phys. Crystallogr.*, 17 (1972) 811.
8. S.K. Sharma and S.L. Pandey, *Thin Solid Films*, 62 (1979) 209.
9. S. Singh, S.L. Pandey, and R.N. Saxena, *Phys. Stat. Sol. (a)*, 54 (1979) K 91.
10. R.N. Saxena, S.L. Pandey, Sooraj Singh, and S.K.Sharma, *Indian J. Phys.*, 53A (1979) 257.
11. A. Rahman and P.C. Mahanta, *Indian J. Pure. Appl. Phys.*, 12 (1974) 815.

12. S.K. Saha, Indian J. Pure. Appl. Phys., 17 (1979) 185.
13. S.P.S. Arya and H.P. Singh, Thin Solid Films, 62 (1979) 353.
14. S.L. Pandey, S. Singh, and R.N. Saxena, Indian J. Pure. Appl. Phys., 18 (1980) 452.
15. W.C. Schumb and E.S. Rittner, J. Am. Chem. Soc., 65 (1943) 1055.
16. E.M. Levin and R.S. Roth, J. Res. Nat. Bur. Standards, Ser. A, 68 (1964) 189.
17. L.P. Fomchenkov, A.A. Maier, and N.A. Gracheva, Inorg. Mater., 10 (1974) 1733,
18. J.W. Medernach and R.L. Snyder, J. Am. Ceramic Soc., 61 (1978) 494.
19. J. George, K.S. Joseph and C.K. Valsalakumari, Int. J. Electronics, 52 (1982) 299.
20. J. George and K.S. Joseph, Solid State Commun., 46 (1983) 541.
21. J.W. Medernach, J. Solid State Chem., 15 (1975) 352.

CHAPTER VI

BISMUTH OXIDE FILMS PREPARED BY REACTIVE
EVAPORATION6.1 INTRODUCTION

Bismuth oxide films have been used as good dielectric films in many applications like optical coatings, Schottky barrier solar cells and also in MIS capacitors /1-6/. These films are physically robust but suffer from the possibility of easy chemical reaction with acids /6/. Thermal evaporation of bismuth oxide is rather difficult due to the fact that molten bismuth oxide attacks almost all crucible materials except platinum /7, 8/. Reactive sputtering in an atmosphere of oxygen and argon has been successfully employed to get good quality films of bismuth oxide and the optical properties of these films have been extensively studied /4, 6, 9, 10/. Another method of obtaining bismuth oxide films is by the thermal oxidation of bismuth films /11, 12/. The films obtained by this method are rather poor in quality and often are a mixture of the different phases of bismuth oxide.

Methods have been worked out to obtain single phase films of bismuth oxide from bismuth films and are discussed in detail in chapter V.

Another method which can yield good quality films of bismuth oxide is the reactive evaporation where bismuth is evaporated into an atmosphere of oxygen /13/. Unfortunately the rate of deposition reported in this case is very low (0.05 Å/Sec to 0.2 Å/Sec). In this chapter is reported the preparation of bismuth oxide films by reactive evaporation at different substrate temperatures and bismuth evaporation rates. Deposition rates from 3 Å/Sec to 20 Å/Sec have been obtained.

6.2 EXPERIMENTAL

Details of the preparation of bismuth oxide films by reactive evaporation is given in chapter III, 3.8. The following deposition conditions, calculated using equations (3.8.2) and (3.8.3), were used for the preparation of the films:

Bismuth impingement rate = $8.5 \times 10^{14} - 5.6 \times 10^{15}$ atoms $\text{cm}^{-2} \text{Sec}^{-1}$

Oxygen impingement rate $\approx 3.6 \times 10^{17}$ molecules $\text{cm}^{-2} \text{Sec}^{-1}$

Substrate temperature was varied from 300 K to 575 K in 50 K interval.

Annealing in air was performed in the specially designed furnace described in chapter III, 3.7. The specimens were slowly heated to the annealing temperature and maintained at that temperature for one hour, and cooled slowly. Vacuum annealing was done in the high vacuum system itself in which the film was prepared, at a pressure of $\approx 10^{-5}$ Torr.

X-ray diffraction studies were performed on samples of film thickness $\approx 2500 \text{ \AA}$. An accelerating potential of 25 KV and a tube current of 14 mA were used for the x-ray diffractometer.

6.3 RESULTS AND DISCUSSION

Reactive evaporation was performed at different substrate temperatures (T_s) and bismuth evaporation rates. Deposition rate of bismuth oxide films varied from 2 $\text{\AA}/\text{Sec}$ to 20 $\text{\AA}/\text{Sec}$ and the substrate temperature from 300 K to 575 K. Beyond $T_s = 575 \text{ K}$ no deposit was obtained. Table I gives the substrate temperature, rate of deposition and the phases obtained for a few of the typical samples. Figure 1 gives the corresponding x-ray diffractograms. It can be seen that the films prepared below a substrate temperature of 400 K are amorphous in nature

TABLE I

Preparation conditions and phases obtained in the
case of RE

Specimen	Sub. Temp. K	Rate of deposition Å/S	Phases obtained
a	300	3.0	Amorphous
b	475	4	β - Bi ₂ O ₃
c	560	4	β - Bi ₂ O ₃
d	300	6.7	Amorphous
e	475	20	β - Bi ₂ O ₃
f	560	18	β - Bi ₂ O ₃

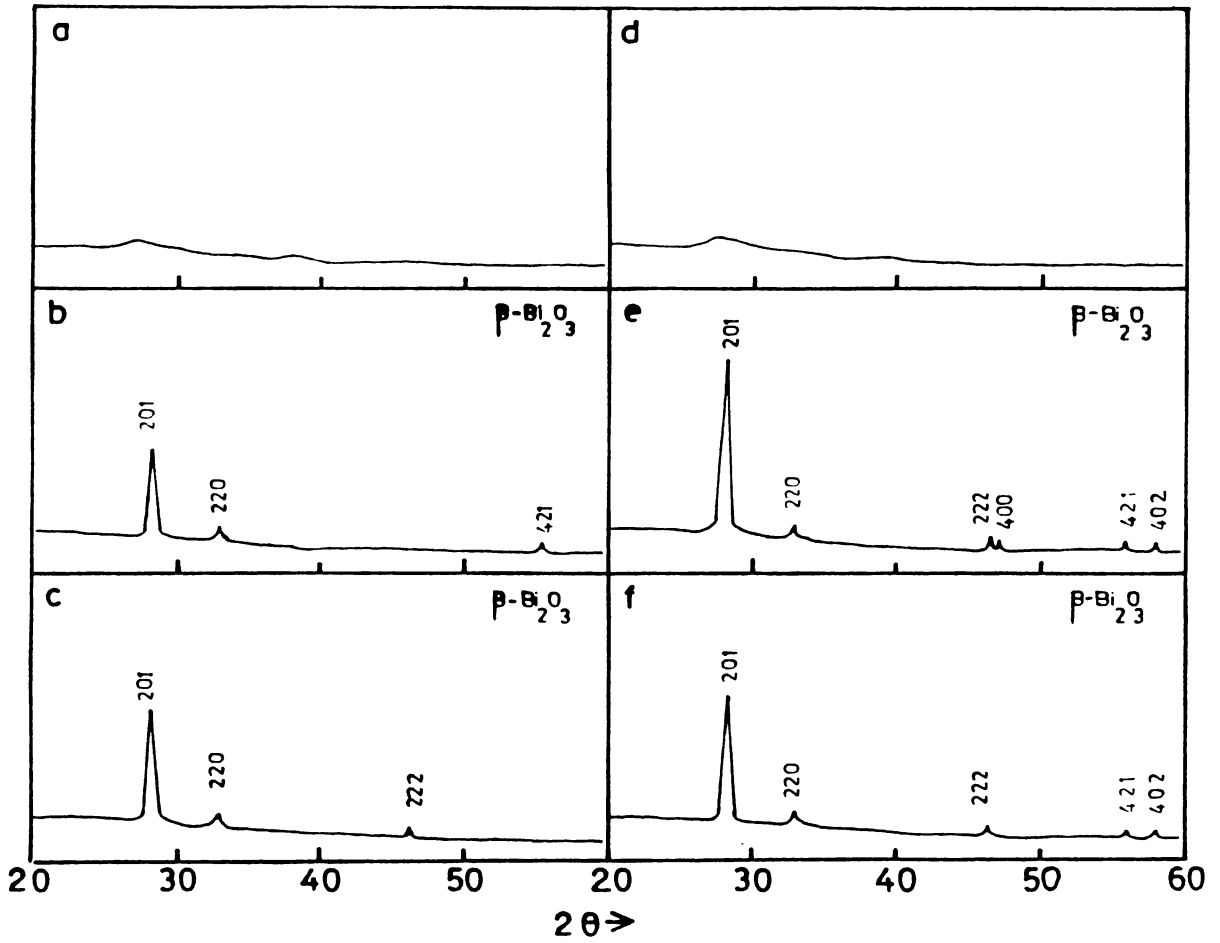


Figure 1. X-ray diffractogram of films prepared by reactive evaporation. a-f referring to the specimens indicated in table I.

(figure 1a & 1d). As the substrate temperature was increased further, polycrystalline films of bismuth oxide were formed. The films thus obtained were of tetragonal phase (β -Bi₂O₃, PDF No. 27-50).

These films had poor optical transmission. Figure 2 shows the transmission spectra of two typical samples of bismuth oxide prepared by reactive evaporation at different substrate temperatures on optically flat glass substrates. The films obtained were of yellow in colour. At low deposition rate ($\approx 2\text{\AA}/\text{Sec}$) fairly good quality films were obtained. When the deposition rate was increased the optical transmission of the films were found to decrease.

Only Milch /13/ has reported the reactive evaporation of bismuth in an oxygen atmosphere. He used a lower oxygen pressure of $7.5 - 9 \times 10^{-4}$ Torr, which is less than the pressure used in the present case. But the deposition rate of his films were very low, ie. $0.05 - 0.2 \text{\AA}/\text{Sec}$. Comparing this with the rate of deposition used in the present case ($\sim 10 \text{\AA} / \text{Sec}$), it is not surprising that the film quality in the present case is poor. At high deposition rate used, bismuth will not be

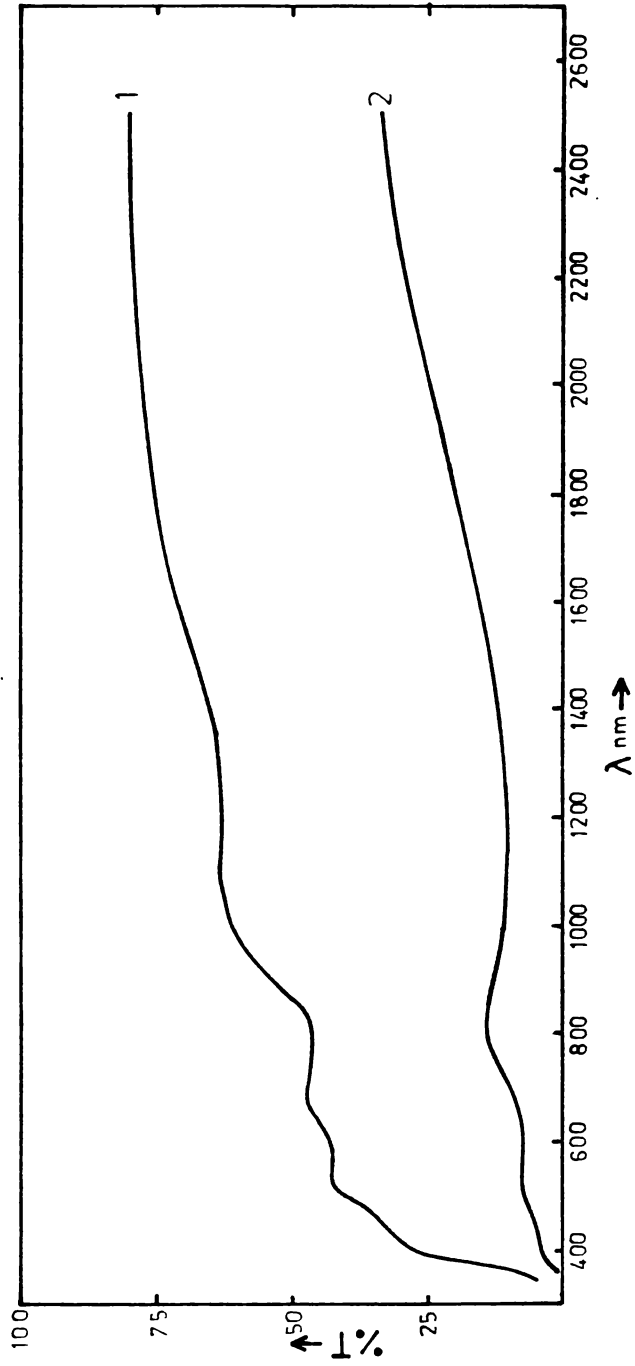


Figure 2. Transmission spectra of two typical samples (1) $T_s = 550$ K, (2) $T_s = 300$ K.

reacting rapidly enough with oxygen on the surface of the substrate, as the activation energy for the formation of β - Bi_2O_3 is 1.2 eV /14/. From our measurements also it is found to be 1.5 eV (Chapter V). Hence in the present films, the possibility of unreacted bismuth getting entrapped in the growing film is rather high and consequent optical absorption.

Milch /13/ has also reported that no bismuth oxide films are obtained when the substrate temperature is greater than the melting point of bismuth. In the present case also no films are obtained, when the substrate temperature is increased beyond this range. This is probably because of the reevaporation of bismuth atoms from the substrate surface before it reacts with adsorbed oxygen molecules to form bismuth oxide at these elevated temperatures.

6.4 ANNEALING OF FILMS

The films prepared by reactive evaporation at substrate temperatures of 300 K and 475 K were used for annealing studies. Table II summarises the results of high temperature annealing of the bismuth oxide films. The corresponding x-ray diffractograms are given in figure 3. Air annealing was performed at 635 K for one hour and high vacuum annealing was performed at 700 K for one hour in a vacuum $\approx 10^{-5}$ Torr. It can be seen

TABLE II

Results of annealing of RE prepared films

Specimen	Film preparation conditions			Annealing	phases obtained
	Sub. Temp. K	Rate of deposition Å/S	Heat Treatment		
a	300	3.2	-	for one hour in high vacuum at 700 K	α -Bi ₂ O ₃ traces of β -Bi ₂ O ₃
b	300	3.2	annealed for one hour in high vacuum at 700 K	for one hour in air at 635 K	β -Bi ₂ O ₃
c	475	4.3	-	for one hour in high vacuum at 700 K	α -Bi ₂ O ₃
d	475	4.3	annealed for one hour in high vacuum at 700 K	for one hour in air at 635 K	α -Bi ₂ O ₃ & β -Bi ₂ O ₃

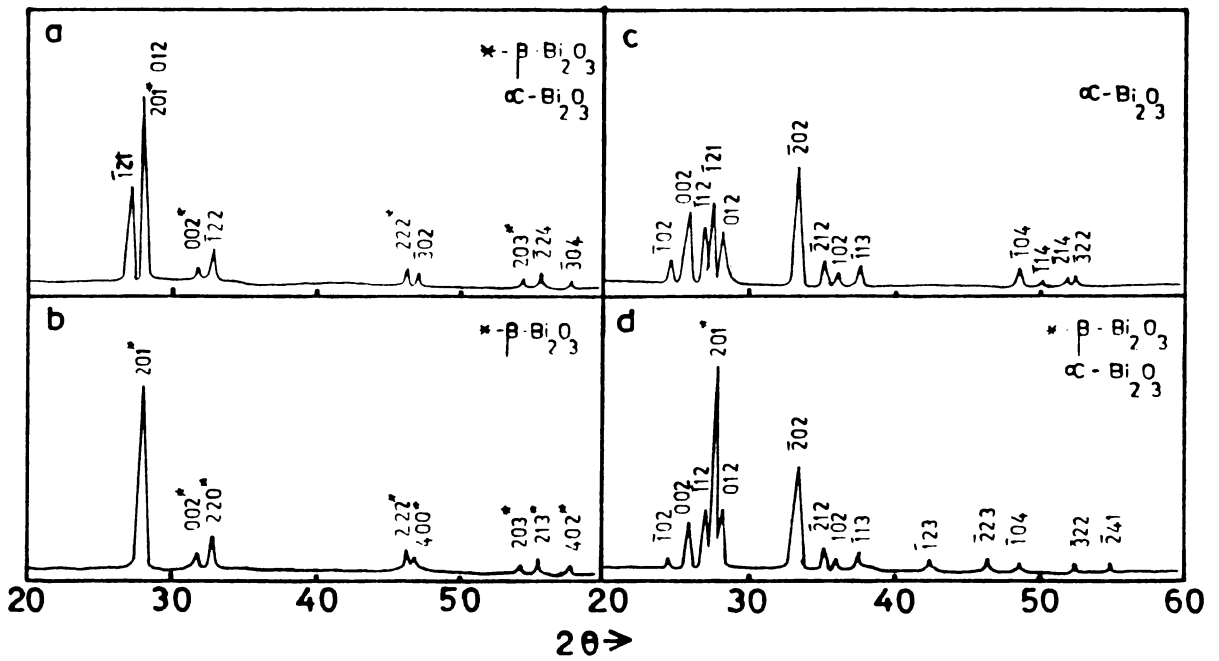
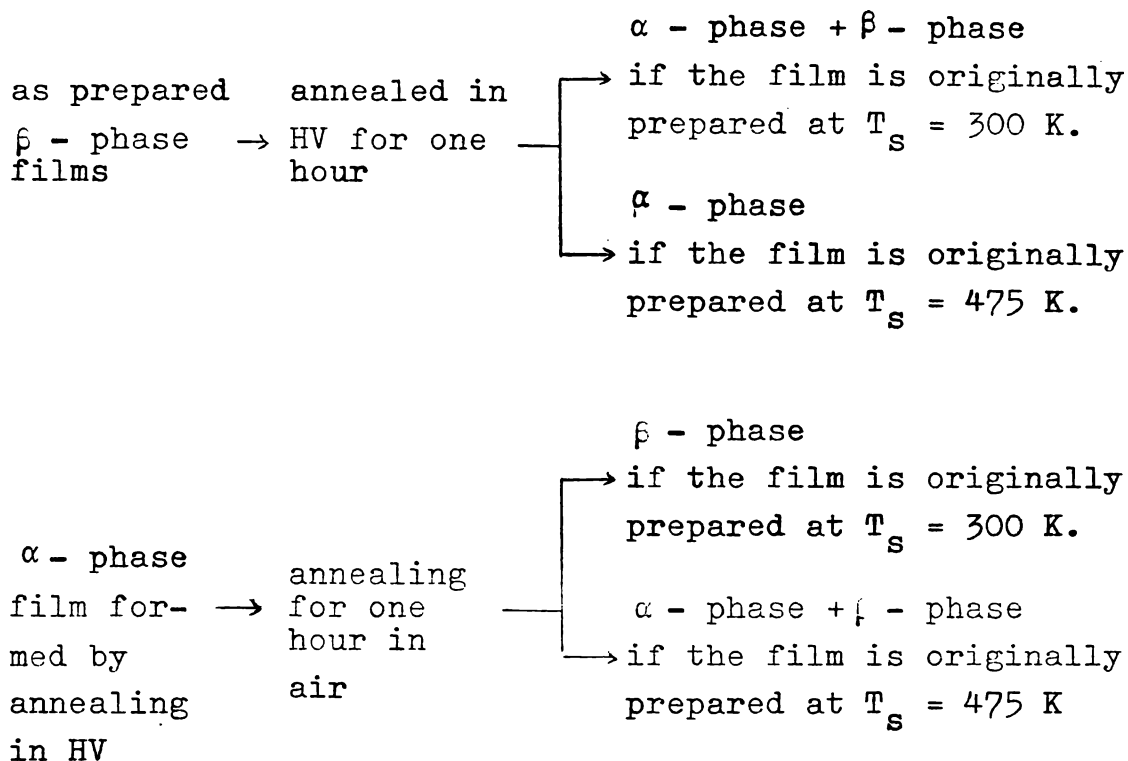


Figure 3. X-ray diffractograms of RE prepared films annealed in air and high vacuum. a-d referring to specimens shown in table II.

from Table II that when an amorphous β - phase film is annealed in high vacuum, it is converted to the α - phase, with some traces of β - phase. This shows that when an amorphous bismuth oxide film is annealed in high vacuum, it is first converted to crystalline β - phase and on further annealing, the relative oxygen deficient α - phase is formed. When the α - phase film so obtained is again annealed in air, the oxygen rich β - phase film is formed.

When crystalline β - phase film is annealed in high vacuum, it is fully converted to α - phase. This is probably due to the outward diffusion of oxygen. But when the α - phase films so obtained are annealed again, in air, they are not fully converted to β - Bi_2O_3 . This may be due to the reported /15/ low temperature stability of the α - phase of bismuth oxide.

The above results of the annealing experiments conducted on bismuth oxide films can be summarized as follows:



The difference between β - phase films prepared onto substrates kept at two different temperatures can only be in their respective grain size. Room temperature prepared films will be amorphous in nature and when they crystallize, their grain size will be small compared to films prepared at high substrate temperature. It is not clear at present how the difference in grain size produce different final phases under annealing.

6.5. CONCLUSION

Only β - phase films are formed by reactive

evaporation. When β - phase films are annealed in an oxygen deficient atmosphere (high vacuum), α - phase films are obtained. α - phase films are stable compared to β - phase films except in ~~the~~ case of very small grained α - phase films

REFERENCES

1. K. Hammer, *Optik.*, 3 (1948) 495.
2. E.J. Gillham and J.S. Preston, *Proc. Phys. Soc. B*, 65 (1952) 649.
3. L. Holland and T. Putner, *J. Sci. Instrum.*, 36 (1959) 81.
4. P.B. Clapham, *Brit. J. Appl. Phys.*, 18 (1967) 363.
5. E.V. Wang and K.A. Pandelisev, *J. Appl. Phys.*, 52 (1981) 4818.
6. T.A. Raju and A.S. Talwai, *J. Appl. Phys.*, 52 (1981) 4877.
7. J.W. Mellor, "A Comprehensive Treatise on Inorganic and Theoretical Chemistry", Vol.IX, p.646, Longman, Green and Company, New York, (1922).
8. L.G. Sillen, *Ark. Kemi.*, 18 (1937) 1.
9. K.Spring and Barton, *Vacuum*, 4 (1954) 20.
10. M.L. Lieberman and R.C. Medrud, *J. Electrochem. Soc.*, 116 (1969) 242.
11. P.S. Aggarwal and A. Goswami, *Z. Naturforsch, Teil A*, 13 (1958) 885.
12. A.A. Zav'yalova, R.M. Imamov and Z.G. Pinsker, *Sov. Phys. Crystallogr.*, 9 (1965) 724.

13. A. Milch, *Thin Solid Films*, 17 (1973) 231.
14. M.G. Hapase, V.B. Tare and A.B. Biswas, *Acta Metallurgica*, 15 (1967) 131.
15. W.C. Schumb and E.S. Rittner, *J. Am. Chem. Soc.*, 65 (1943) 1055.

CHAPTER VII

BISMUTH OXIDE FILMS PREPARED BY ACTIVATED
REACTIVE EVAPORATION7.1 INTRODUCTION

Two methods of preparation of bismuth oxide films are discussed in detail in chapter V and VI. In chapter V is reported the preparation of bismuth oxide films by the oxidation of bismuth films. But the films obtained by this method are poor in quality because of the strain caused by the heating and cooling of the films and it is impossible to obtain optical quality films. Another method of preparation is the reactive evaporation, where bismuth is evaporated into an atmosphere of oxygen /1/. Here, although fairly good quality films have been obtained, unfortunately, the rate of deposition is rather low (0.05 Å/Sec to 0.2 Å/Sec). When high deposition rates are used, as described in chapter VI films of poor optical quality, with high optical absorption, are only obtained even at high substrate temperatures. The high optical absorption is due to the presence of unoxidized bismuth in the films prepared. So it was thought that a method which will completely oxidize the bismuth atoms during their

deposition will yield good quality films of bismuth oxide. The obvious choice is the activated reactive evaporation (ARE) perfected by R.F. Bunshah of UCLA /2/. In this method the reactive gas is activated by an electric discharge obtained with the help of a low voltage electron gun and a magnetic field. A slightly modified technique, which dispenses with the magnetic field, has been used here to deposit good quality films of bismuth oxide. In this chapter is reported the deposition conditions and also the phases obtained by ARE and the change of phases of bismuth oxide of different annealing conditions.

7.2 EXPERIMENTAL

The deposition of bismuth oxide films was performed in the vacuum system discussed in chapter III, 3.9. The system was first evacuated to $\sim 2 \times 10^{-5}$ Torr. Then the substrates were heated to the required temperature. Optically flat glass substrates of dimensions 3.5 cm x 2.4 cm x 0.1 cm were used as the substrates. After the substrates attaining the required temperature, it was allowed to remain at that temperature for 15 minutes for stabilizing the temperature. Then oxygen was admitted to the work chamber through a narrow tube. Industrial grade

oxygen was used as the reactive gas. The pressure inside the chamber was controlled by adjusting the flow of oxygen through the narrow tube by the needle valve. Then the high tension supply to the anode was switched on and the filament supply was also switched on. Then the current through the tungsten filament was increased slowly till a bluish glow appeared between the cathode and anode.

Oxygen partial pressure inside the chamber was so adjusted that the glow filled the whole chamber. The discharge current was maintained between 1.6 A and 2 A by adjusting the emission of the tungsten filament. The pressure inside the chamber was maintained at $\approx 5 \times 10^{-4}$ Torr. Current through the bismuth source containing 5 N purity bismuth was then switched on and slowly increased. The source current was adjusted to get the required flux of bismuth. During deposition, some oxygen would be consumed and hence a slight adjustment of needle valve was required to maintain the plasma. The following deposition conditions, calculated using equations (3.8.2) and (3.8.3) were used to deposit the bismuth oxide films.

β - phase films:

$$\text{Bismuth impingement rate} = 3.4-5.6 \times 10^{25} \text{ atom cm}^{-2} \text{ sec}^{-1} \quad (7.2.1)$$

$$\text{Oxygen impingement rate} \approx 1.8 \times 10^{20} \text{ molecules cm}^{-2} \text{ Sec}^{-1} \quad (7.2.2)$$

α - phase films:

$$\text{Bismuth impingement rate} = 1.1-1.5 \times 10^{16} \text{ atoms cm}^{-2} \text{Sec}^{-1} \quad (7.2.3)$$

$$\text{Oxygen impingement rate} \approx 1.8 \times 10^{18} \text{ molecules cm}^{-2} \text{Sec}^{-1} \quad (7.2.4)$$

Substrate temperature was varied from 300 K to 675 K in steps of 25 K.

Annealing of the samples were done in the specially constructed furnace (discussed in chapter III, 3.7). The specimens were slowly heated to the annealing temperature, then maintained at that temperature for one hour before cooling slowly to room temperature. High vacuum annealing was done in the same vacuum system in which the specimens were prepared. During vacuum annealing, pressure was maintained at $\approx 10^{-5}$ Torr.

X-ray diffraction studies were performed with the x-ray diffractometer discussed in chapter III, 3.4. Films $\approx 5000 \text{ \AA}$ thick were used for the x-ray diffraction studies. A tube current of 14 mA and an accelerating

potential of 25 KV was used for the diffraction study. The diffraction pattern obtained was compared with the powder diffraction file.

7.3 RESULTS AND DISCUSSION

Activated reactive evaporation was done at various substrate temperatures and deposition rates. In the case of reactive evaporation films will not be obtained if the substrate temperature is maintained above the melting point of bismuth. Here, films could be obtained at substrate temperatures as high as 650 K. The deposition rate was also varied from 10 Å/Sec to 52 Å/Sec. Table I summarizes the conditions of deposition and the phases obtained. The corresponding x-ray diffractograms are shown in figure 1. It is seen that the films obtained at low substrate temperatures are amorphous in nature to x-ray diffraction (figures 1a & d). As the substrate temperature was increased, the films crystallize, resulting in polycrystalline films.

It can be seen from Table I that low rates of deposition (< 20 Å/Sec) always gives β - Bi_2O_3 (PDF No.27.50) films, whereas high rates of deposition

TABLE I

Preparation conditions and phases obtained in ARE

Speci- men	Sub. Temp. K	Rate of de- position Å/S	Phases obtained
a	300	12	Amorphous
b	475	14	β - Bi_2O_3
c	650	7	β - Bi_2O_3
d	300	38	Amorphous
e	510	48	α - Bi_2O_3
f	660	52	α - Bi_2O_3

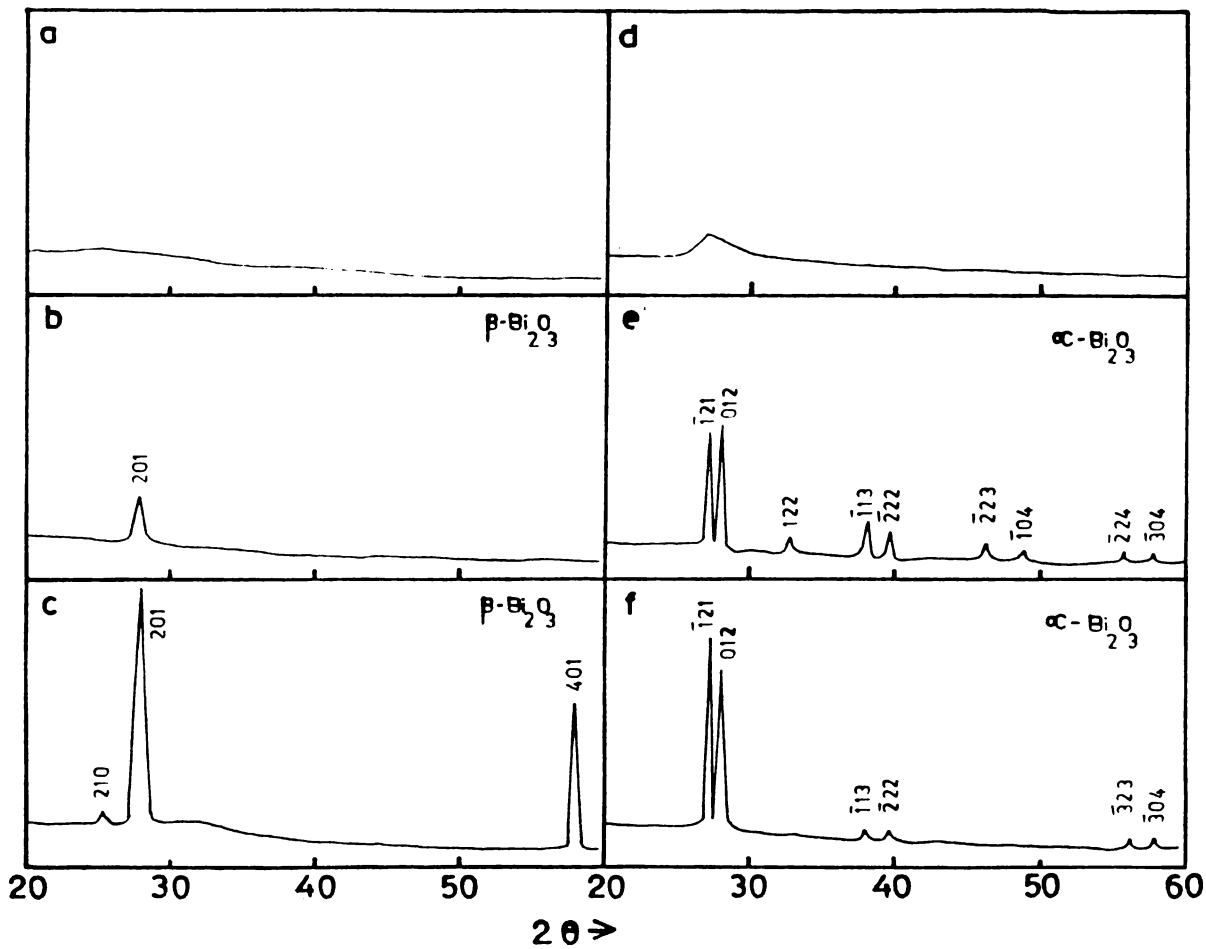


Figure 1. X-ray diffractograms of films prepared by ARE
a-f referring to the specimens shown in Table I.

($> 35 \text{ \AA}/\text{Sec}$) gives α - Bi_2O_3 (PDF No.27.53) films for a given substrate temperature. α - phase films were obtained when the evaporation rate of bismuth was increased, keeping the oxygen pressure in the chamber constant. When the deposition rate was increased keeping the oxygen pressure constant, from the data given in (7.2.1), (7.2.2), (7.2.3) & (7.2.4), it may be inferred that, there was effectively a short supply of oxygen molecules, and this seems to induce the formation of α - phase.

It has been reported by many authors that β - phase is the most oxygen rich of various Bi_2O_3 phases /3-5/. For constant oxygen pressure inside the chamber and at low bismuth atom arrival rates, there was effectively a high oxygen pressure at the reaction site and in terms of chemical equilibria it may be said that the oxygen rich β - phase was formed. But when the bismuth atom arrival rate was increased, for constant oxygen pressure, the effective oxygen pressure was reduced and the chemical equilibrium shifted and a comparatively oxygen lean α - phase was formed.

α - phase films of Bi_2O_3 were also obtained when bismuth films were oxidized in oxygen deficient atmosphere (chapter V).

Bi_2O_3 films prepared by this technique have got excellent optical transmission and also have very good adhesion to the substrate.

7.4 ANNEALING OF FILMS

Table II summarizes annealing of ARE prepared Bi_2O_3 films. The corresponding x-ray diffractograms are given in figure 2. It can be seen from the table that all the films when annealed in high vacuum, irrespective of their temperature of preparation and the rate of deposition, were converted to α - phase. When α - phase films prepared by oxidizing bismuth, were annealed in air for one hour they were fully converted to β - Bi_2O_3 (chapter V), But α - phase films, prepared at high substrate temperature and high deposition rate, was not converted to β - phase when annealed in air, whereas α - phase films prepared at high deposition rates and low substrate temperature was partly converted to β - phase when annealed in air and this may be due to the reported low temperature stability /6/ of the α - phase.

TABLE II

Results of annealing of ARE prepared
films

Specimen	Film preparation conditions			Heat Treatment	Annealing	Phases obtained
	Sub. Temp. K	Rate of deposition Å/S	Phases formed			
a	300	13	β	-	for one hour in high vacuum at 700 K	α - Bi_2O_3
b	300	13	β	Annealed for one hour in high vacuum at 700 K	for one hour in air at 635 K	α - Bi_2O_3
c	300	39	α	-	for one hour in air at 635 K	β - Bi_2O_3 & α - Bi_2O_3
d	300	39	α	-	for one hour in high vacuum at 700 K	α - Bi_2O_3
e	550	12	β	-	for one hour in high vacuum at 700 K	α - Bi_2O_3
f	550	12	β	Annealed for one hour in high vacuum at 700 K	for one hour in air at 635 K	α - Bi_2O_3
g	550	45	α	-	for one hour in air at 635 K	α - Bi_2O_3

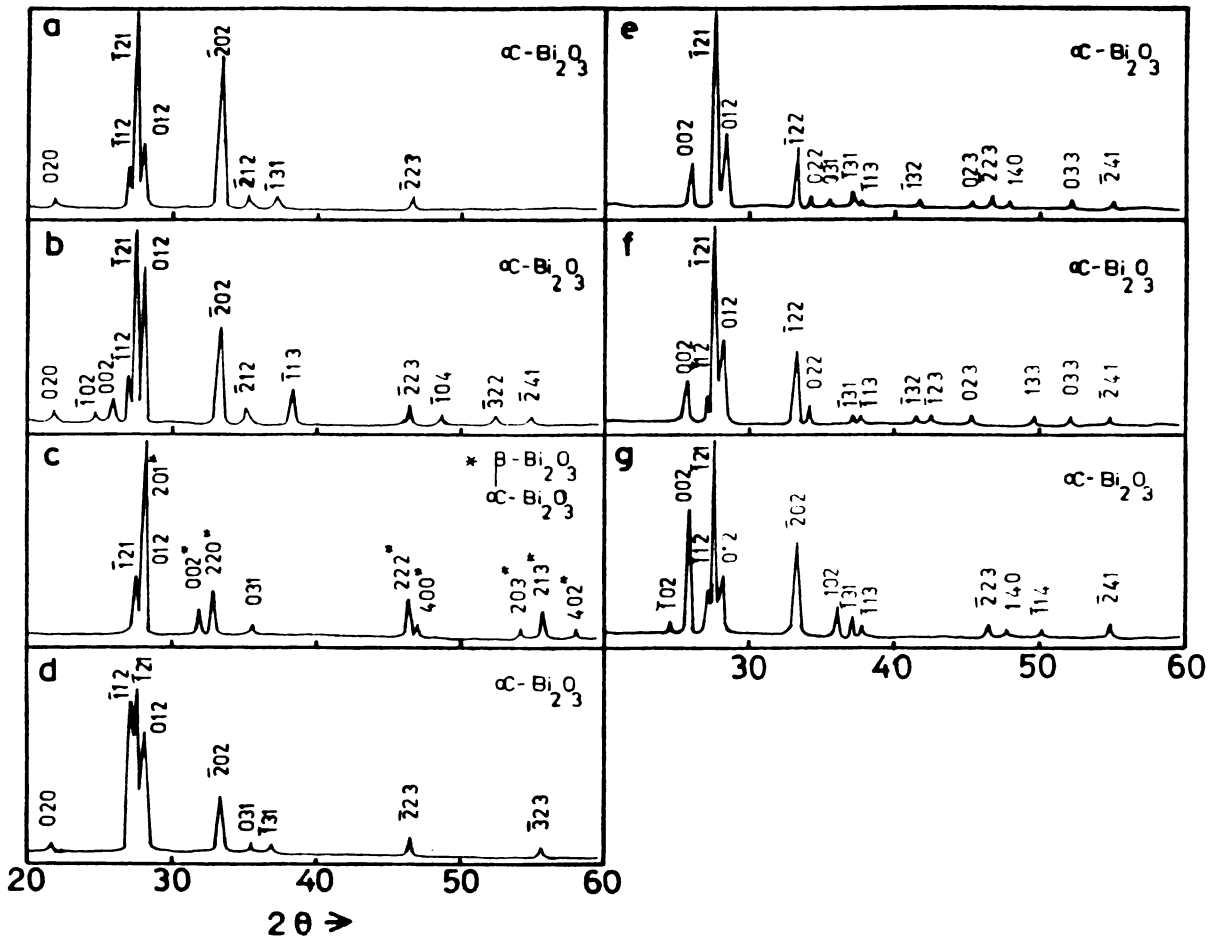


Figure 2. X-ray diffractogram of ARE prepared films annealed in air and high vacuum a-g referring to the specimens indicated in Table II.

The difference between α - phase films prepared onto substrates kept at two different temperatures can only be in their respective grain size. Room temperature prepared films will be amorphous in nature and when they crystallize, their grain size will be small compared to films prepared at high substrate temperature. The same phenomena was also observed in the case of reactively evaporated films of bismuth oxide.

7.5 CONCLUSION

The following conclusions may be drawn:

- (1) β - phase films are obtained when there is abundant supply of oxygen during deposition otherwise α - phase films are obtained.
- (2) When β - phase films are annealed in an oxygen deficient atmosphere (high vacuum), α - phase films are obtained.
- (3) α - phase films are stable compared to β - phase films except in the case of very small grained α - phase films.

REFERENCES

1. A. Milch, Thin Solid Films, 17 (1973) 231.
2. R.F. Bunshah and A.C. Raghuram, J. Vac. Sci. Tech., 9 (1972) 1389.
3. A.A. Zav'yalova, R.M. Imamov, and Z.G. Pinsker, Sov. Phys. Crystallogr., 9 (1965) 724.
4. M.G. Hapase, V.B. Tare and A.B. Biswas, Indian J. Pure Appl. Phys., 5 (1967) 401.
5. A.A. Zav'yalova, and R.M. Imamov, Sov. Phys. Crystallogr., 17 (1972) 811.
6. W.C. Schumb and E.S. Rittner, J. Am. Chem. Soc., 15 (1943) 1055.

CHAPTER VIII

OPTICAL AND ELECTRICAL PROPERTIES OF β - Bi₂O₃ FILMS8.1 INTRODUCTION

β - Bi₂O₃ films have been used as a good dielectric film in many applications including optical coatings /1-3/. These films are highly insulating, having a high refractive index and are physically robust. The optical properties of β - Bi₂O₃ films are reported by many authors. The optical studies of bismuth oxide film was first reported by Doyle /4/. He reported the band gap of the material as 3.2 eV. Later the band gap of β - Bi₂O₃ was reported as 2.6 eV by Dolocan and Iova /5/. They also reported that the fundamental absorption of β - Bi₂O₃ is due to indirect transition. The refractive index of Bi₂O₃ had also been determined and reported /1, 6/.

Electrical properties of bismuth oxide films were also reported by many authors /7-13/. Hapase et.al / 7/ used aquadag as end contacts for electrical

measurements. All others used metal-insulator-metal structure for electrical studies. Space charge limited conduction in Bi_2O_3 was reported by Albin and Sathianandan /8/ and Arya and Singh /12/. An activation energy of 0.9 eV for conduction had been reported by Fedorov and Davydov /11/.

In this chapter is reported the optical and electrical properties of β - Bi_2O_3 thin films prepared by activated reactive evaporation.

8.2 EXPERIMENTAL

The preparation of bismuth oxide thin films is discussed in detail in the last chapter. For optical measurements, samples were prepared on optically flat glass substrates of dimensions 3 cm x 1.2 cm x 0.1 cm. Before deposition of the films, the substrates were cleaned in boiling nitric acid and then with industrial detergent followed by ultrasonic agitation (described in chapter III, 3.8). The films were prepared at different substrate temperatures from 300 K to 600 K. The transmission spectra were taken in the region 2500 nm

to cut off, using a UV - Vis - NIR spectrophotometer, with the sample in the sample beam.

For electrical measurements quartz substrates were used, because bismuth oxide being a highly insulating material. Films were prepared with 2 cm length, 0.4 cm width and ~ 1 micron thick, by properly masking the quartz plates. Substrate temperatures were varied from room temperature to 600 K. After deposition of bismuth oxide films, the specimens were transferred to another vacuum coating unit in which indium was deposited at both the ends of the films, as contacts with a separation of 1 cm. From this indium film, the electrical contacts were made with silver paint to copper foil pressed over it by using teflon strips. A potential difference of 150 Volts was applied across the film from a well regulated power supply. A micro heater was provided below the specimen to maintain the sample at different temperatures. Measurements were done under a vacuum of $\approx 10^{-2}$ Torr in an all metal cell (described in chapter III, 3.1). The current through the specimen was measured by an electrometer. The temperature was varied from 300 K

to 660 K and the current through the film was measured for the applied potential difference of 150 V.

8.3 RESULTS AND DISCUSSION

Optical

Figure 1 a and 1 b respectively shows typical transmission spectra of amorphous and polycrystalline films of $\beta - \text{Bi}_2\text{O}_3$. Film thickness 't' and substrate temperature ' T_s ' during preparation are indicated in the figure. It can be seen that the films show large amplitude interference fringes and good optical transmission. From this figure, it may be inferred that the films are of good optical quality. The amorphous films thus prepared were orange yellow in colour and polycrystalline films were yellow in colour for transmission. Figure 2 a - 2 f shows the refractive index as a function of wavelength. The value of 'n' remains constant ($n = 2.2$) from 2500 nm to 1000 nm and slowly increases with decrease in wavelength.

Figure 3 shows the absorption coefficient as a function of photon energy, in the case of amorphous

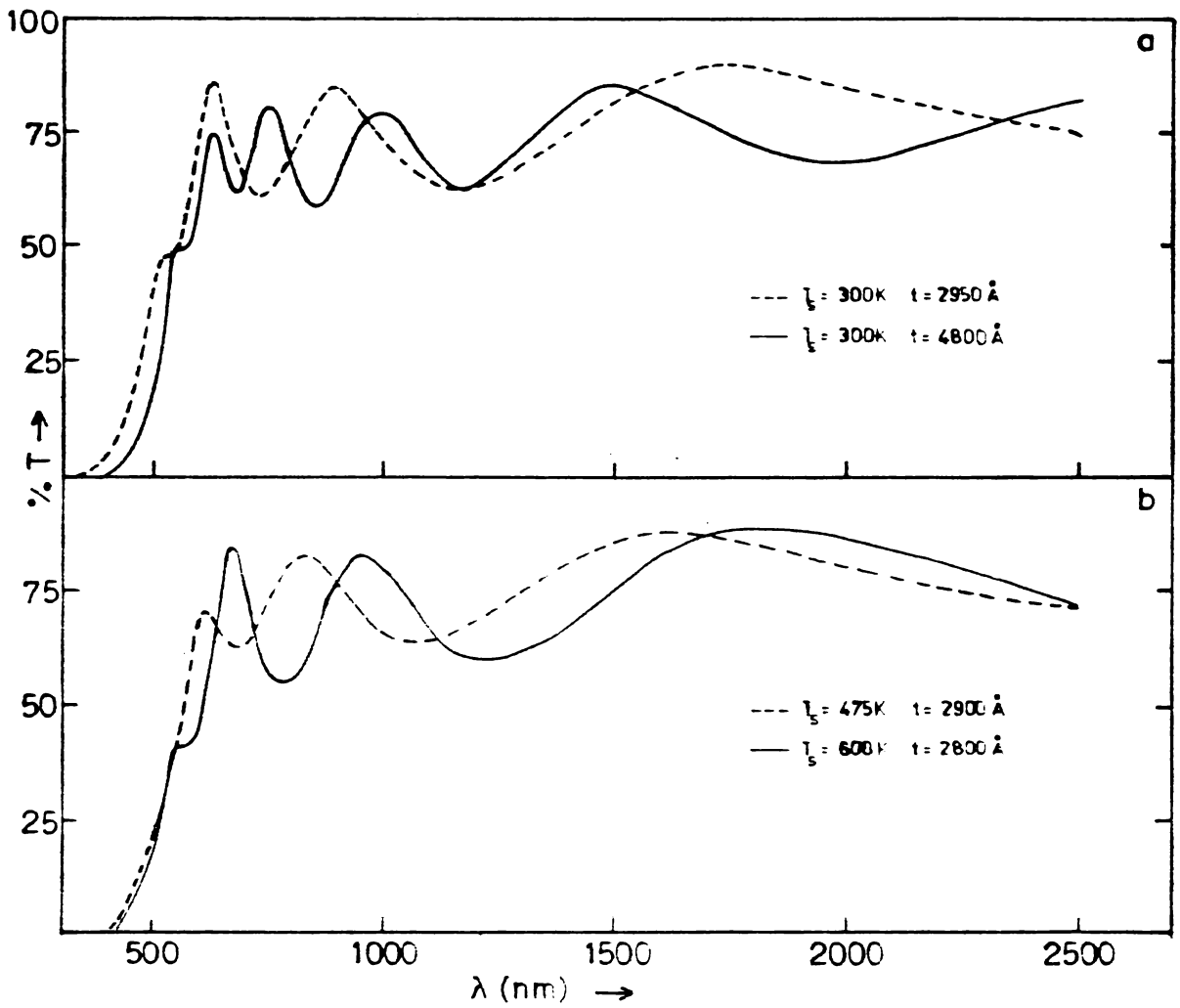


Figure 1. Optical transmission spectra of (a) amorphous, (b) polycrystalline β - Bi_2O_3 .

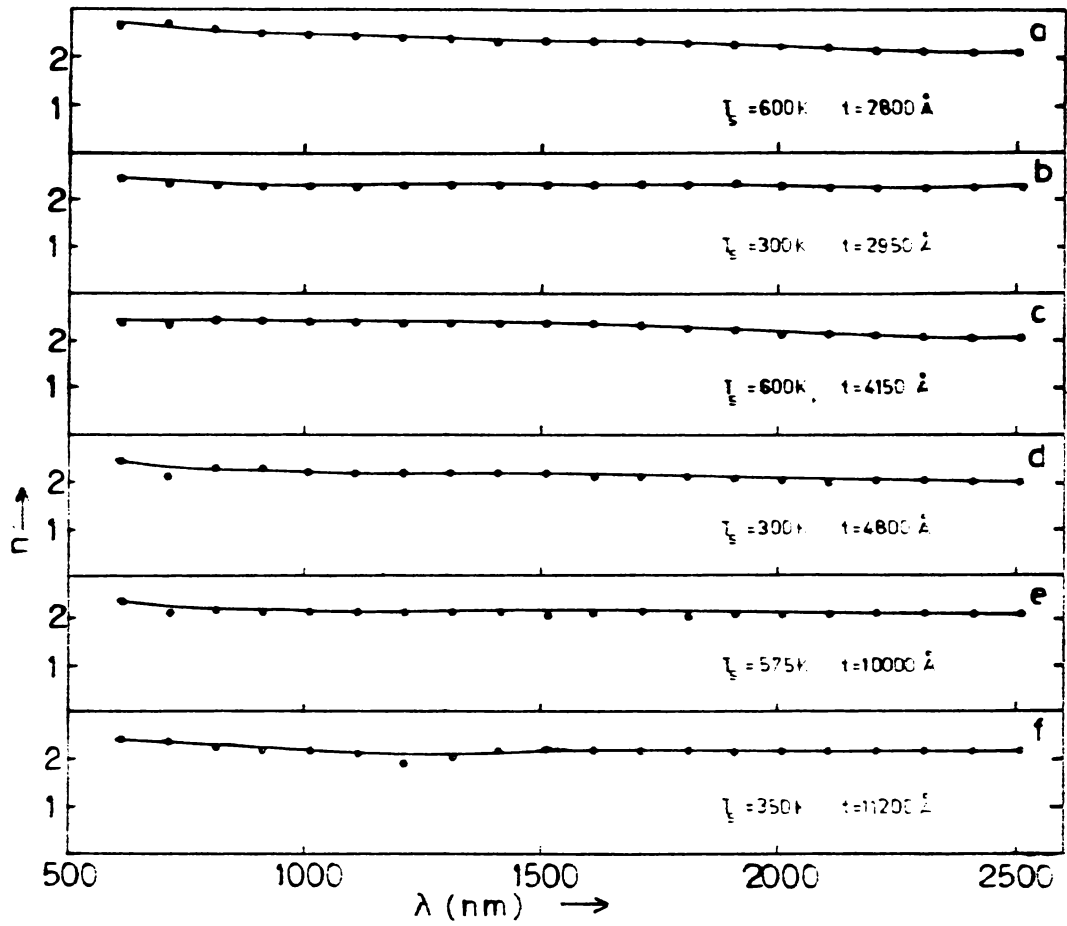


Figure 2. Variation of refractive index as a function of wavelength.

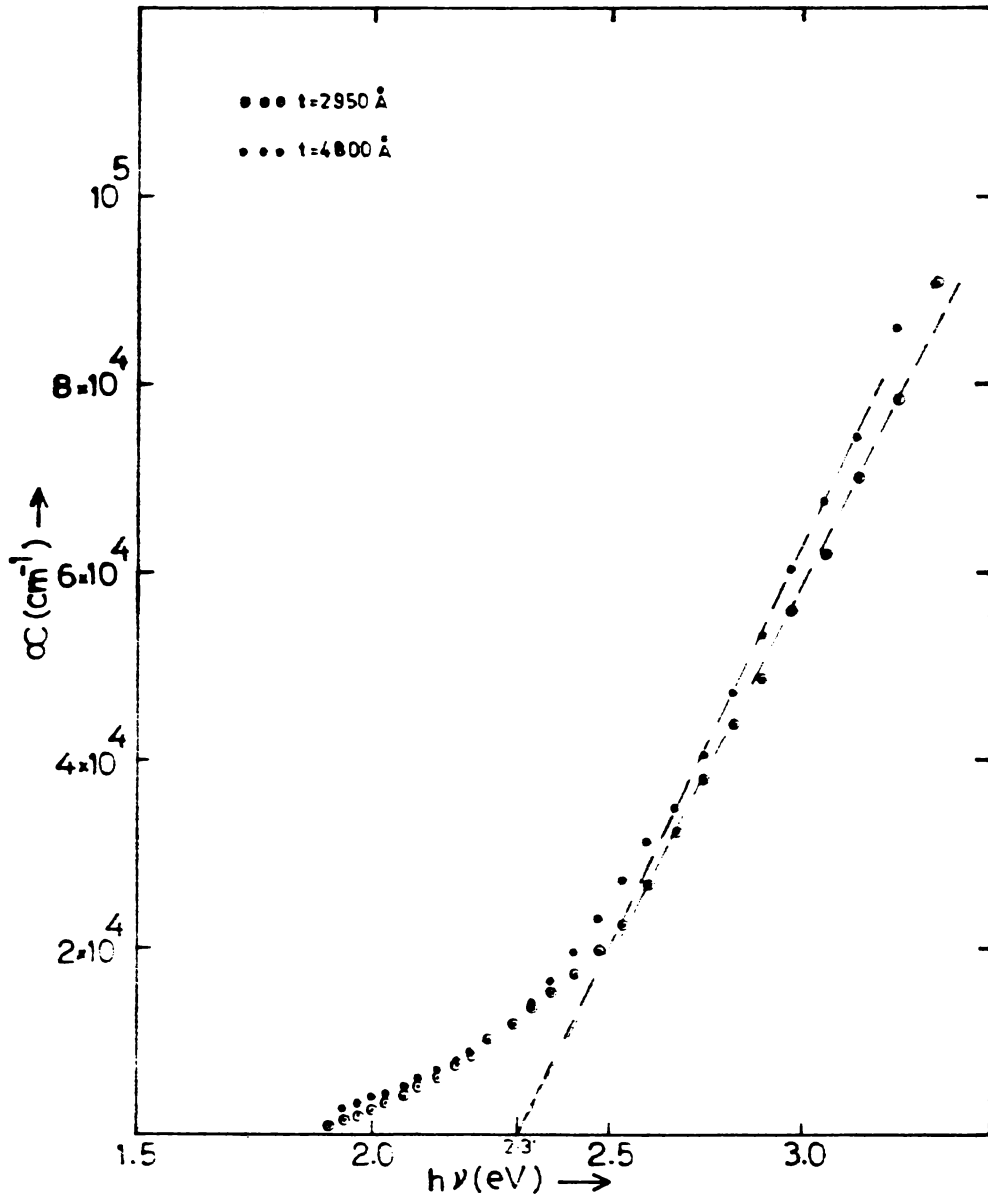


Figure 3. Variation of absorption coefficient as a function of photon energy for amorphous films.

bismuth oxide films. It is known that in the case of amorphous materials, for values of absorption coefficient in the region 10^4 to 10^5 cm^{-1} , is given by

$$\alpha \propto (h\nu - E_g)$$

where $h\nu$ is the photon energy and E_g is the optical band gap. The value of energy gap obtained from this plot is 2.31 ± 0.02 eV, which is a little lower than the reported energy gap (2.6 eV) of crystalline β - Bi_2O_3 /6, 14/. The band gap of amorphous bismuth oxide is not yet seen to be reported in literature and hence no comparison is possible.

Figure 4 shows the dependence of absorption coefficient on photon energy for polycrystalline films of β - Bi_2O_3 at room temperature. The optical absorption data of crystalline β - Bi_2O_3 films were investigated for evidence of either direct or indirect transition. According to Bardeen et.al. /15/, absorption coefficient α due to band to band transition may be described by

$$\alpha = A (h\nu - E_g \pm E_p)^r$$

in the case of indirect transition,

$$r = 2 \text{ for an allowed one}$$

$$r = 3 \text{ for a forbidden one}$$

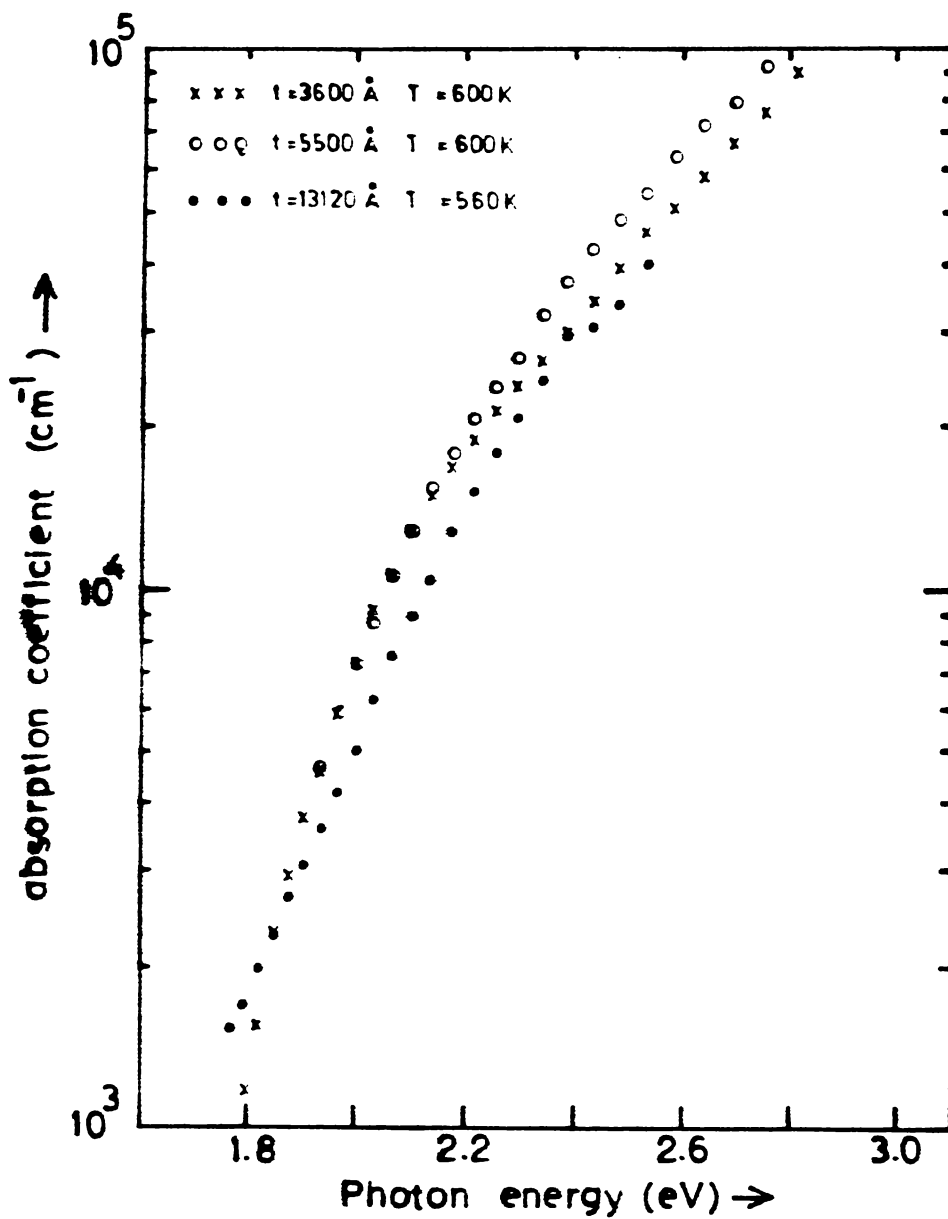


Figure 4. Variation of absorption coefficient as a function of photon energy for polycrystalline films.

and

$$\alpha = A' (h\nu - E_g)^r$$

in the case of a direct transition,

$$r = \frac{1}{2} \text{ for an allowed transition}$$

$$r = \frac{3}{2} \text{ for a forbidden transition}$$

where A and A' are constants, $h\nu$ photon energy and E_g is the direct or indirect band gap.

Optical absorption data for values of absorption coefficient $\lesssim 10^3$ was analyzed for evidence of indirect transition. Figure 5 shows $(\alpha h\nu)^{1/2}$ as a function of $h\nu$. It may be seen that a straight line is obtained. Extrapolating this line we get an indirect band gap of 1.74 ± 0.05 eV. This transition is an allowed one. The dependence of absorption coefficient of $\beta - \text{Bi}_2\text{O}_3$ on photon energy in this range of values has not been investigated earlier and hence this is the first determination of the indirect fundamental absorption edge of $\beta - \text{Bi}_2\text{O}_3$. The absorption coefficient for individual films at a particular photon energy are slightly different probably due to the different oxygen:bismuth ratio.

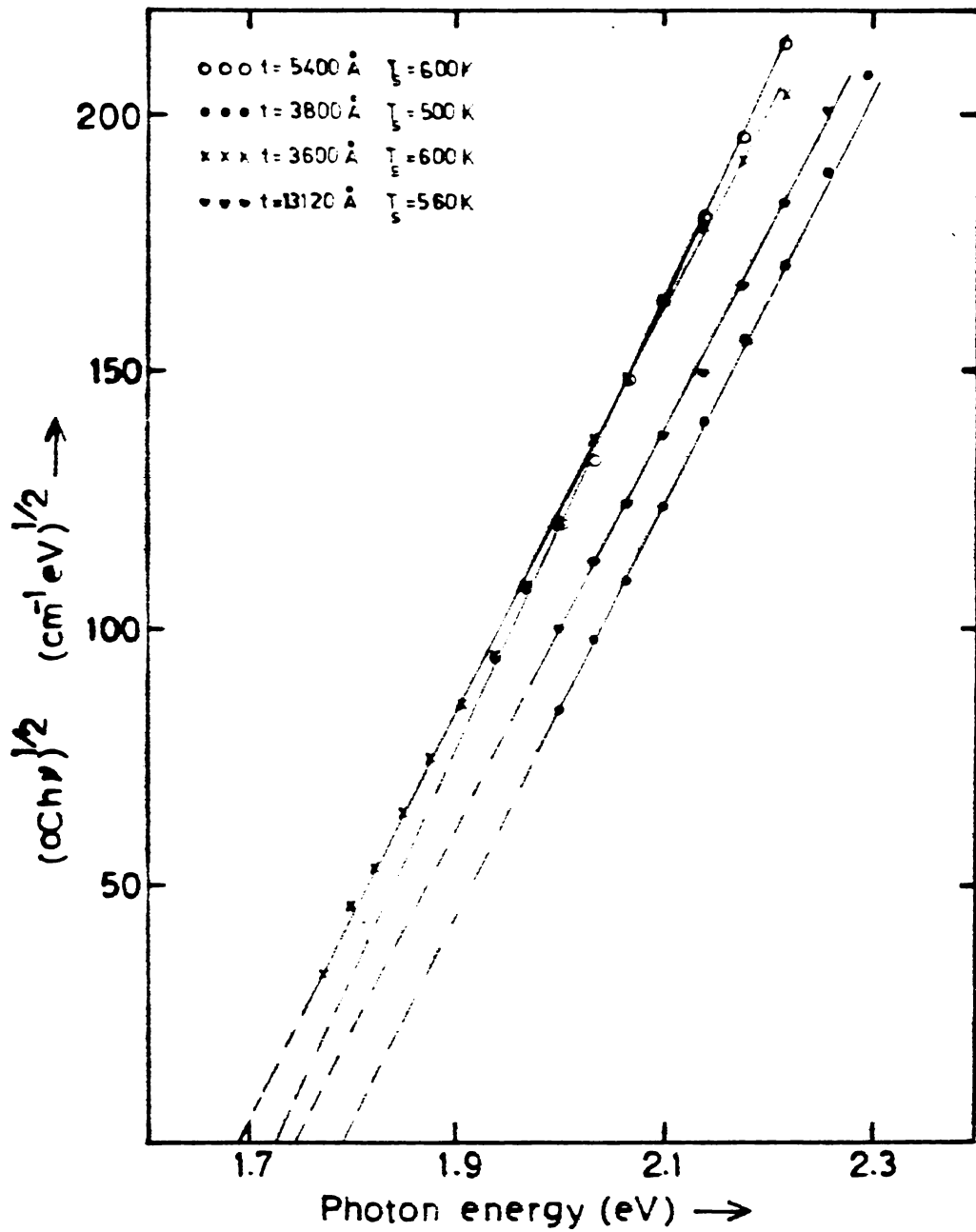


Figure 5. $(\alpha h\nu)^{1/2}$ as a function of photon energy.

For values of absorption coefficient $\geq 10^4$, direct transition was observed. Figure 6 show $(\alpha h\nu)^{2/3}$ as a function of $h\nu$. The turning point at 2.6 ± 0.02 eV is due to the onset of direct transition. From the functional dependence of α on photon energy, it may be seen that this transition is a forbidden one. Dolocan and Iova /5/ and Dolocan /14/ have reported that β - Bi_2O_3 is an indirect band gap semiconductor with a band gap of 2.6 eV at 300 K. Present measurements also indicate that β - Bi_2O_3 is an indirect band gap semiconductor. But fundamental absorption starts at 1.74 ± 0.05 eV and not at 2.6 eV. It is also established here that the 2.6 eV transition reported by Dolocan and Iova /5/ and Dolocan /14/ is actually a direct forbidden transition.

Electrical

The current passing through the film for a given applied voltage at different temperatures was measured and the $\log I$ is plotted as a function of reciprocal of temperature in figure 7. It can be seen from the figure that all the films prepared, at different substrate temperatures showing the same property.

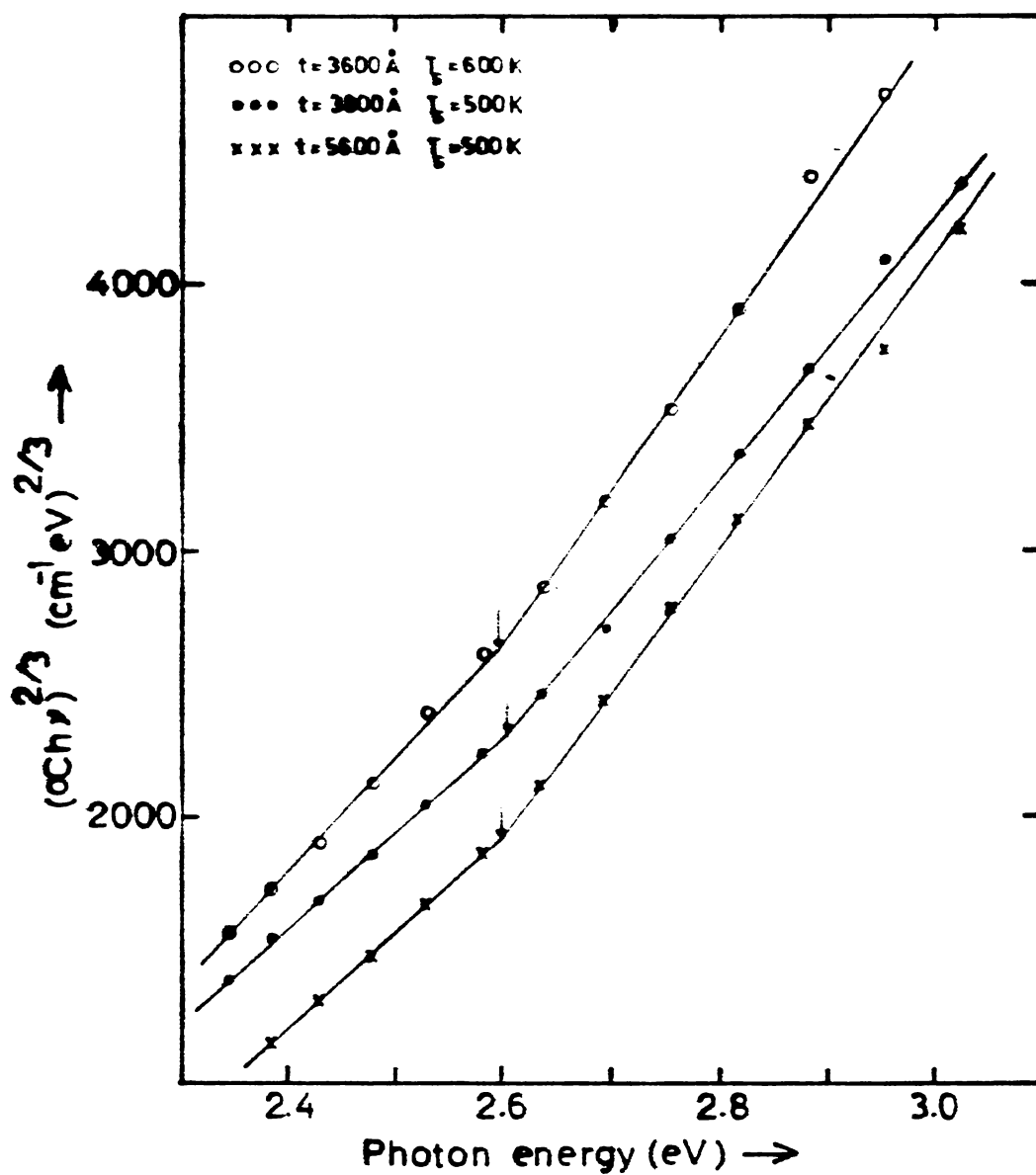


Figure 6. $(\alpha h\nu)^{2/3}$ as a function of photon energy.

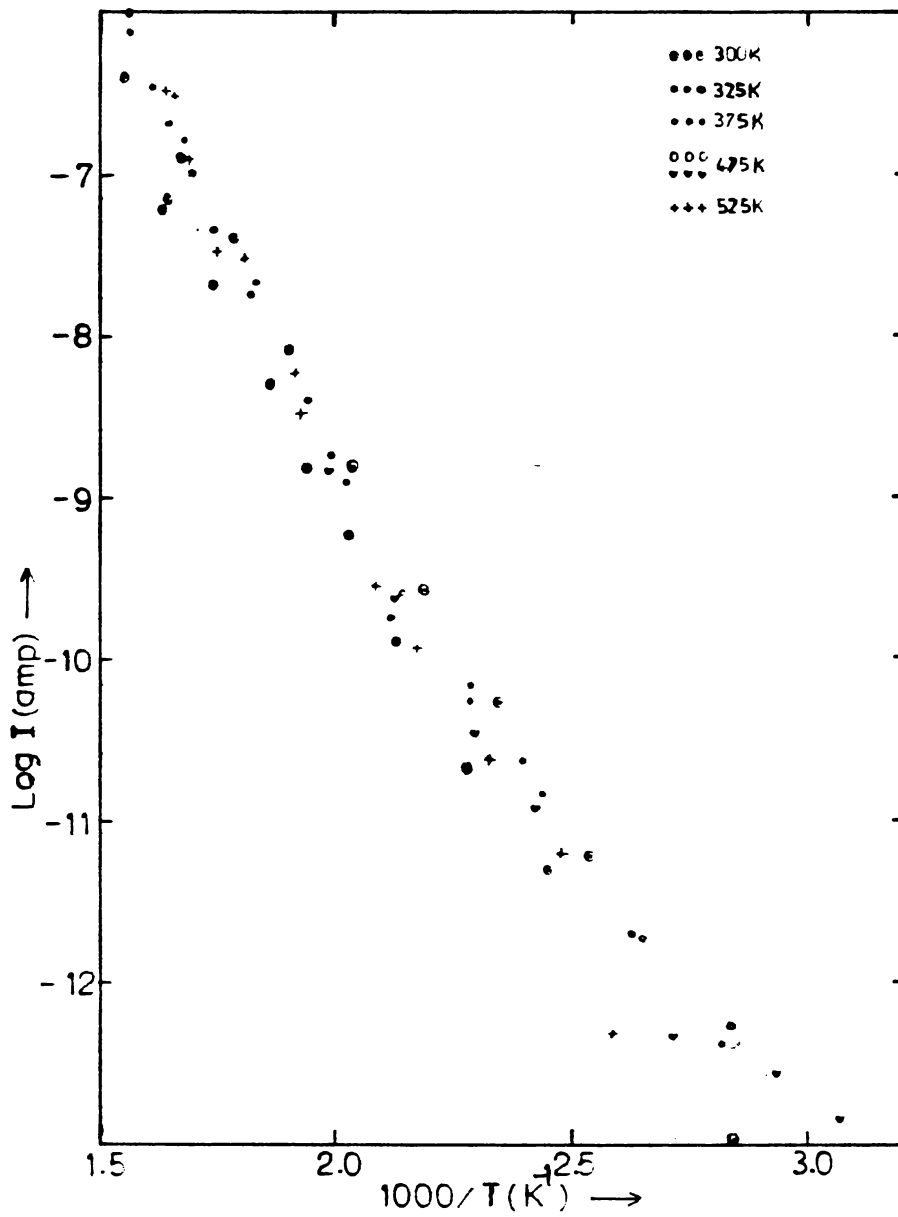


Figure 7. Current through the films as a function of temperature.

ie. the amorphous and polycrystalline films of bismuth oxide showing the same variation in conductivity with temperature. The activation energy can be calculated from this plot and the value obtained is 0.82 eV which in agreement with the reported value /11/.

8.4 CONCLUSION

β - Bi_2O_3 is an indirect band gap semiconductor, The fundamental absorption starts at 1.74 ± 0.05 eV and the optical transition leading to this is an indirect allowed one. The direct band gap of β - Bi_2O_3 is at 2.6 ± 0.02 eV. The optical transition leading to this is a forbidden one. The thermal activation energy is determined as 0.82 eV from the electrical measurements.

REFERENCES

1. P.B. Clapham, Brit. J. Appl. Phys., 18(1967)363.
2. E.V. Wang and K.A. Pandelisev, J. Appl. Phys., 52 (1981) 4818.
3. T.A. Raju and A.S. Talwai, J. Appl. Phys., 52 (1981) 4877.
4. W.P. Doyle, J. Phys. Chem. Solids, 4 (1958) 144.
5. V. Dolocan and F. Iova, Phys. Stat. Sol. (a), 64 (1981) 755.
6. M.L. Lieberman and R.C. Medrud, J. Electrochem. Soc., 116 (1969) 242.
7. M.G. Hapase, V.B. Tare and A.B. Biswas, I.J. Pure & Appl. Phys., 5 (1967) 401.
8. S.Albin and K. Sathianandan, Thin Solid Films, 24 (1974) 339.
9. R. Rahman and P.C. Mahanta, I.J. Pure & Appl. Phys., 12 (1974) 815.
10. V. Dolocan, Phys. Stat. Sol. (a), 45 (1978) K 155.
11. V.I. Fedorov and I. Ya. Davydov, High Temp., 16 (1978) 654.
12. S.P.S. Arya and H.P. Singh, Thin Solid Films, 62 (1979) 353.

13. V.S. Dharmadhikari and A. Goswami, J. Vac. Sci. Technol. A, 2 (1983) 383.
14. V. Dolocan, Appl. Phys., 16 (1978) 405.
15. J. Bardeen, F.J. Blatt, and L.H. Hall, Proceedings of Photoconductivity Conference, Atlantic City Wiley, New York, (1956), p.146.

CHAPTER IX

PREPARATION OF HEAT MIRRORS USING
BISMUTH OXIDE FILMS9.1 INTRODUCTION

Bismuth oxide is a dielectric material with high refractive index. Its optical band gap is very close to the band gap of CdS, which is a promising material for solar cells. Bismuth oxide films are physically robust, but its optical absorption and chemical activity /1/ forbid its use in many sophisticated applications of thin films. Because of its high refractive index and physical robustness, it is used as a beam splitter /2/. It is also used as a component in two-layer anti-reflection system /3/ and as a base layer for gold films /4/. It is also used in many applications like Schottky barrier solar cells /5/ and MIS capacitors /6/. From the study of the optical properties of bismuth oxide and the fact that it can be used as a base material for gold films, it was thought useful to investigate the possibility

of using bismuth oxide as promising material for the fabrication of heat mirrors.

Heat mirrors are thin films that reflect IR radiations and transmit only the visible radiations. Heat mirrors are first used by Reed /7/ to construct transparent furnaces for the growth of bulk single crystals and epitaxial films at temperatures up to 1000°C . The thermal insulation for a furnace of this type is produced by a gold film about 200 \AA thick, which is coated on the inside of a pyrex tube. This gives a 20% transmission to visible light which is sufficient for high temperature furnaces. John and Frank /8/ prepared heat mirrors using $\text{TiO}_2/\text{Ag}/\text{TiO}_2$ structure and also with Sn-doped In_2O_3 film for solar energy applications. Later Sadafami /9/ used Sn-doped In_2O_3 as heat mirrors for solar thermal conversion. Pracchia and Simon /10/ tried dielectric/metal/dielectric structure using different materials and have shown that smaller refractive indices allow wider transmission region at the cost of a more gradual transmission and smaller infrared reflectivities. On the other hand, sharper transmission may be obtained with

higher indices, but the transmission band becomes narrower. Frank et.al. /11/ used doped In_2O_3 as heat mirror for sodium vapour lamps, solar collectors and in incandescent lamps.

Heat mirrors were fabricated using gold films sandwiched between two bismuth oxide layers. The transmission characteristics were studied by varying the layer thickness of bismuth oxide and gold and also the annealing conditions and are discussed in this chapter.

9.2 THEORY

When an electromagnetic radiation is incident on a boundary separating two media of optical admittance N_o and N_i , part of the incident radiation is reflected back into the incident medium. The reflectance (R) at the interface for an angle of incidence θ is given by

$$R = \left[\frac{\gamma_o - \gamma_1}{\gamma_o + \gamma_1} \right]^2 \quad (9.2.1)$$

where γ is the effective optical admittance and is

given by

$$\begin{aligned} \gamma &= N \cos \theta \quad \text{for TE waves} \\ &= N / \cos \theta \quad \text{for TM waves} \end{aligned}$$

where N is the complex refractive index given by

$$N = n - ik$$

where n is the refractive index and k is the extinction coefficient.

Considering a system consisting of an assembly of l layers with optical admittance N_j and thickness t_j ($j = 1$ to l , with $j = 1$ as the outermost layer) on a substrate of admittance N_s . If Y is the optical admittance of this system, then the normal reflectance in a medium of admittance N_o is given by

$$R = \left[\frac{N_o - Y}{N_o + Y} \right]^2 \quad (9.2.2)$$

The optical admittance for this assembly of thin films is calculated by the matrix method developed by Herpin /13/ and Weinstein /14/. According to this method,

$$Y = C/B \quad (9.2.3)$$

where B and C are the elements of the characteristic matrix of the assembly defined as

$$\begin{bmatrix} B \\ C \end{bmatrix} = \left\{ \prod_{j=1} \begin{bmatrix} \cos \delta_j & i \sin \delta_j / \gamma_j \\ i \gamma_j \sin \delta_j & \cos \delta_j \end{bmatrix} \right\} \begin{bmatrix} 1 \\ \gamma_s \end{bmatrix} \quad (9.2.4)$$

$$\text{where } \delta_j = \frac{2\pi}{\lambda} N_j t_j \cos \theta_j \quad (9.2.5)$$

is the effective phase thickness of the jth layer, λ is the wavelength of incident radiation, and θ_j is the angle of refraction in the jth layer.

Equation 9.2.2 and 9.2.4 are of utmost importance and form the basis of almost all thin film calculations.

Here a three layer structure was used consisting Bi_2O_3 - Au - Bi_2O_3 over the glass substrate, for the preparation of heat mirror. The thickness of the individual layers are so chosen by solving the characteristic matrix for minimum reflectivity for the incident wavelength of 550 nm. The refractive index of bismuth oxide was taken as 2.5 and that of glass as 1.51. The optimum condition of minimum reflectivity

was determined by solving the characteristic matrix for all permutation combinations with the thickness of bismuth oxide layers varying from 100 Å to 1200 Å in steps of 50 Å and that of gold from 50 Å to 150 Å in steps of 25 Å. The optimum condition was chosen for the preparation of the heat mirrors.

9.3 EXPERIMENTAL

One of the optimum combination of dielectric/metal/dielectric thicknesses obtained from theoretical calculations had been used to study their characteristics for use as a heat mirror and, was prepared on optically flat glass substrates of dimensions 3 cm x 1.2 cm x 0.1 cm. The deposition was performed in the setup discussed in chapter III, 3.9. The vacuum system was fitted with three resistively heated sources, each for the deposition of corresponding layers. 5N purity bismuth and 24 carat gold were used for the deposition.

The vacuum system was first pumped to $\sim 10^{-5}$ Torr. Then the substrates were heated to 560 K. After the thermal stabilization of the substrates, first layer of bismuth oxide was deposited by the procedure described in chapter VII. After completion of bismuth

oxide deposition, the plasma was switched off and a little interval was given. Gold was evaporated from the second source in three steps, giving adequate intervals in between. If all the gold was evaporated continuously, the base layer of bismuth oxide will get melted, resulting poor quality films. The melting was caused by the high insulating nature of bismuth oxide.

After completion of gold film deposition the plasma was again produced and the third layer was deposited over the gold film without breaking the vacuum, from the third source. After deposition of the third layer of bismuth oxide, the system was cooled slowly to room temperature. Then the prepared film assembly was taken out of vacuum and a set of samples were annealed in atmosphere to study the effect of annealing on the transmission characteristics. Annealing was done in the furnace (discussed in chapter III, 3.7) and also over a hot plate of 1 KW (figure 1a). The temperature of annealing were varied from 625 K to 725 K in steps of 50 K and the duration of annealing were also varied. The transmission spectra of the assembly system were taken by a

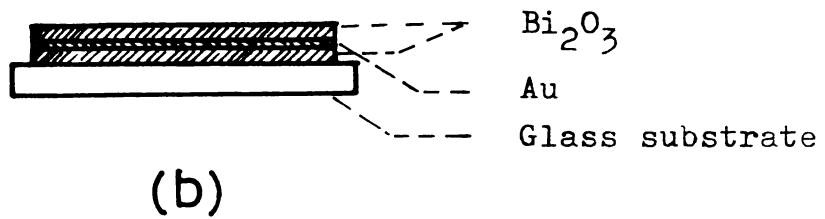
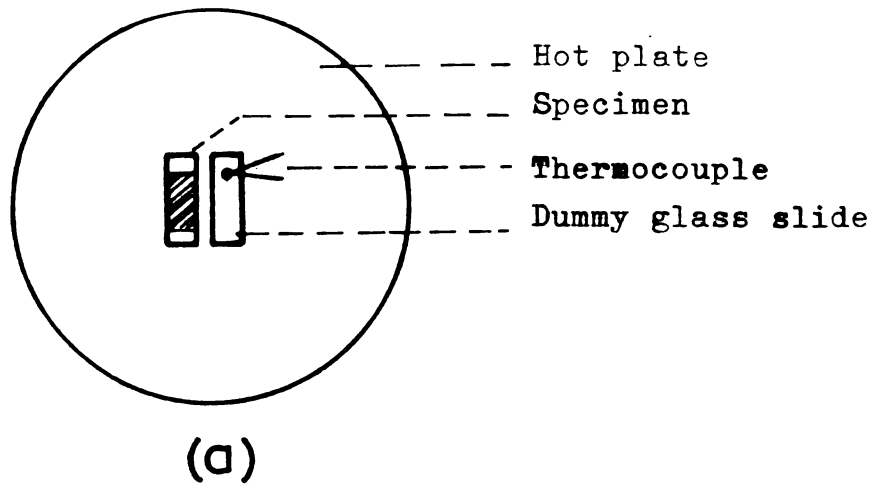


Figure 1. (a) Setup for annealing the specimen
(b) Cross section of a heat mirror assembly.

UV-Vis spectrophotometer, before and after annealing. The experiment was repeated for other optimum conditions of dielectric/metal/dielectric thicknesses after the conditions of annealing temperature and thickness had been determined to get the best transmission characteristics.

9.4 RESULTS AND DISCUSSION

The structure used for the fabrication of heat mirror is shown in figure 1b. Weighed quantities of bismuth and gold, for the required thickness were, used for the deposition. 6 mg of bismuth will give 100 Å thickness of bismuth oxide film and 6 mg of gold will give 50 Å thickness of gold film for this source substrate geometry and position, and the substrate temperature used. Four specimen assembly were prepared in each run.

Eventhough John et.al. /8/ and Kienel /12/ had shown that silver is the best suitable metal layer for fabricating heat mirrors with structure insulator/metal/insulator, gold has been chosen here for the fabrication of heat mirror. This is because, copper or

silver will get oxidized in the presence of oxygen plasma while depositing the third layer of heat mirror, and this oxide layer will absorb the incident radiation.

Figure 2 a (broken curve) shows the transmission spectrum of the assembly consisting of bismuth oxide layer each of thickness $\approx 600 \text{ \AA}$ and gold $\approx 135 \text{ \AA}$. The continuous curve shown is that of an identical specimen annealed at 675 K over the hot plate for one minute. Figure 2 b and 2 c shows the transmission spectra of the specimen annealed for 10 minutes and 60 minutes respectively. It can be seen from figure 2 a - c, that longer annealing time will produce poor quality films. That is, if the film is annealed for a longer time, the transmission in the region 800 - 900 nm is found to increase. By comparison of these curves it can be seen that the annealing time, to get the optimum result is ≈ 10 minutes.

Figure 2 d - 2 f shows the transmission spectra of the specimens of the same batch, annealed at different temperatures, inside the furnace. These

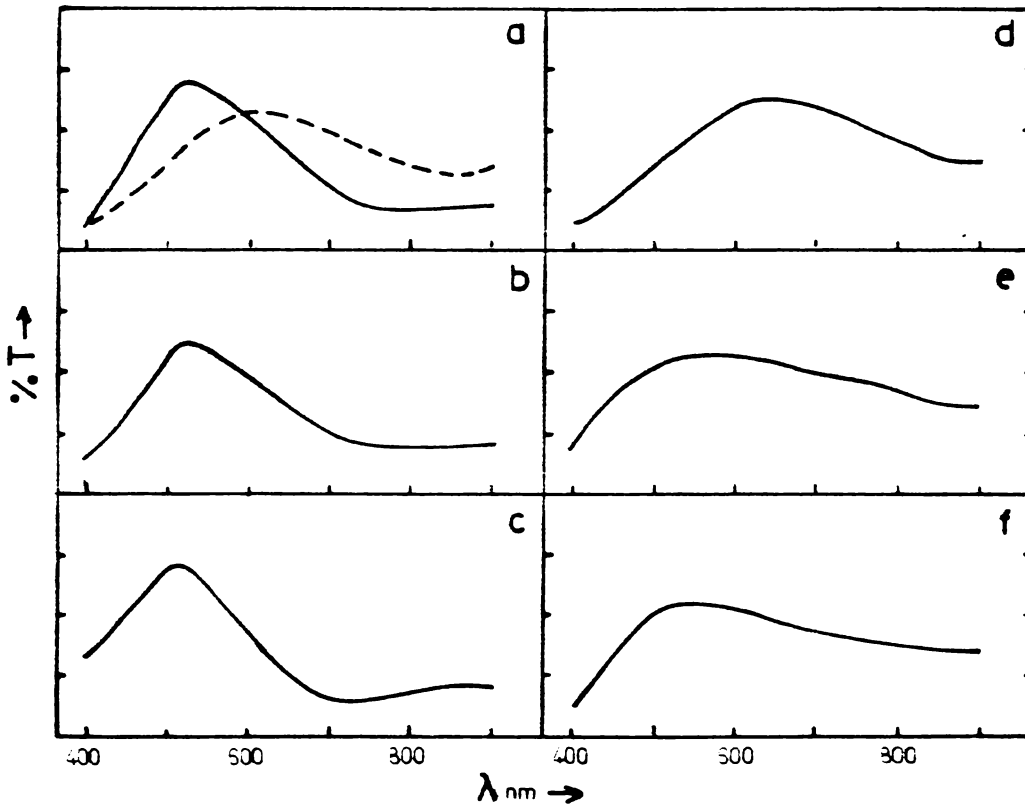


Figure 2. Transmission spectra of heat mirror assembly with thickness $\text{Bi}_2\text{O}_3 : \text{Au} : \text{Bi}_2\text{O}_3 = 600 \text{ \AA} : 135 \text{ \AA} : 600 \text{ \AA}$. (a) - (c) annealed at 675 K over hot-plate for 1 minute, 10 mts. and 60 mts. (d) - (f) annealed inside furnace for 1 hour at 625 K, 675 K and 725 K. - - - - unannealed specimen.

curves shows that there is no appreciable change in the transmission spectra even after annealing in such a high temperature as 725 K. Comparison of these spectra with that obtained for specimens annealed over hot plate (figure 2 a - c), shows that better results can be obtained when the samples are annealed over the hot plate. Unlike the samples annealed inside the furnace, the samples annealed over the hot plate will always have a current of fresh air over the surface of this sample and this large convection current may be influencing the changes that take place in this sample during annealing. Thus it can be seen that best results are obtained with the film annealed over the hot plate at 675 K for about 10 minutes. It is also seen that annealing the assembly at higher temperature over the hot plate only lowers the quality.

After optimising the conditions for heat treatment of the sample system to get the best results for a particular combination of thickness, it has been thought useful to vary the thickness of

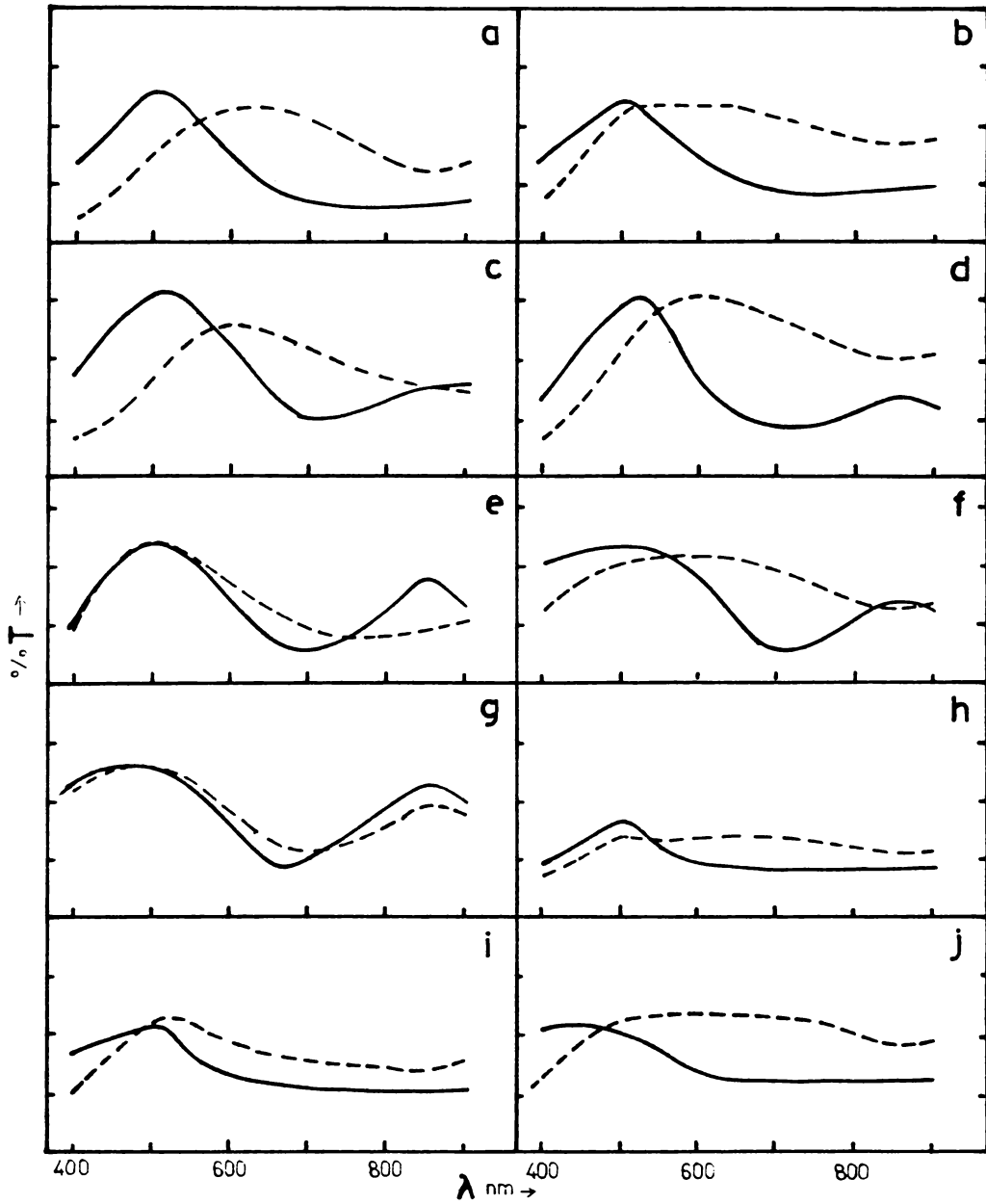


Figure 3. Transmission spectra of heat mirrors with different thickness ratio of Bi_2O_3 : Au : Bi_2O_3 (a) 500:130:500 (b) 450:130:450, (c) 560:80:560, (d) 530:75:550, (e) 60:75:60, (f) 150:65:510, (g) 50:50:50, (h) 300:140:610, (i) 255:140:510, (j) 500:140:245
 - - - - unannealed specimen.

each layer independently and then heat treat the system to improve the transmission characteristics of the heat mirror assembly. The transmission spectra for different combinations of thickness are given in figure 3 a - 3 j. These changes in transmission after annealing, may be due to the inter-diffusion of bismuth oxide and gold at the layer boundaries. From figure 3 a - 3 j it can be seen that the system with a bismuth oxide layer of 500 Å thick and gold layer of 130 Å thick is giving the minimum transmission in the infrared region (figure 3 b) and a fairly good transmission in the visible region. As such it can be said that this combination of thickness of $\text{Bi}_2\text{O}_3/\text{Au}/\text{Bi}_2\text{O}_3$ is best suited for the fabrication of heat mirrors.

9.5 CONCLUSION

Heat mirrors can be prepared using $\text{Bi}_2\text{O}_3/\text{Au}/\text{Bi}_2\text{O}_3$ structure. The optimum properties of heat mirrors are obtained with Bi_2O_3 layer each of thickness ≈ 500 Å and gold layer ≈ 130 Å. Heat treatment over hot-plate at 675 K is necessary for obtaining good quality heat mirrors.

REFERENCES

1. P.B. Clapham, Brit. J. Appl. Phys., 18 (1967)363.
2. K. Hammer, Optik., 3 (1948) 495.
3. L. Holland and T. Putner, J. Sci. Instrum.,
36 (1959) 81.
4. E.J. Gillham and J.S. Preston, Proc. Phys. Soc.
B, 65 (1952) 649.
5. E.V. Wang and K.A. Pandelisev, J. Appl. Phys.,
52 (1981) 4818.
6. T.A. Raju and A.S. Talwai, J. Appl. Phys., 52
(1981) 4877.
7. T.B. Reed, Solid State Research Report, MIT Lincoln
Laboratories (1969:1), p.21.
8. John C.C. Fan and Frank J. Bachner, Appl. Optics,
15 (1976) 1012.
9. Sadafami Yoshida, Appl. Optics, 17 (1978) 145.
10. J.A. Pracchia and J.M. Simon, Appl. Optics,
20 (1981) 251.
11. G. Frank, E. Kauer and H. Köstlin, Thin Solid
Films, 77 (1981) 107.

- 12. G. Kienel, *Thin Solid Films*, 77 (1981) 213.
- 13. A. Herpin, *Compt. Rend.*, 225 (1947) 182.
- 14. W. Weinstein, *Vacuum*, 4 (1954) 3.

ACKNOWLEDGEMENT

I would like to use this opportunity to express my sincere thanks and gratitude to Dr. Joy George, Professor in Industrial Physics for his able and invaluable guidance and constant encouragement throughout the stages of my research work.

I also wish to express my thanks to Prof. K. Sathianandan, former Head of the Department of Physics and Prof. M.G. Krishna Pillai, Head of the Department of Physics, for providing laboratory and library facilities.

I acknowledge the cooperative and helpful attitude of all my fellow research scholars, especially Dr. (Fr.) E.C. Joy, Dr. M.K. Radhakrishnan, Dr. K.S. Joseph, Mr. T.I. Palson, Mr. P.K. Sarangadharan, Dr.S.K.Premachandran, Fr. George Peter and Dr. (Mrs.) C.K. Valsalakumari of our Solid State Physics Group.

I am extremely thankful to all the faculty members, office and technical staff of the Physics Department and the staff of USIC for friendly assistance throughout the period of my research work.

My thanks are also due to Prof. Paul A. Vadakancheri,, Department of Applied Chemistry; Prof. Joseph Francis, Polymer and Rubber Technology; Dr. P.K. Joy,

Er. P.B. Sudharma Dev and V. Ramachandran Pillai of Travancore Titanium Products, for providing various instrumentation facilities during the course of my work.

I wish to thank the Department of Science and Technology, New Delhi and Cochin University of Science and Technology for the financial assistance during the tenure of my work.

Thanks are also due to Mrs. Giriyamma for her excellent typing and to Mr. Peter for nicely binding the thesis.